



DISSERTATION

Titel der Dissertation

Dissecting sperm provided polarity in *C. elegans*
embryo: study of centrosome movement and sperm
provided mitochondria

Verfasserin

Dominika Bienkowska

angestrebter akademischer Grad

Doktorin der Naturwissenschaften (Dr.rer.nat.)

Wien, 1-2-2012

Studienkennzahl lt. Studienblatt: A 091490
Dissertationsgebiet lt. Studienblatt: Molekulare Biologie
Betreuerin / Betreuer: Carrie Cowan, PhD

Abstract

Cell polarity provides essential spatial information to guide developmental decisions. One-cell *C. elegans* embryos have proven an important model system for understanding cell polarity, largely because of their highly stereotyped development, including the process of polarization. While much is known about the maintenance of cell polarity, the requirements for the initiation of polarity are less well understood. Centrosomes are required for polarity establishment in one-cell *C. elegans* embryos. It has been proposed that the movement of the centrosome to the cell cortex determines the time and place of polarization, and a current model proposes that direct centrosome-cortex interactions are necessary for polarity establishment. I assessed how centrosome position relative to the cortex affects polarity establishment. I found that centrosomes can initiate polarity from any position within the embryo volume, but centrosome-cortex proximity decreases the time required to initiate polarity. Polarization itself brings about close centrosome-cortex proximity. Prior to polarization, cytoplasmic microtubules constrained centrosome movement near the cortex, expanding the controversial role of microtubules during polarity establishment in *C. elegans*. The ability of centrosomes to induce a single polarity axis from any position within the egg emphasizes the flexible, self-organizing properties of polarization in *C. elegans* embryos and contrasts the common view of *C. elegans* development as invariant.

Furthermore I investigated the presence of sperm provided mitochondria in the zygote. Sperm mitochondria cluster around the centrosome before symmetry breaking and disperse once symmetry is broken. Their distribution during later development appears to be random. Sperm mitochondria can be seen in late in the development (beyond 300 cells). However, paternal mitochondria may be selectively excluded from the germline progenitor cells thus limiting transmission of heteroplasmic mtDNA to the next generation.

Der Beitrag des Spermiums zur Zellpolarität in *C. elegans* Embryos: Eine Analyse von Zentrosombewegung und paternalen Mitochondrien

Zellpolarität bietet notwendige räumliche Informationen, die Entscheidungen in der Entwicklung eines Organismus leiten. *C. elegans* Einzell-Embryos sind ein wichtiges Modellsystem, um ein besseres Verständnis von Zellpolarität zu erlangen. Dies liegt zu einem großen Teil an einem hochgradig reproduzierbaren Ablauf ihrer Entwicklung, was auch den Prozess der Polarisierung umfasst. Während viel über die Aufrechterhaltung von Zellpolarität bekannt ist, sind die auslösenden Faktoren der Polarisierung weniger gut untersucht. Es wurde vorgeschlagen, dass die Bewegung des Zentrosoms zum Zellkortex die Zeit und den Ort der Polarisierung bestimmt, und ein aktuelles Modell nimmt an, dass eine direkte Verbindung und Kommunikation von Zentrosom und Kortex notwendig für die Polarisierung sind. Ich habe den Einfluss der Zentrosomposition relativ zum Kortex auf die Polarisierung des Embryos untersucht und gefunden, dass Zentrosomen die Polarisierung zwar von jeder Position im Embryo initiieren können, die Nähe zum Zellkortex jedoch die dafür notwendige Zeit verringert. Die Polarisierung selbst bewirkt eine Annäherung von Zentrosom und Kortex. Vor der Polarisierung beschränken zytoplasmatische Mikrotubuli die Bewegung des Zentrosoms in der Nähe des Kortex, was wiederum die kontroversielle Rolle von Mikrotubuli bei der Initiierung der Polarität unterstreicht. Die Fähigkeit von Zentrosomen, eine einzige Polaritätsachse von jeder Position im Embryo festzulegen, betont die Flexibilität und die selbstorganisierenden Eigenschaften der Polarisierung von *C. elegans* Embryos und steht somit im Gegensatz zu dem verbreiteten Bild von der Unveränderlichkeit in der Entwicklung dieses Nematoden.

Des Weiteren habe ich das Vorhandensein und Verhalten der Mitochondrien des Spermiums in der Zygote untersucht. Die Mitochondrien des Spermiums sind

vor der Polarisierung des Embryos um das Zentrosom konzentriert und zerstreuen sich erst nach der Initiierung der Polarisierung. Ihre Verbreitung in späteren Stufen der Entwicklung scheint zufällig zu sein. Die Mitochondrien des Spermiums können auch noch in späteren Stadien (über 300 Zellen) beobachtet werden, sie könnten jedoch spezifisch aus den Vorläuferzellen der Keimbahn eliminiert werden, um eine Weitergabe von heteroplasmischer mitochondrialer DNA an die nächste Generation zu vermeiden.

Table of Contents

1. Introduction

- 1.1 What is polarity
- 1.2 Symmetry Breaking
 - 1.2.1 Spontaneous symmetry breaking in actin-based motility
- 1.3 Polarity establishment in *C. elegans* embryo
 - 1.3.1 Oocyte and fertilization
 - 1.3.2 Polarity in the embryo
 - 1.3.3 Centrosome as the symmetry breaking cue
 - 1.3.4 Microtubule nucleation at the centrosome
 - 1.3.5 Symmetry breaking – cortical relaxation model
 - 1.3.6 Symmetry breaking – identity of centrosomal signal
- 1.4 Symmetry breaking and polarity establishment in other systems
 - 1.4.1 *Drosophila* oocyte
 - 1.4.2 Mouse embryo
 - 1.4.3 Ascidian egg
 - 1.4.4 Nodal flow
- 1.5 Centrosome position in polarized cells
 - 1.5.1 Asymmetric cell division
 - 1.5.2 Migrating fibroblast
 - 1.5.3 Neuronal polarization
 - 1.5.4 T Lymphocyte
- 1.6 The role of sperm contributed mitochondria in polarity
 - 1.6.1 Mitochondria and mitochondrial DNA
 - 1.6.2 Significance of uniparental inheritance
 - 1.6.3 Mitochondria heteroplasmy
 - 1.6.4 Fate of paternal mitochondria in *C. elegans* embryo

2. Materials and Methods

- 2.1 Worm strains and imaging
- 2.2 Image processing and data analysis
 - 2.2.1 Assignment of Symmetry Breaking time
 - 2.2.2 Centrosome tracking.
 - 2.2.3 Cortex detection
 - 2.2.4 Closest cortex.
 - 2.2.5 Symmetry breaking site
 - 2.2.6 Velocity.
 - 2.2.7 Frequency histogram.
 - 2.2.8 Net Displacement.
 - 2.2.9 Color-plotted trajectory.
 - 2.2.10 Distance to cortex in NMY-2::GFP expressing movies.
 - 2.2.11 Kymograph.
 - 2.2.12 PIV
 - 2.2.13 Bead Tracking
- 2.3 RNAi
- 2.4 Immunofluorescence
- 2.5 Bead Injection
- 2.6 Drug treatment
- 2.7 Cellular markers
- 2.8 Worm mating

3. Results

- 3.1 Analysis of wildtype movement
- 3.2 Assignment of symmetry breaking
- 3.3 Random walk of centrosome
- 3.4 Centrosome-cortex distance: closest cortex
- 3.5 Centrosome-cortex distance: polarity site
- 3.6 Centrosome-cortex distance at symmetry breaking
- 3.7 Centrosome movement in centrifuged embryos
- 3.8 Cytoplasmic flow: endogeneous granules
- 3.9 Cytoplasmic flow: beads
- 3.10 The role of actin in centrosome movement
- 3.11 The role of microtubules in centrosome movement
- 3.12 The role of centrosomal microtubules in centrosome movement
- 3.13 The role of gamma-tubulin in centrosome movement
- 3.14 Contribution of microtubules regulators
- 3.15 The effect of centrosome-cortex distance on polarity: NMY-2 and PAR-2
- 3.16 Visualizing sperm mitochondria in the zygote
- 3.17 Sperm mitochondria in the zygote
- 3.18 Mitochondria cluster around the male pronucleus and leave the cluster at symmetry breaking

- 3.19 Paternal mitochondria in the zygote during development
- 3.20 Exclusion of sperm mitochondria from a germline progenitor
- 3.21 LGG-1 dependent autophagy

4. Discussion

- 4.1 High temporal resolution imaging of centrosome movement
- 4.2 Random walk of centrosomes
- 4.3 Cortical constraint of centrosome movement
- 4.4 Movement of centrosome to the cortex after symmetry breaking
- 4.5 Posteriorization
- 4.6 How centrosome-cortex distance affects polarity
- 4.7 Centrosome-cortex communication to break symmetry
- 4.8 Centrosome cortical constraint: a polarity-independent function?
- 4.9 Does the centrosome return to a predetermined spot on the cortex?
- 4.10 The sperm mitochondria contribution to the zygote
- 4.11 Sperm mitochondria are an isolated population in the embryo
- 4.12 Do paternal mitochondria disappear completely during development?

5. References

6. Appendix

- 6.1 Acknowledgments
- 6.2 Matlab scripts
- 6.3 Curriculum vitae

Table of figures

- Figure 1. Scheme for hanging drop mounting method.
- Figure 2. Detection of the cortex
- Figure 3. Symmetry breaking assignment
- Figure 4. Analysis of GFP::SPD-2 timelapse.
- Figure 5. Analysis centrosome movement: turning and velocity
- Figure 6. Analysis of wildtype motion
- Figure 7. Centrosome-to-cortex distance
- Figure 8. Distance to symmetry breaking site
- Figure 9. Distance to cortex analysis
- Figure 10. Centrosome in a centrifuged embryo
- Figure 11. Polarity establishment moves centrosomes, beads and granules to the cortex
- Figure 12. Tracking beads
- Figure 13. Centrosome motion in a latrunculin-treated embryo
- Figure 14. Centrosome-cortex distance in nocadazole treated embryos
- Figure 15. Radius of gyration in wildtype and nocadazole treated embryos
- Figure 16. Trajectory travelled by centrosome in nocadazole treated embryo
- Figure 17. Immunofluorescence of a meiotic embryo showing cytoplasmic microtubules
- Figure 18. Dynamic noncentrosomal microtubules
- Figure 19. Centrosome movement in *spd-5*(RNAi)
- Figure 20. Consequences of TBG-1 depletion on movement of centrosome and microtubules cytoskeleton
- Figure 21. Depletion of RAN-1.
- Figure 22. Symmetry breaking at a distance
- Figure 23. Distance to cortex vs polarity establishment efficiency
- Figure 24. Mitochondria in *C. elegans* embryo
- Figure 25. Behavior of sperm mitochondria before and after symmetry breaking
- Figure 26. Sperm mitochondria and ER morphology prior to symmetry breaking
- Figure 27. Sperm mitochondria persist during development
- Figure 28. Photobleaching of mitochondrial stain
- Figure 29. Exclusion of sperm mitochondria from germline
- Figure 30. Localization of paternal mitochondria and autophagy components
- Figure 31. Model for centrosome constraint close to the cortex

1. Introduction

Biological systems require both spatial and temporal information to function effectively. How do cells know when and where to perform particular functions? Internal regulatory mechanisms or external cues must be able to provide robust positional information during development. I am interested in one particular source of positional information: cell polarity.

1.1 What is polarity?

Polarity refers to an asymmetric organization of cytoskeleton along an axis, which drives nonrandom distribution of organelle and of mobile components, usually regulatory molecules. Specification of an axis facilitates generation of diverse regions within an organism or cell. The first axis specified during development is usually anterior-posterior axis, followed by dorsal-ventral and finally left-right axis.

Polarity of a cell lies at the basis of cell division, motility, fate specification or tissue generation. Regional specialization of a cell allows generation of diverse cell shapes as well as cellular structures such as axons, filopodia, microvilia or cilia. Furthermore, asymmetric cell division and the consequent tissue formation are (Knoblich, 2008) possible due to cell polarity (Knoblich, 2008). The existence of polarity is essential for development and functioning of organisms, and consequently, disruption of polarity results in malfunctioning and disease. Cancer is just one of several instances of what can happen when cells lose their polarity (Caussinus and Gonzalez, 2005).

The establishment of cell polarity occurs through three generalizable steps: symmetry breaking, cortical reorganization, and functional polarization. Symmetry breaking is the initial change that dictates when and where a cell polarizes. Cortical reorganization is the formation of two domains on the plasma membrane, which is

associated with cytoskeleton reorganization and localization of polarity markers. Finally, functional polarization is the distribution of the cellular functions in the cytoplasm. I am interested in understanding how spatial information is provided during the very first step in polarization, symmetry breaking.

1.2 Symmetry Breaking

Symmetry in biology is a homogenous distribution of components. According to the rules of entropy, nature favors disorder. Correspondingly, a symmetric state is unstable and cannot persist, thus leading to redistribution of the components into an asymmetrical, energetically more favorable state. In 1952, Alan Turing attempted to understand how a homogenous system could spontaneously form a heterogeneous pattern that is more thermodynamically stable (Turing, 1952; Howard et al., 2011). He proposed a reaction-diffusion model in which he speculated how two substances - morphogens - establish an irregular pattern. Initially it may seem counterintuitive that diffusion can be a destabilizing influence instead of leading to homogenization of a system, however, diffusion-driven instability has a symmetry breaking capacity. In biology, symmetry breaking can be driven in response to mechanical or biochemical instability. During polarity establishment, symmetry breaking manifests as a local disruption of the cytoskeletal network and/or proteins attached to plasma membrane.

1.2.1 Spontaneous Symmetry Breaking in actin-based motility

Symmetry breaking is an inherent property of actin networks and has been reconstituted *in vitro*. A well-studied example is actin gel assembly around beads (Noireaux et al., 2000) Actin monomers assemble around beads coated with proteins that activate actin polymerization. Eventually high stress builds up in such a network. When stress exceeds a critical threshold, a local rupture in the actin shell can be observed, usually at the weakest point of the gel (Paluch et al., 2006). A result of breakage in the system is local relaxation: release of elastic energy followed by movement of the bead driven by an “actin comet”. Symmetry breaking in this case

derives from a mechanical instability and occurs spontaneously.

A similar behavior can be recognized in the unicellular slime mold *Dictyostelium discoideum*. A single *Dictyostelium* breaks symmetry spontaneously, eliciting motility and growth of the cell but with randomized directionality. However, *Dictyostelium* can also break symmetry in response to a spatial signal: chemoattractant. A gradient of chemoattractant induces oriented growth and motility towards the source of the attractant (Devreotes and Zigmond, 1988).

Thus symmetry breaking in a biological system can be envisioned as way of generating further complexity and specialization, for instance cell motility, as stated above. Symmetry breaking is the first event that leads to development of cell polarity and directional migration, in other words, to the functional specialization of a cell

1.3 Polarity establishment in *C. elegans* embryo

A symmetric cell can become asymmetric upon an extrinsic or intrinsic instability. This initial cue initiates cytoskeleton reorganization and results in a polarized cell with spatially distributed functions. A remarkable example of such cell polarity occurs in the one-cell zygote of the nematode *Caenorabditis elegans*. The embryo of *C. elegans* is a well-established research system for elucidating mechanisms of cell polarity due to its optical transparency, rapid cell cycle and genetic flexibility, which allows for manipulation and visualization of the embryos. The worm zygote is particularly interesting because the segregation of soma and germ line occurs during the first cell division, which is asymmetric (SULSTON and HORVITZ, 2003; Sulston and HORVITZ, 1977). Asymmetry in one-cell *C. elegans* embryos is established soon after fertilization, upon completion of meiosis. The anterior-posterior (AP) axis of the embryo can be easily distinguished based on molecular differences, highlighted by the asymmetric distribution of the conserved polarity regulators, Par proteins, which were first described in *C. elegans* (Kemphues et al., 1988). Previous investigations have shown that an intrinsic factor

delivered by sperm allows for establishment of polarity in *C. elegans* embryos (Goldstein and Hird, 1996). The spatial cue is provided by the centrosomes, however mechanism of the polarizing signal is not well understood (Cowan and Hyman, 2004b; 2004a).

1.3.1 Oocyte and fertilization

In laboratory conditions, *C. elegans* is found mostly as a hermaphrodite with sporadic males. In hermaphrodites, sperm is produced during a larval stage. The spermatozoa are then stored in a specialized structure, the spermatheca. Spermatogenesis is followed by transition to oogenesis, oocytes are continually produced during the lifetime of an adult, but they arrest in prophase I of meiosis and resume meiotic progression after fertilization (Kosinski et al., 2005). Upon reception of a sperm signal, a mature oocyte passes through the spermatheca, where fertilization takes place. The newly fertilized egg generates a covering on its surface that blocks multiple fertilizations and later becomes the vitelline layer of the eggshell. Subsequently, around meiotic metaphase I, the chitin layer of the eggshell is formed, which is then followed by formation of lipid-rich-layer that provides an osmotic barrier between the embryo and its environment. The lipid-rich-layer is separated from embryo plasma membrane by perivitelline space (Johnston and Dennis, 2011). Due to the process of eggshell formation, the embryo is sensitive to the osmotic and mechanical environment where it resides in during meiosis.

1.3.2 Polarity in the *C. elegans* embryo

The worm oocyte possesses no inherent developmental asymmetry (Goldstein and Hird, 1996). Despite the fact that the maternal nucleus is asymmetrically positioned toward one pole in oocytes, any part of the oocyte can become the posterior and give rise to the germline lineage. In this aspect, the worm oocyte is “axially naïve” (Goldstein and Hird, 1996). The sperm delivers a signal to specify the AP axis. Once meiosis II is complete and the second polar body is extruded, myosin and F-actin become enriched at the cortex, assembling into foci

and cables to generate a tensioned actomyosin network. This dynamic network undergoes cortical invaginations over the entire surface of the egg (Munro et al., 2004). Furthermore, anterior polarity markers PAR-3 and PAR-6 are evenly and symmetrically distributed on the cortex (Munro et al., 2004). The posterior polarity determinant PAR-2 is present in the cytoplasm (Hao et al., 2006).

The symmetry breaking signal induces downregulation of actomyosin contractility in the vicinity of the centrosomes, generating cortical flow away from the symmetry breaking site and a counteracting cytoplasmic flow toward the site. Concurrent with the appearance of flows, PAR-2 localizes on the myosin-reduced cortex, forming the posterior domain. The actomyosin enriched half of the embryo is marked by polarity regulators PAR-3, PAR-6, and aPKC and defines the anterior. Consistent with the importance of contractility and cortical/cytoplasmic flows in polarity establishment, an intact actomyosin cortex is required for embryo polarization. Genetic perturbation of actin, myosin or disruptions of actin filament assembly with pharmacological agents inhibit contractility of the cortex, symmetry breaking, consequent cortical flow and overall embryo polarization.

Following establishment of the anterior and posterior Par protein domains, PAR-2 and PAR-1 mediate the asymmetric distribution of cell fate determinants and control posterior spindle positioning, leading to an asymmetric cell division. The posterior cell will give rise to the germline; the anterior cell will become somatic tissues.

How does the position of polarity establishment relate to the position of fertilization? Previous studies (Jenkins et al., 2006; Goldstein and Hird, 1996) were not able to visualize the position where sperm entry occurred in a living specimen. The difficulty of such an observation comes from sensitivity of newly fertilized zygote to the external environment on a slide during visualization. Another obstacle is lack of tools for visualization of sperm. Previous investigations have associated position of sperm pronucleus and other organelles delivered during fertilization

with sperm entry site. However, such an assumption may not be entirely correct, as the sperm complex may not be immobilized within the embryo. Therefore, careful analysis should be performed to monitor correlation of centrosome position at the time of symmetry breaking with its position after fertilization.

1.3.3 Centrosomes as the symmetry breaking cue

The contractile acto-myosin cortex in one-cell *C. elegans* embryos is not able to break symmetry spontaneously, as occurs in other actin-based systems, but instead requires a polarizing cue. Several lines of evidence attribute this role to paternally supplied centrosomes. First, genetic perturbation of the core centrosome components SPD-2 or SPD-5 prevent polarization (Hamill et al., 2002; OCONNELL et al., 2000). Second, mechanical disruption of the centrosome with laser ablation prevents symmetry breaking (Cowan and Hyman, 2004). Moreover, cell cycle regulators that control activation of centrosome assembly, such as cyclin E and CDK-2, are required for symmetry breaking (Cowan and Hyman, 2006). Conversely, fertilization with nucleus-free sperm does not perturb polarity, further substantiating the role of centrosomes (Sadler and Shakes, 2000).

Beyond their role as microtubule organizing centers (MTOCs), centrosomes also act as signaling hubs in eukaryotic cells. In *C. elegans* embryos, the centrosome is necessary for symmetry breaking, most likely acting as a signaling center. Previous studies have observed that centrosomes can be found close to cortex during polarization (Cowan and Hyman, 2004). Moreover, failure in centrosome-cortex juxtaposition correlated with polarity defects in several mutants (Cowan and Hyman, 2004b; Rappleye et al., 2003; 2002), further suggesting that centrosome-cortex proximity may be an important prerequisite for centrosomes to break symmetry.

1.3.4 Microtubule nucleation at the centrosome

In *C. elegans*, as in the majority of sexually reproducing organisms, centrioles are removed from the oocytes and the sperm brings a functional pair of centrioles to the zygote. Only a few centrosome markers can be found at the sperm derived centrosomes immediately after fertilization in *C. elegans*: SAS-4, SAS-5, and SAS-6, core centriole components; and SPD-2, a centriole and pericentriolar material (PCM) protein. Once meiosis II is completed, centrosome starts to accumulate pericentriolar material (ie. SPD-5) and gamma-tubulin (TUBG-1). At this time, centrosomes become capable of nucleating microtubules. Thus, from fertilization until the end of meiosis II, centrosomes are not functional MTOCs (Cowan and Hyman, 2004). The role of centrosomes in symmetry breaking also appears to be independent of microtubule nucleation capacity as neither gamma-tubulin depletion nor microtubule depolymerization prevents polarity establishment. The role of microtubules in polarization in *C. elegans*, however, remains controversial.

1.3.5 Symmetry Breaking – cortical relaxation model

One of the first attempts to explain symmetry breaking and subsequent cortical domain establishment in a contractile acto-myosin system was the cortical relaxation model. Contracting cortex was predicted to locally relax in response to a point of instability. Actin filaments from the relaxed region would be pulled towards the highly contracted region. This model speculated the existence of gradients in cortical tension that could drive cortical flow – a bulk movement of actin filaments residing underneath the plasma membrane - from the relaxed to the contracted region (Bray, White, 1988). In one-cell *C. elegans* embryos, detailed mapping of cortical tension using laser cutting excluded the presence of tension gradients during cortical flow (Mayer et al., 2010), opposing the cortical relaxation model. Furthermore, the distance over which cortical flow acts - half of the embryo length - could not be achieved by gradients in tension. Cortical flow can, however, be attributed to the anisotropies in the cortical tension and cortex viscoelasticity. The

magnitude of tension parallel to the AP axis was two-fold lower than tension perpendicular in the anterior domain (Mayer et al., 2010).

A further finding derived from the laser cutting experiments was that mechanical rupture of the actomyosin network was not sufficient to trigger symmetry breaking. This excludes the model that symmetry breaking is solely driven by a mechanical instability. The cortex exhibits viscoelastic properties: upon laser ablation it shortly relaxes but then seals back instead of creating a noncontractile region (Mayer et al., 2010). Furthermore, myosin turns over rapidly, contributing to high cortical dynamicity (Munro et al., 2004). Thus the physical nature of the symmetry breaking event at the cortex still remains to be elucidated.

1.3.6 Symmetry breaking – identity of the centrosomal signal

What is the mechanism of symmetry breaking? Could it be a result of excessive tension or rupture of the acto-myosin network? This scenario is unlikely, as the cortex does not break spontaneously and, additionally, symmetry breaking is spatially localized adjacent to the centrosome (Cowan and Hyman, 2004).

Due to correlation between the time of symmetry breaking and onset of centrosomal microtubule nucleation, several models speculate an importance of microtubules during initiation of polarity. One theory suggested that polymerization of microtubules at the centrosome could trigger activation of the small GTPase Rac that consequently inhibits myosin II activity (Sanders et al., 1999). Due to the onset of centrosomal nucleation of microtubules, a population of microtubules in a region distant to the centrosome may start depolymerizing, consequently activating the small GTPase Rho (Ren, 1999). Rho has previously been shown to control acto-myosin contractions in the worm embryo (Jenkins et al, 2006, Motegi and Sugimoto, 2006, Schonegg and Hyman, 2006). When RhoA is depleted, myosin is not activated. The efficiency of RhoA signaling depends on its activity state, which is determined by presence of GTP or GDP. Regulatory proteins such as GEF contribute to GTPase activation, accelerating dissociation of GDP and binding of GTP. On the other hand, GAPs catalyze GTP hydrolysis, exerting an inhibitory function on the GTPase. The

Mango group has proposed a model in which RhoA is negatively controlled by the RhoGAP CYK-4. Paternally provided CYK-4 would downregulate RhoA activity and consequently suppress acto-myosin network contractions during symmetry breaking. Due to CYK-4 enrichment in proximity of the sperm derived centrosome, CYK-4 could also provide a spatial cue for downregulation of contractility. The authors attribute the RhoGEF role to ECT-2 as its depletion phenocopies inactivation of RhoA, resulting in a failure to activate myosin. Furthermore, ECT-2 colocalizes with myosin II foci.

Polarization of *C. elegans* appears to be a result of multiple, distinct mechanisms working in parallel to ensure proper functioning of this essential process. In the absence of contractility and the consequent cortical flow, embryos still manage to break symmetry, namely to localize PAR-2 onto the cortex. A main player in contractility independent pathway is PAR-2 itself. Recently the Seydoux group (Motegi et al., 2011) reported that in zygotes with severely impaired myosin activity, achieved upon ECT-2 depletion, PAR-2 binds to the cortex in the vicinity of the male pronucleus. The initial breaking of symmetry next to the centrosome could be facilitated by binding of PAR-2 to centrosomal microtubules, which the authors suggest protects PAR-2 from an inhibitory phosphorylation by aPKC. This population of PAR-2 - resistant to aPKC and bound to microtubules - could then access the cortex. Thus association of PAR-2 with microtubules and then PAR-2's interaction with phospholipids on the cortex could promote symmetry breaking. Due to the enrichment of PAR-2 around centrosomes and the neighboring microtubules, symmetry would be broken close to centrosomes. But how does PAR-2 remove PAR-3, PAR-6, and aPKC from the cortex during polarization? Once on the cortex, PAR-2 could antagonize the anterior Par proteins through competition for similar sites on the cortex or by affecting binding of PAR-3 to myosin. An intriguing observation showed that PAR-2 depleted zygotes can still break symmetry, with defects noticeable only later during maintenance of the anterior Par domain. There were no defects in the establishment of polarity upon depletion of PAR-2 (Cuenca et al., 2003).

Currently, much is known about how polarity develops in the *C. elegans* embryo. However, the molecular identity of symmetry breaking cue provided by centrosome is still missing.

1.4 Symmetry breaking and polarity establishment in other systems

1.4.1 Drosophila oocyte

In contrast to *C. elegans* embryo, the *Drosophila* oocyte establishes the AP axis prior to fertilization. Still, the majority of the polarity regulators are homologous to the worm polarization machinery. Initiation of AP axis formation is not completely understood. The symmetry breaking signal originates from follicle cells that surround the oocyte. In response to an as yet unknown yet cue, PAR-1 localizes to the posterior cortex, excluding Bazooka (PAR-3 homologue) from the cortex (Doerflinger et al., 2006; 2010). The complex of the anterior polarity regulators consisting of Bazooka, PAR-6 and aPKC localize to the lateral sides of the oocyte, the anterior. aPKC negatively controls PAR-1 by phosphorylation. Another posterior regulator is LGL (lethal giant larvae). LGL was shown to localize PAR-1 to the posterior cortex and to inhibit aPKC activity (Betschinger et al., 2003, Wirtz-Peitz et al., 2008). Cortical polarity of the *Drosophila* oocyte directs microtubule-dependent distribution of regulatory mRNAs. Localization of mRNA plays a role in axis formation. The minus ends of microtubules, including anchoring and nucleation sites, are enriched at the anterior of the egg with dynein transporting *bicoid* mRNA to the anterior (Bastock and St Johnston, 2008). The localization of posterior determinant - *oskar* mRNA results from a small bias in organization of microtubules. The motion of *oskar* resembles a random walk - it moves along microtubules. Microtubule plus ends extend in all directions but there is small bias towards posterior, tracking of plus ends indicated that around 57 % of tracks have a net posterior vector (Bastock and St Johnston, 2008, Zimyanin et al., 2008). This is

sufficient to localize *oskar* mRNA posteriorly. All in all, the bias in cytoskeleton constitutes symmetry breaking leading to distribution of cytoplasmic determinants.

1.4.2 Mouse embryo

Intrinsic polarity in mammals does not appear to be present during early embryogenesis. The existence of polarity in the oocyte or after fertilization was indeed a highly controversial topic during recent years. Despite previous experimental data that supported that sperm entry site and the position of the polar body specify the AP the axis (Motosugi et al., 2006) or that the position of blastomeres influences the lineage, the concept of prepatterning in mouse blastomeres has been challenged. Lineage divergence in mouse embryo appears to occur from the 8-cell stage, during compaction (Motosugi et al., 2006; Hiiragi and Solter, 2004)(Motosugi et al., 2006)(Motosugi et al., 2006)(Motosugi et al., 2006) Blastocoel formation leads to establishment of the first axis of developmental importance in the embryo: Embryonic-Abembryonic (Em-Ab). The outer layer of blastomeres at the blastocyst stage secretes droplets and vesicles forming fluid, which coalesce, into small extracellular cavities. Distribution of the cavities is completely random. Spatial constraints imposed by ellipsoidal geometry of the zona pellucida relocates the cavities along the long axis where they form blastocoel. Thus the formation of the first embryonic Em-Ab axis is independent of first cleavage plane or sperm entry position (Motosugi et al., 2005) and has a self-organizing character that can be attributed to geometry of the embryo.

1.4.3 Ascidian Egg

The ascidians, also known as sea squirts, present an example of a model organism where sperm entry specifies the AP axis. In the unfertilized egg, arrested in meiosis I, the position of the meiotic spindle and the subsequent site of polar body extrusion are defined as the animal pole; the opposite site is the vegetal pole, with enrichment

of the mitochondria in a region known as myoplasm and a cortical ER domain. Several mRNAs show a polarized distribution, being most concentrated at the vegetal pole (Sardet et al., 2005). However, the animal-vegetal axis does not persist past fertilization. Upon sperm entry, the egg remodels its axis. Sperm entry triggers a dramatic reorganization of the egg- so called ooplasmic segregation- initiated by a calcium wave (Speksnijder et al., 1986) that triggers contraction of the cortical actin towards the vegetal pole. During the second phase of the ooplasmic segregation, most of cellular components from the vegetal pole are transported to what will later become posterior pole. This reorganization is mediated by sperm centrosome nucleated microtubules (Sardet et al., 1989; Roegiers et al., 1995). The posterior pole coincides with sperm entry site, but more accurately with the position of the centrosome.

1.4.4 Nodal Flow

Embryos need to specify a left-right (LR) axis that serves to position internal organs. Specification of this LR asymmetry is achieved using the positional information from previously established AP and DV axes. In vertebrate embryos, a physical process accomplishes symmetry breaking: nodal flow, namely a flow of extra-embryonic fluid with imposed chirality at the midline (a concave region formed during gastrulation). Nodal flow is generated by a specialized population of monocilia. To produce a leftward-directed flow, the monocilia are tilted at an angle of 30-40 degrees towards the posterior, such that their rotatory movement drives a directional flow rather than circular “stirring” (Nonaka et al., 2005; Okada et al., 2005). The mechanism by which nodal flow breaks symmetry is not entirely understood. Nodal flow may transport a signal – fate determinant molecule - towards the left side of the lateral mesoderm plate, which would be transduced into differential expression of *Nodal* at that side of the lateral mesoderm plate. Recent data indicates that upon induction of the nodal flow, concurrent FGF signalling triggers release of nodal vesicular parcels, which are preferentially circulated

toward the left part of the node (Hirokawa et al., 2009). The contents deposited by the nodal vesicular parcels elicit calcium increases, which induce expression of several genes including *Nodal*. The differential expression of *Nodal* leads to asymmetric organogenesis. Symmetry breaking in the case of the nodal flow has a self-organizing character coming from a physical process. It is the flow generated by cilia which transports the determinant and contributes to establishment of the LR axis.

1.5 Centrosome position in polarized cells

The centrosome, despite its small size, fulfills a multitude of important roles in a cell. The best-known role of the centrosome is as an MTOC. In their role as MTOCs, centrosomes are involved in organizing the mitotic spindle, and thus centrosomal defects may lead to chromosomal aberrations that may result in disease. Centrosomes consist of a centriole pair that is surrounded by PCM that contains microtubule nucleators, anchors and several other regulatory proteins. In addition, centrosomes appear to provide platforms for the integration of various signaling cascades or protein regulatory machines such as the proteasome. Thus centrosomes have important functions in many biological processes distinct from microtubule organization.

1.5.1 Asymmetric cell division

The position of the centrosome within the cell is an essential component of establishing and maintaining cell polarity in a variety of contexts. Proliferation of male germline stem cells in *Drosophila melanogaster* relies primarily on centrosome position (Yamashita and Fuller, 2008). The orientation of centrosomes in relation to the stem cell niche determines the developmental fate of a cell, providing an extrinsic cell polarity cue. In male germline stem cells of *D. melanogaster*, centrosomes are required for spindle orientation, which provides an intrinsic cue for deciding whether both daughter cells will inherit stem cell fate (spindle oriented

parallel to niche) or whether one cell will differentiate and the other one will maintain stem cell status (spindle oriented perpendicular) (Yamashita and Fuller, 2008). Perturbations in the cell polarity machinery in *Drosophila*, including several centrosomal proteins, renders cells unresponsive to mechanisms ensuring correct cell proliferation and leads to excessive growth resembling human carcinomas (Caussinus and Gonzalez, 2005).

The importance of centrosome positioning in assigning cell fate was recently documented in *Drosophila* neuroblasts, nervous system progenitors. An asymmetric cell division of the neuroblast gives rise to another self-renewing neuroblast and a ganglion mother cell that undergoes differentiation and divides into a neuron or glia. During interphase, the apically positioned centrosome splits into two. One of the resulting centrosomes terminates incorporating PCM and moves towards the basal cortex. The motile centrosome is the mother centrosome; the daughter one is retained apically (Conduit and Raff, 2010; Januschke et al., 2011; Rebollo et al., 2007). The basis of this centrosome movement is not well understood, but it has been described as „unrestricted movement“ due to randomized motion (Rebollo et al., 2007). Since the motile centriole is not associated with PCM it is unlikely to nucleate microtubules and thus may be able to move more than a centriole associated with microtubules and thus under microtubule-dependent forces. Similar behavior has been reported in HeLa cells, where the centriole not nucleating microtubules undergoes „wild excursions“, traveling substantial distances (Piel et al., 2000). Compared to mother centriole nucleating microtubules, which remains stationary and examples of centrosome motility from other systems, daughter centriole motion is quite the opposite.

1.5.2 Neuronal polarization

Repositioning of the centrosomes has been correlated with important developmental events during the neuronal polarization. In the rodent cortex, cortical interneurons undergoing tangential migration exhibit forward movement of

organelles. The centrosome, together with the Golgi apparatus, was shown to displace forward into the leading edge of these cells. The nucleus translocates towards the front in the second phase in a myosin II driven motion (Bellion et al., 2005). In parallel to centrosome movement in *Drosophila* neuroblasts and in HeLa cells, the moving centrosome may not be associated with microtubules, as the microtubule anchoring protein - ninein - is absent. Relocation of centrosomes to the cell edge was also observed during initial axon formation (Solecki et al., 2006) although the importance of centrosome position in determining axon identity still remains to be clarified. However, position of centrosome and Golgi apparatus correlates with position where the neurite forms and in case of multiple centrosomes in the neuron number of axon corresponds to position and number of centrosomes (de Anda et al., 2005). Therefore centrosome positioning plays an important role in differentiation of a nervous cell.

1.5.3 Migrating Fibroblast

Similar to migrating cortical interneurons, the centrosome in migrating fibroblasts displaces towards the direction of migration, most likely driving polarization of cells as they become migratory. In a fibroblast initiating migration, centrosome relocation relative to the nucleus was thought to be the first event of the process. However, careful analysis of the translocation process revealed that the nucleus moves rearward while the centrosome remains stationary (GOMES and GUNDERSEN, 2006). Activation of Cdc42 and consequent phosphorylation of myosin leads to retrograde flow of actin which drives relocation of the nucleus. Dynamic microtubules tethered by dynein exert pulling forces to maintain the centrosome at the front while the nucleus is being translocated. What is the function of centrosome relocation? The function may be to position the microtubule array together with the Golgi apparatus toward the leading edge to facilitate membrane trafficking and secretion.

1.5.4 T Lymphocyte

Cytotoxic T lymphocytes release lytic granules to kill tumorigenic cells. This process is mediated through a formation of an immunological synapse to connect the two cells. The centrosome was reported to translocate to the synapse and contact the plasma membrane, specifying the position where granule secretion occurs. The site where the lymphocyte attaches to the cell which will be lysed, is demarcated by accumulation of actin (Ryser and Vassalli, 1982). Actin retracts away from the synapse in the form of a ring, simultaneously moving the microtubule plus ends with the actin. Furthermore, dynein – minus-end directed microtubules motor - was shown to localize to the clear zone (Quann et al., 2009). The centrosome is subsequently pulled by dynein towards the central supramolecular activation cluster (Stinchcombe et al., 2006). The centrosome docks at the plasma membrane.

In my thesis, I wanted to understand how the centrosome supplies spatial information information to mediate acto-myosin downregulation during polarity establishment. Is centrosome-cortex contact essential for symmetry breaking? And how does the centrosome find the cortex?

1.6 The role of sperm contributed mitochondria in polarity

Since sperm contributed centriole has an essential role during the polarization of the zygote, I was interested in examining whether other sperm components are present in the embryo and are significant for polarization. Spermatogenesis in *C. elegans* reduces the number of components in the male germ cells to mitochondria, membranous organelles, cytoplasm and plasma membrane. I chose to concentrate on the mitochondria due to their role in cell signaling in other systems.

1.6.1 Mitochondria and mitochondrial DNA

Mitochondria are well known as cellular powerhouses, supplying cells with ATP. Beyond the energetic function, mitochondria participate in a multitude of other processes such as

calcium homeostasis, heat generation and apoptosis. Evolutionary theories claim that mitochondria may have contributed to the birth of multicellularity (Emelyanov, 2001) Mitochondria appear to be a product of endosymbiosis between methanogens and alpha-bacteria (Gupta, 2003). The remnant of this merge and the subsequent billions of years of evolution is mitochondrial DNA (mtDNA), which encodes only a few genes that are completely essential for mitochondrial function. In humans there is 13, in *C. elegans* only 12 genes encoded in mitochondria (Tsang and Lemire, 2002). The mtDNA genes are largely subunits of respiratory chain. The majority of mitochondrial-resident proteins are encoded by genes, which have been transferred into the nuclear genome.

1.6.2 Significance of uniparental inheritance

Most sexually reproducing species ensure transmission of mitochondria from only one parent – so-called uniparental transmission (Hoekstra, 2000). The strictly maternal inheritance of mitochondria is more a well-accepted dogma than a thoroughly proven hypothesis. What is the significance of selective mitochondria inheritance from one parent solely?

Evolutionary biologists believe that existence of nonautosomal DNA in the cytoplasm, such as mitochondrial DNA, arises an intracellular population genetics issue (Cosmides and Tooby, 1981). The mtDNA exists in multiple, frequently diverse copies within one cell. Its division is not subject to the surveillance control of the cell. Thus, a deleterious selfish mutation of mtDNA could theoretically gain advantage over the rest of mtDNA population and divide infinitely at the cost of its host. Uniparental – most commonly maternal – inheritance contributes to minimizing spread of such harmful cytoplasmic DNA. Uniparental transmission ensures that only daughters – half of population – would inherit a “selfish” mitochondrial mutation (CUMMINS, 2004).

The significance of uniparental inheritance may also concern the bioenergetical consequences of assembling protein complexes from more than one genome-template (DNA). Mitochondrial and nuclear genes aim for a perfect synchrony in assembled complexes. Variants lowering respiration efficiency disappear immediately due to natural selection, as they would not satisfy the energetic needs of a cell (CUMMINS, 2004). Female germline selects for oocytes that have the energetically fittest mitochondria.

Mouse oocytes with severe defects in oxidative phosphorylation are selectively eliminated (Fan et al., 2008). On the other hand, male germ cells due to small size contain few mitochondria. Paternal mitochondria were long believed to be eliminated due to potential oxidative damage they accumulate during fertilization (Sutovsky et al., 2000).

1.6.3 Mitochondrial heteroplasmy

Heteroplasmy in mitochondria stands for multiple mitochondrial genotypes within one cell. Mitochondrial heteroplasmy may be generated by mitochondrial inheritance from two parents (CUMMINS, 2004). However, heteroplasmy within a cell could also arise due to mutations in mtDNA and its retention. Mitochondrial DNA mutates 20-50 times faster than nuclear DNA due to the presence of reactive species within mitochondria (Wallace, 2010). It remains interesting to investigate the effects of heteroplasmy within one organism. Recently, one patient suffering from mitochondrial disease was reported to show mitochondrial heterogeneity. Analysis showed disparity in the mtDNA sequence, paternally contributed mitochondria were present in his defective muscle tissue (Kraytsberg et al., 2004). It is not known whether the maternal and paternal mitochondria coexisted or whether they recombined with each other.

Originally believed to be rare in healthy organisms, mitochondrial heteroplasmy appears to be more frequent than once expected (Ivanov et al., 1996; Li et al., 2010; Jazin et al., 1996). Digital sequencing of mtDNA genomes revealed widespread mtDNA heterogeneity in normal human cell (He et al., 2010). Above-mentioned studies investigated mitochondria in somatic cells. So far, there is no direct study of whether heterogeneous mitochondrial populations exist in the germ cells.

1.6.4 Fate of paternal mitochondria in *C. elegans* embryo

Sperm mitochondria are present in the *C. elegans* embryo after fertilization. Recent data suggests that the paternal mitochondria are degraded soon after fertilization through the autophagy machinery (Rawi et al., 2011; Sato and Sato, 2011). These studies leave open the question of whether degradation occurs throughout the embryo or instead if it is restricted to certain lineages – for instance, the germline – as small numbers of

mitochondria could still be detected very late in embryogenesis. Furthermore, it remains to be elucidated if paternal mitochondria play any role during development or if they are immediately targeted for degradation. I was interested in understanding two aspects of paternal mitochondria in one-cell *C. elegans* embryos: first, if paternal mitochondria have a role in cell polarity, and second, if and how paternal mitochondria are excluded specifically from the germline.

2. Materials and Methods

2.1 Worm strains and imaging

Worm maintenance was done at 16°C according to standard *C. elegans* methods (Stiernagle, 2006) L4 larvae were shifted to 25°C 20-24 hrs prior to imaging. Strains used in the study: CB4108 (*fog-2(q71)*) (McCarter et al., 1999), DA2123 (*LGG-1::GFP::ROL-6(su1006)*) (Meléndez et al., 2003), JH1327 (*PIE-1::GFP::ROL-6(axEx73)*) (Reese et al., 2000)(McCarter et al., 1999)(McCarter et al., 1999)(McCarter et al., 1999), TH42 (Pelletier et al., 2004), UE33 (*mCH::H2B;NMY-2::GFP;GFP::SPD-2*, cross between RW10226, JJ1473, and TH42), and UE42 (*mCH::PAR-2;GFP::SPD-2*, created by crossing JH2759 and TH42). To preserve normal embryo geometry, embryos were mounted on poly-L-lysine coated coverslips attached gently to the slide. Embryo dissection was a glass coverslips double coated with 15 µl of 0.01% poly-L-lysine in 5 µL of EGM (Edgar, 1995). One worm was dissected on slide per coverslip. The coverslip was suspended from a glass slide with 2 strips of double-sided tape, about 2 cm apart, creating space for specimen. In order to apply compression, embryos were mounted on agarose pads, following standard protocols. Embryos were squeezed to ~24 µm in the z-axis, compared to ~30 µm diameter in uncompressed samples. In squeezed embryos with large centrosome- cortex distances [γ -tubulin(RNAi)], symmetry occurring from „top“ or „bottom“ of the embryo was observed more frequently. Such samples were not included in the analysis. Only embryos where symmetry breaking occurs in a similar z-axis and within the middle third of the embryo were analyzed. This measurement also forms the basis of our error estimate of 8 µm. Centrosome imaging was performed on a Zeiss Axiovert equipped with a Perkin Elmer spinning disk using a 63X lens and 2X binning. Images in GFP channel were acquired at 3 frames per second; z-position was manually adjusted to keep centrosome in focus. Furthermore, brightfield reference images were acquired every 10 seconds. A subset of centrosome imaging in wild type and latrunculin-treated embryos and all *GFP::SPD-2; mCH::PAR-2* embryos was performed using a wide-field Delta Vision microscope (Applied Precision) with a 60X lens and 2x binning. z-stacks of 0.5 µm spacing were acquired at intervals of 10 seconds; a reference image in brightfield was collected from the midplane of the stack. Myosin

and histone imaging was performed on spinning disk. Z-stack with spacing of 1 μm was acquired in GFP and mCherry channels to include majority of the embryo. Stacks were acquired constantly, with 7-9 seconds required per stack.

2.2 Image processing and data analysis

The data analysis of centrosome data was performed in MatLab (R2010a, MathWorks), ImageJ64 and FiJi. Immunofluorescence images were processed in SoftWorx (Applied Precision). All graphs were created in Prism (v5, GraphPad Software).

Time “0” assignment. To provide polarity-independent time standardization, time “0” was assigned according to completion of female meiosis II. The assignment of meiosis end II were the formation of a mature male pronucleus, telophase of meiosis II and the second polar body extrusion. Those events consistently correlate with the male pronucleus reaching 3 μm diameter. Pronuclear size is the only quantitative aspect of this particular developmental stage, thus I used male pronuclear size of 3 μm to assign completion of meiosis II.

2.2.1 Assignemt of timeSB.

The time of symmetry breaking was assigned according to cessation in the contractility of the cortex or clearing of NMY-2 GFP from the cortex. In DICimages, I looked for formation of a small cortical protrusion resembling a membrane bleb. The retraction of this protrusion correlated with the onset of non-contractile domain on the cortex. In the case of NMY-2::GFP I relied on the change in (loss of) NMY-2 foci from the cortex around the origin of the non-contractile domain, and the accompanying DIC images.

2.2.2 Centrosome tracking.

Raw images were first processed to remove blur. This was done by subtracting image filtered with low-pass Gaussian filter with kernel equal to 1, from high-pass Gaussian filter with kernel 30. The obtained image was normalized and thresholded. Position of centrosome was detected corresponding to the highest intensity. Trajectory was constructed by assembling detected positions of centrosome only when consecutive positions were less than 8 pixels apart, dismissing all the noise pixels that did not correspond to the actual path travelled by centrosome.

2.2.3 Cortex detection

The outline of the embryo corresponding to the edge of cytoplasmic fluorescence was automatically detected for each frame in the timelapse. Images were processed with Gaussian filtering and thresholded using graythresh function. Next the binary image was smoothed and single noise pixels were removed. The cortex mask was created using the edge function (MatLab).

2.2.4 Closest cortex.

Closest point from centrosome to the cortex was calculated for each frame when centrosome was detected.

2.2.5 Symmetry breaking site.

Polarity site was assigned as an approximate spot on the cortex where noncontractile domain could first be seen (either using reference brightfield frame or gfp channel where nmy-2 signal was acquired). Distance to the polarity site was measured by calculating distance from centrosome to the polarity site at each timepoint.

2.2.6 Velocity

Positions of the centrosome were smoothed with the running average of window size 10. Next a vector containing positions of centrosome every 5 sec apart was created and velocity was calculated.

2.2.7 Frequency histogram

Velocities calculated for each embryo of given treatment until symmetry breaking were pooled into one set and then sorted. Histogram was produced using sorted values and bin equal 50. The histograms were normalized to 1.

2.2.8 Net Displacement

Distance travelled towards the cortex between specified time points, subtracting the distance to cortex of the second position.

2.2.9 Color-plotted trajectory

Time vector of length 900 units was created; each unit represents one second and is given one of the consecutive colors from colormap 'jet'. Position of the centrosome and its corresponding closest cortex are colored in the same shade.

2.2.10 Distance to cortex in NMY-2::GFP expressing movies

Distance to the closest cortex was calculated in a frame from Z-stack where centrosome

could be observed.

2.2.11 Kymograph

Projection of the z-stack of maximum intensity was made for each timepoint (encompassing three frames per stack with one μm spacing). Next line corresponding to the outline of the embryo sampled every 10 units was obtained from the frame where symmetry breaking occurs. Integrated intensity along line marked by the outline of the embryo of width 10 was measured. The kymograph was obtained for each timepoint and stored into a matrix where x-axis corresponds to time in seconds and y-axis represents integrated intensity. Embryos used for kymograph were mounted on agar pads with slight compression.

2.2.12 PIV

Movement analysis of yolk granules and lipid droplets in the cytoplasm was performed using brightfield images quantified with PIV algorithm in Matlab as previously described (Mayer et al., 2010).

2.2.13 Bead Tracking

Bead tracking was performed using particle tracking algorithm downloaded from The Matlab Tracking Repository (<http://physics.georgetown.edu/matlab/code.html>), no gaps in the trajectory were allowed and the maximum distance that bead could be apart between two consecutive frames was 8 pixels.

2.3 RNAi

L4 worms were placed on RNAi plates (as previously described) and grown at 25 C for 25-30 hrs.

2.4 Immunofluorescence

Immunofluorescence was performed as previously described using SAS-4 (1:200, Rabbit), DM1a (1:300, Mouse) and DAPI (10 $\mu\text{g}/\text{ml}$). Widefield images were taken at the Delta Vision. Deconvolved images were projected in the GFP channel (5 frames).

2.4 Bead Injection

Fluorescent carboxylate modified red fluorescent microspheres of 0.1 μm size (FluoreSperes, Molecular Probes) were injected into the gonad of young N2 adults. After injection worms were recovered into a 50 μL of S-basal on standard NGM+OP50 plate and incubated at 20 degrees for about 4 hrs. Embryos were dissected and observed in TRITC channel on Delta Vision. Z-stack with 1 μm spacing was taken to include most of the embryo. Imaging was done at a rate of 5 sec per stack. A reference frame in brightfield was collected from the midplane after each stack was acquired.

2.6 Drug treatment

Chemical agents were added to the EGM buffer in which worms were dissected at the following concentrations: latrunculin A, 0.6 mM; nocadazole, 2-3.25 μM ; taxol, 10 mM. Drug could enter the embryos because of eggshell permeability during meiosis II (Rappleye et al., 2003). Efficiency of latrunculin treatment was judged by defects in polarity establishment and lack of cortical flows.

2.7 Cellular markers

Lysotracker Green DND-26, 1 mM in DMSO, JC-1, 2 mM in DMSO, TMRE, 1mM in DMSO, Mitotracker Green FM, 1mM in DMSO, Mitotracker Red CMXRos 1mM in DMSO. All from Molecular Probes.

2.8 Matings

5 μL of dye was diluted in 25 μL of water and pipetted on a plate with worms. After overnight incubation at 16 C in a dark container, worms were placed on a clean plate for about half an hour.

Next, worms were put on a mating plate.

Matings were done overnight at 25 C. Mating plates consisted of NGM plates with two drops of OP50 (50 μL).

3. Results

3.1 Analysis of wildtype centrosome movement

Previously the centrosome has been reported to be at the cortex during polarity establishment, however little is known about the dynamics of this process. It remains unknown, for instance, whether the centrosome is at the cortex prior to symmetry breaking or instead if it moves there during the polarization process. To get insights into this question, I first needed to find conditions that would allow for visualization of one-cell *C. elegans* embryos prior to symmetry breaking by time-lapse fluorescence microscopy. So far, such imaging has not been performed due to the high frequency of embryo lethality caused by the sensitivity of meiotic embryos to the external environment and mechanical pressure. Thus, I attempted to find experimental conditions that would preserve embryo geometry and provide favorable osmotic conditions so that viability would be maintained. There were two important factors that affected the success of time-lapse imaging of meiotic embryos, namely the incubation medium and the method of mounting. Embryonic – or Edgar’s - Growth Medium (EGM) allows for reliable maintenance of zygotes and isolated blastomeres during early stages of development (Edgar, 1995). Accordingly, EGM provided a well-balanced medium for maintenance of early embryos. Further, a hanging drop mounting technique exerts no physical compression on the sample. Hanging drop preparation permitted imaging without compromising embryo viability (fig. 1).

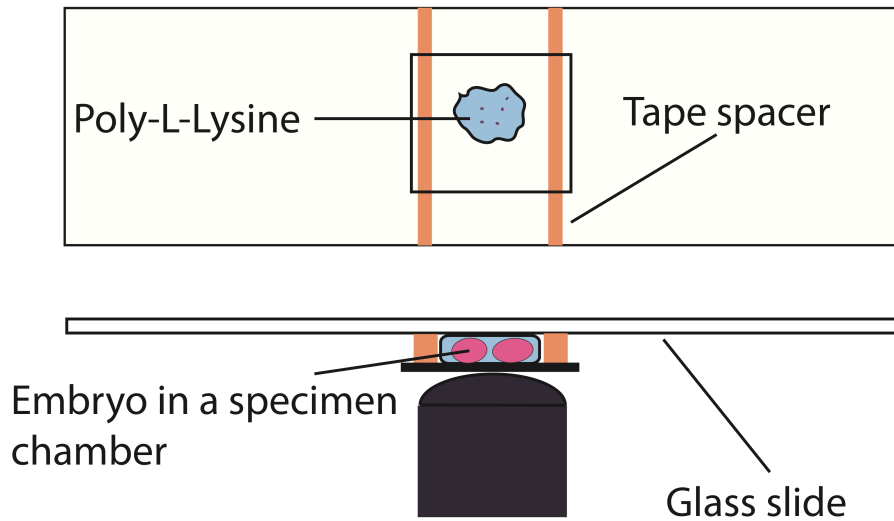


Figure 1. Scheme for hanging drop mounting method. The drop of buffer is placed on double Poly-L-Lysine coated slide. Tape strips create a specimen chamber where embryo geometry can be preserved.

Meiotic embryos do not have a completely formed eggshell and thus are susceptible to geometric deformation. When mounted on an agar pad, such embryos may be flattened to the point that they die. This can be observed readily in bright-field imaging as “embryo freezing”, where random motion of the cytoplasmic granule ceases, the embryo shrinks and does not proceed in the cell cycle. Another sign of unhealthy embryos appeared to be spinning of the cytoplasm in a washing machine type of rotation. On the other hand, zygotes visualized in a hanging drop and EGM look healthy: cytoplasmic granules move but do not show bulk rotational motion, and there is a space between the embryo edge and eggshell outline.

Having established conditions that maintained embryo viability, I attempted to gain insights into cortex-centrosome communication and the role of centrosome movement at the time polarity onset. To achieve this goal I performed a time-lapse analysis of centrosome motility preceding symmetry breaking using fluorescence microscopy of living *C. elegans* embryos. SPD-2::GFP is an established marker for visualizing centrosomes (Pelletier et al., 2004) and can be used to quantitatively analyze position of

centrosomes in relation to the cortex. Detection of the cortex is possible in SPD-2::GFP expressing embryos from the cytoplasmic fluorescence which demarcates the boundary of the embryo – how I define the cortex (fig 2).

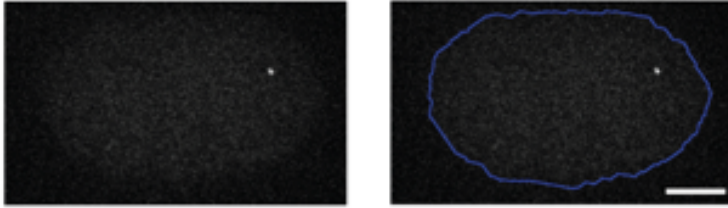


Figure 2. Detection of the cortex from the cytoplasmic fluorescence, picture on the left represent a GFP image with centrosome visible being the brightest spot. Right shows the GFP image overlaid with cortex outline extraction (blue line).

The analysis of centrosome movement is executed in 2D, due to isotropy of the movement in x and y dimension ($\langle x^2 \rangle = \langle y^2 \rangle$) precluding the need for 3D tracking of centrosome. I further investigated centrosome motility by xyz imaging and likewise found no differential contribution of the third dimension.

3.2 Assignment of symmetry breaking

Reproducible standardization of developmental time is important to make comparisons among samples. The time standard should be polarity-independent, so that embryos with compromised polarity can still be assessed temporally. In my analysis, time “0” refers to the end of meiosis II, which can be judged from the size of the male pronucleus (corresponding to 3 μm in diameter). Symmetry breaking occurs about 2 minutes after this cell cycle event (Cowan and Hyman, 2004).

Symmetry breaking could be reproducibly assigned according to cessation of cortical contractility observed in brightfield images or by retraction of myosin foci in embryos expressing NMY-2::GFP (fig. 3). Symmetry breaking is followed by significant cytoskeleton reorganizations such as onset of cortical and cytoplasmic flows. Thus, watching the timelapse backwards until no signs of spatially coherent reorganization were observed facilitates assignment of the symmetry breaking time.

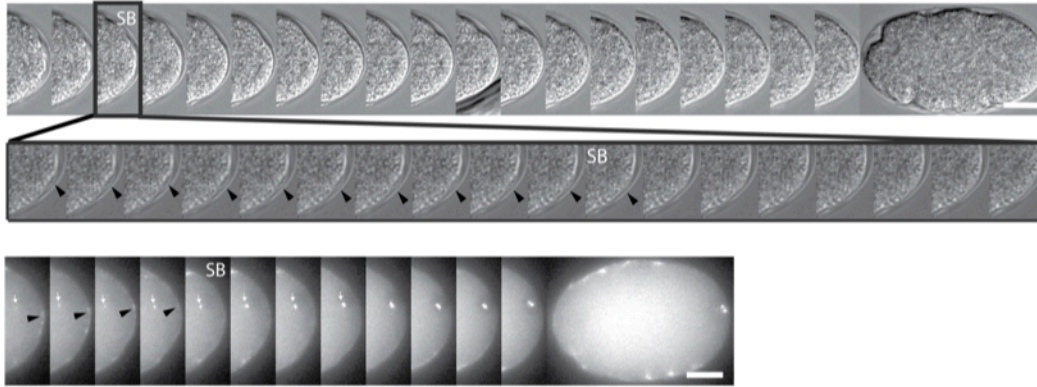


Figure 3. Symmetry Breaking assignment. **(Top)** DIC image. Symmetry breaking is defined according to progressive cessation of cortical contractions. Immediately prior to symmetry breaking, there is a cortical protrusion (black arrowhead in the blow-up) that disappears as the non-contractile domain is established. Symmetry breaking is defined as the time of the disappearance of this protrusion. **(Bottom)** In GFP::SPD-2; NMY-2::GFP images, symmetry breaking was defined by progressive loss of myosin foci and cessation of cortical contractions. White arrows indicate the centrosome signal; black arrowhead points to cortical NMY-2 that disappears, defining symmetry breaking. In both time series, “SB” indicates the frame assigned as symmetry breaking. Scale bars, 10 μ m.

3.3 Random walk of centrosomes

Using the imaging conditions described above I set out to analyze my timelapse images of centrosome position relative to the cortex during symmetry breaking. Since manual tracking of the centrosome and the corresponding closest spot on the cortex was inefficient and highly biased, I developed an automated tracking protocol in MatLab. I first applied image filtering to detect the centrosome according to the highest intensity pixels in the image. The detected list of points was next assembled into a trajectory travelled by the centrosome, with the assumption that the distance travelled by centrosomes between two consecutive frames was not large. Thus, only the brightest points in the vicinity of each other at subsequent time points were used. Further, there is only one centrosome visible in pre-polarity embryos, so that the brightest pixel within the embryo corresponds to the centrosome. It was necessary to extract the entire cortex coordinates at each timepoint as the embryo changes its shape over time. To achieve this I applied an edge function to a binary image corresponding to the embryo based on cytoplasmic GFP::SPD-2. This function takes advantage of high fluctuation in the frequency domain, which occurs when edges are present in the image. To verify that the

described image processing procedure worked, I compared results obtained in MatLab to manual tracking. The results were in a very good agreement. Furthermore, a trajectory assembled in Matlab closely resembled a projection of the entire timelapse, in which the path travelled by the centrosome can be seen clearly (fig. 4bc).

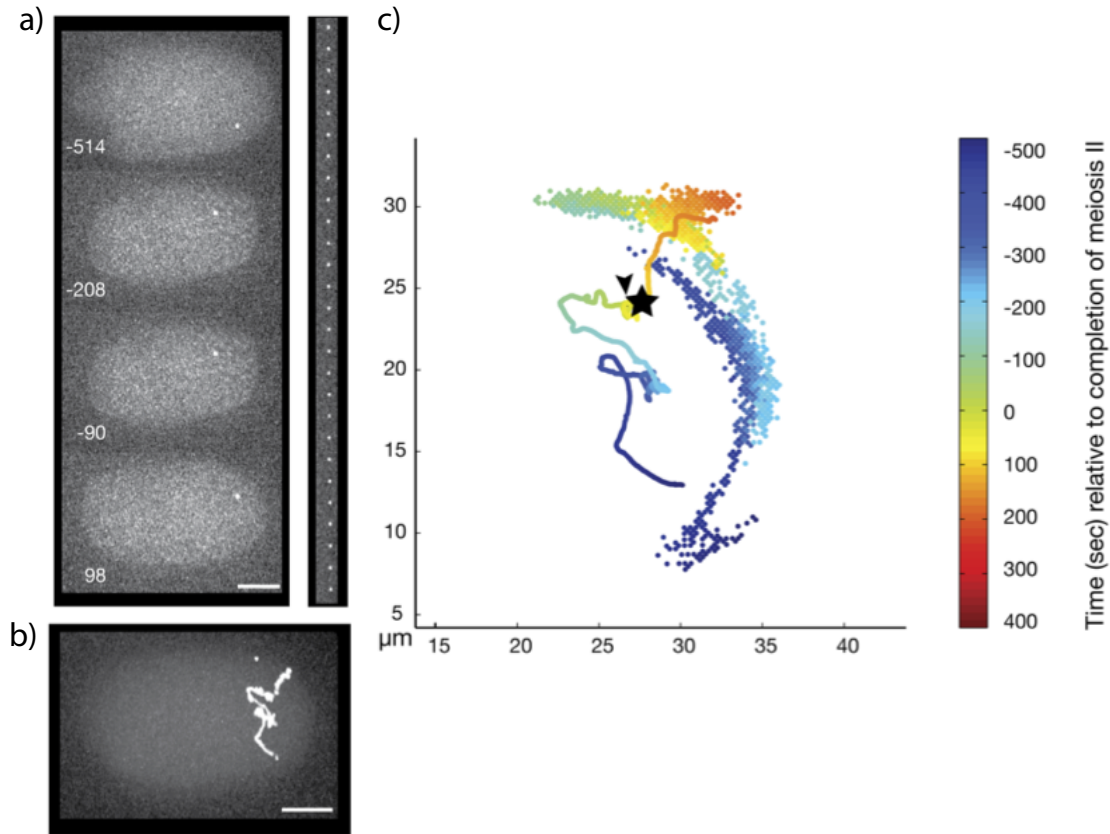


Figure 4. Analysis of GFP::SPD-2 timelapse. **(a)** Time-lapse images of GFP::SPD-2 labeled centrosome in one-cell *C. elegans* embryos before symmetry breaking. Left sequence: embryo view; right sequence: centrosome detail at actual temporal resolution (3 frames per second). Time is indicated relative to completion of meiosis II (time “0”). **(b)** Projection of centrosome images from the time-lapse series shown. **(c)** Centrosome position (linear track) and closest cortical point (dots) extracted from time-lapse series in **a,b**. Colors indicate time scale (blue: -500, red: 400). YX axes indicate absolute position. Centrosome position at time “0” is indicated by an arrowhead. Centrosome position at time of symmetry breaking is indicated by a star. Scale bars, 10 μm .

Centrosome movement was very dynamic, and when imaged at the rate of 3 frames per second, manual adjustment of the Z-axis position was necessary to account for upward

and downward movement. However, only embryos where the centrosome was within the middle planes were analyzed. Centrosomes that moved to the top or bottom of the egg were excluded from analysis, as their closest cortex position is difficult to assign and may introduce error to the analysis.

To characterize the movement of the centrosome, I measured several motion characteristics, such as velocity, turning angles, step size or size of the trajectory. Instantaneous velocity varied a lot, ranging from 0.01 to a maximal velocity of 0.45 μm per second (fig. 5b). The peaks of high velocity could be observed for no more than a few seconds. It was difficult to determine if periods of accelerated motion in different embryos all occurred during a particular cell cycle stage or instead if these were random phases of fast motion. Measurement the consecutive angles of centrosome trajectories revealed no directionality of the movement (fig. 5a).

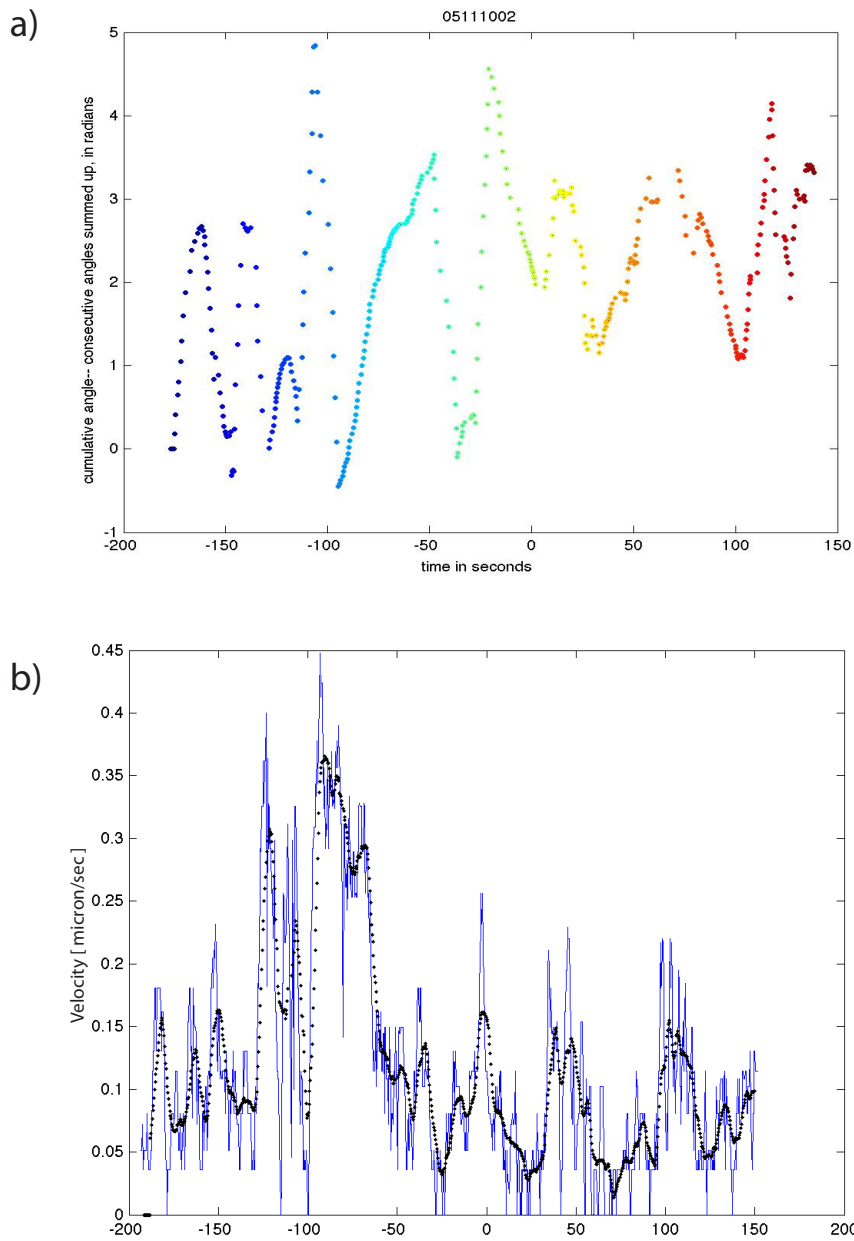


Figure 5. Analysis centrosome movement: turning and velocity **(a)** Trajectory of a centrosome is presented as summation of consecutive angles over time. Centrosome shows high frequency of changes in directionality. **(b)** Instantaneous velocity (blue) and average velocity (black, calculated with running average of window 20). In both graphs time “0” is represented as “0” and symmetry breaking occurs at 90 sec.

Centrosomes do not follow a straight path, but rather may move for several seconds in a straight path and then dwell in one position, turning frequently.

Pooled measurements of the step size exhibited by centrosomes in wild type embryos resembled a half normal distribution skewed at the values close to zero. The skewed distribution around 0 may be because it is impossible to visualize centrosome step sizes smaller than the limit of spatial resolution of the microscope. The average step size measured in the SPD-2::GFP strain fell in the range of $0.1 \mu\text{m}$ (fig. 6a). Centrosomes have the ability to travel large distances, in some cases over $50 \mu\text{m}$ during 10 minutes.

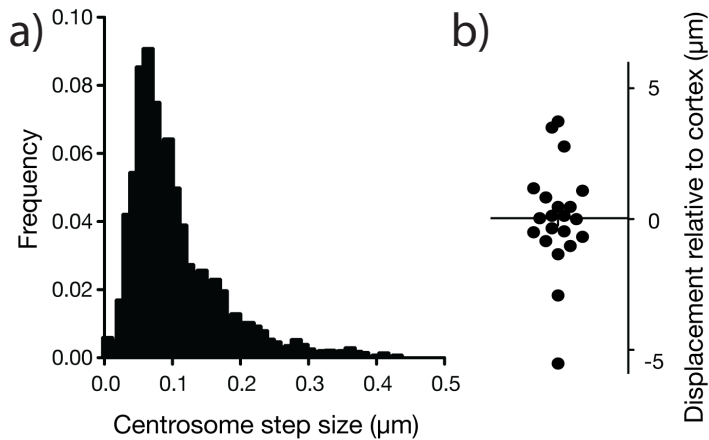


Figure 6. Analysis of wildtype motion. **(a)** Frequency histogram of centrosome step sizes ($n=13$). **(b)** Net centrosome displacement relative to the cortex before symmetry breaking ($-200 - 0$).

Altogether, the motion of the centrosome resembles a random walk, instantaneously losing its directional memory. Furthermore, centrosome does not return to its initial position from the onset of tracking. The exception to purely random motion was the preference of centrosomes to stay close to the embryo periphery rather than to explore the middle of the egg.

3.4 Centrosome-cortex distance: closest cortex

To measure the tendency of centrosome to stay in vicinity of the cortex I determined the distance of centrosomes to the closest point on the cortex over time. Centrosomes and the cortex were detected automatically at each timepoint of the timelapse series. Next, the

point on the cortex closest to the centrosome was found by comparing all possible centrosome-cortex distances and choosing the minimal distance. Such a measurement allowed me to assess how close to the cortex the centrosome was before symmetry breaking. This analysis showed that the distance of the centrosome to the cortex varied from embryo to embryo (Fig 7).

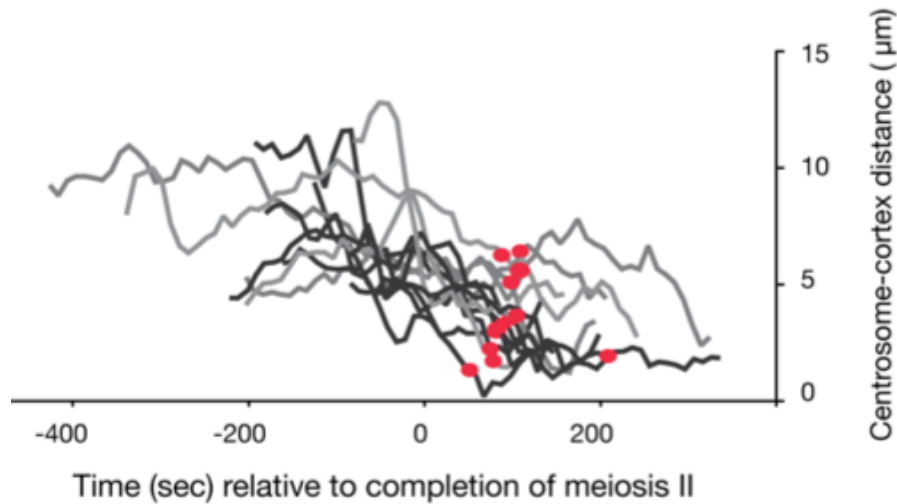


Figure 7. Centrosome-to-cortex distance. The distance from the centrosome to the symmetry breaking site over time. Each line represents one centrosome. Centrosome-cortex distances at the time of symmetry breaking is indicated with red dots.

Centrosomes were on the average 5 µm away from the cortex before symmetry breaking (fig. 8b). Considering egg dimensions, particularly the width of the embryo, the maximum achievable distance is around 14-15 µm. Thus, centrosomes appear to be cortically constrained. Centrosomes were observed moving away from the cortex and then later approaching the cortex at a different spot once symmetry was broken (fig. 7). Analysis of centrosome trajectories indicated that centrosomes did not return to the point of origin. However, my data did not include time right after fertilization so I cannot rule out entirely that centrosomes may respond to spatial information provided by fertilization. Overall, centrosomes are not immobile within the embryo and the pattern of centrosome movement differs substantially between embryos, indicating high heterogeneity – or randomness - of the movement.

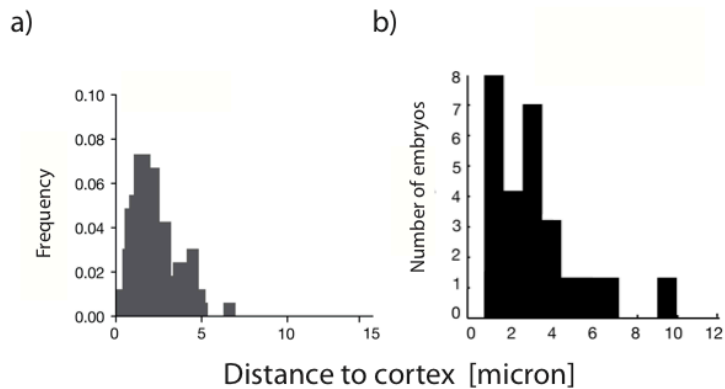


Figure 8. Distance to cortex analysis (a) Frequency histogram of cumulative distances to cortex before symmetry breaking measured every 5 sec. (b) Distance of centrosome to the cortex at the time of symmetry breaking. On y-axis is the number of embryos for each bin.

3.5 Centrosome-cortex distance: polarity site

Is the point to which centrosome moves during symmetry breaking a predetermined site? To investigate this question further, I measured centrosome position relative to the point on the cortex where symmetry is broken, called the polarity site. The distance of the centrosome to the polarity site was measured at each timepoint. This analysis revealed that the distance to the polarity site over time was highly variable instead of decreasing constantly over time, as might be expected for prior spatial information for centrosome movement (fig 9). Such behavior argues that centrosome is not traveling towards a predetermined spot but rather moves in a stochastic way.

Comparison of the closest cortex and polarity site graph for a given embryo showed that the two graphs did not overlap before symmetry breaking, suggesting that only at the time of symmetry breaking does the centrosome exhibit a spatial relationship to the symmetry breaking site (fig 9a).

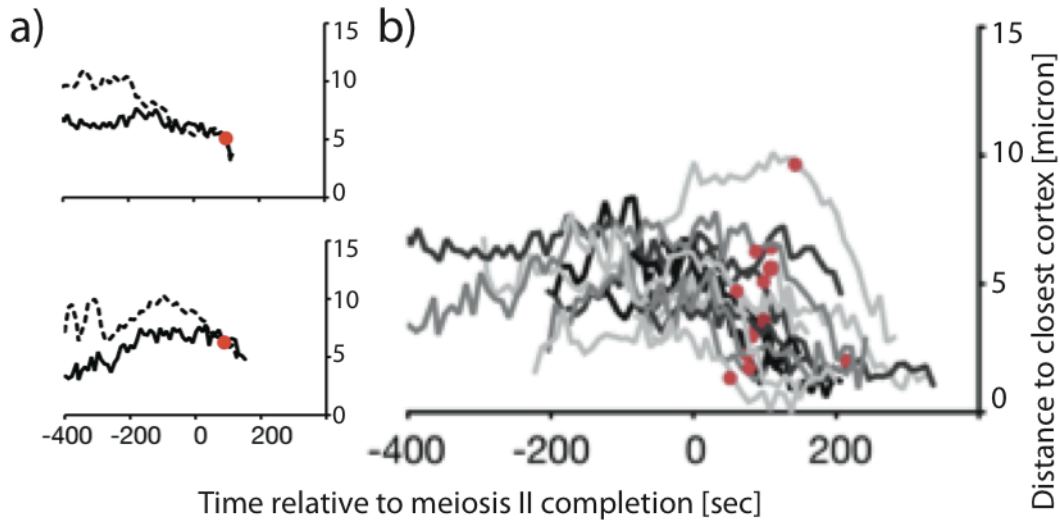


Figure 9. Distance to symmetry breaking site. **(a)** Centrosome distance to symmetry breaking site (dotted line) and closest cortex (solid line). Two individual centrosomes from representative wild type embryos are shown. Distance at of symmetry breaking is indicated with a red dot. **(b)** The distance from centrosomes to the site of symmetry breaking on the cortex over time. Each line represents one centrosome. Centrosome-cortex distance at the time of symmetry breaking indicated with a red dot.

3.6 Centrosome-cortex distance at symmetry breaking

In wild type embryos, centrosomes were not at the cortex (within 2 μm) at the time of symmetry breaking in several embryos. The frequency distribution of the distances at the time of symmetry breaking showed a range from 2 to 7 μm (fig. 8b).

Once symmetry was broken, however, centrosomes approached the cortex (fig 7). The centrosome movement after symmetry breaking was direct: the path taken towards the cortex had high straightness and the result was close centrosome-cortex juxtaposition. After centrosomes achieved close contact with the cortex, a process of posteriorization occurred, in which the entire embryo rotates within the eggshell so that centrosomes become positioned along the long axis of the eggshell. Comparison of displacement towards the closest cortex before and after symmetry breaking indicates that centrosome displaces towards cortex in a highly directional manner after symmetry breaking.

3.7 Centrosome movement in centrifuged embryos

Since centrosome in the wild type embryos did not exhibit large net movements away from their starting points, I decided to further investigate the question of a predetermined polarity site by more dramatic displacement of the centrosome away from its initial position. If centrosomes move to a predetermined point on the cortex, then physical displacement of centrosomes away from the potential „polarity site“ should perturb polarity establishment because of deficient centrosome-cortex communication. To address this question I briefly centrifuged worms prior to dissection. The centrifuged embryos were viable and could establish polarity and proceed with cell cycle assignment of the time from brightfield is very difficult in the centrifuged embryo). The centrifuged cytoplasm had a layered appearance suggesting that centrifugation was sufficient to segregate lipid droplets and yolk granules, which have different densities. Analysis of centrosomes in centrifuged embryos showed that, despite mechanical displacement, the centrosome moved towards the closest cortex shortly after meiosis II was completed (fig. 10). Centrosomes were not observed to travel significant distances, for instance to a distant origin. Centrifugation displaced all organelles, which did not allow for any spatial control. To perform a more accurate manipulation of centrosome position, I used an optical trap to try to displace centrosomes. Unfortunately, the trap strength was not sufficient to hold yolk granules in the embryo. I thus chose not to pursue physical manipulation of centrosome position any further but instead sought genetic means of altering centrosome position relative to the cortex (section 3.13-3.14).

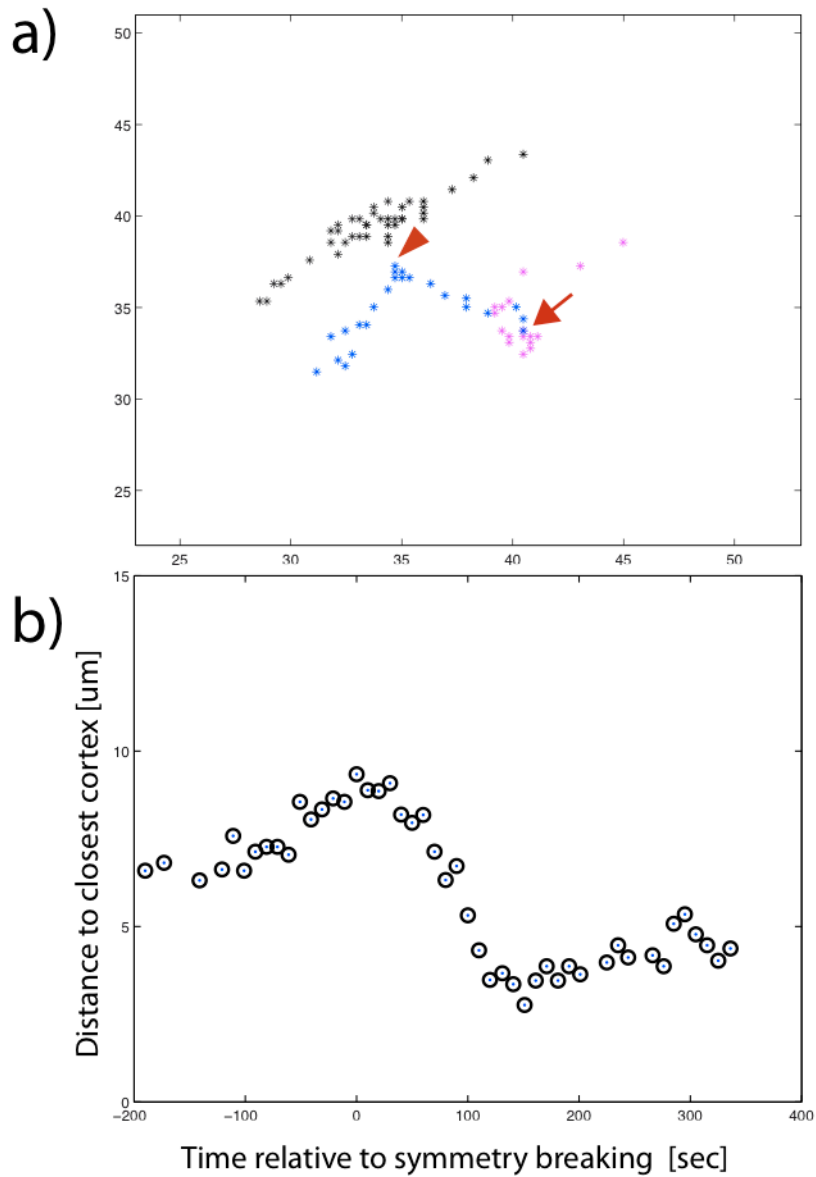


Figure 10. Centrosome in a centrifuged embryo reaches the cortex. **(a)** Path travelled by the centrosome in a centrifuged embryo (pink is prior to symmetry breaking, blue is after symmetry breaking. Corresponding closest cortex is plotted (black prior to symmetry breaking, red after symmetry breaking, red arrow indicates symmetry breaking). Red arrowhead points to centrosome being close to the cortex. **(b)** Distance to closest cortex over time. Time “0” here corresponds to symmetry breaking (not to completion of meiosis II).

3.8 Cytoplasmic flow: endogenous granules

As my results indicated that centrosome position was constrained near the cortex prior to symmetry breaking, I wanted to determine how this cortical bias was transmitted to centrosomes. Symmetry breaking induces cytoplasmic flow towards the cortex. I was curious if there were any cytoplasmic flows directed towards the cortex prior to symmetry breaking that might maintain centrosomes close to the cortex. To address this question I performed Particle Image Velocimetry (PIV). This computational method measures flow directionality. I followed the movement of the cytoplasmic granules visible in DIC images. No directional, coherent flows of yolk granules could be detected prior to symmetry breaking, contrary to after symmetry breaking, when cytoplasmic and cortical flow could be detected by PIV analysis (fig. 11).

The coherent flow could be observed in PIV analyzed images as a high concentration of arrows pointing in the same direction. Conversely, lack of flow was indicated by a lack of arrows.

3.9 Cytoplasmic flow: beads

To further substantiate the result from PIV analysis, I wanted to obtain a higher resolution view of centrosome-sized single particles in the embryo during symmetry breaking. To accomplish this goal, I injected fluorescent beads of $0.1 \mu\text{m}$ diameter into the gonad and recorded time-lapse images of embryos that had incorporated beads in the cytoplasm. The fluorescent beads are assumed to be inert tracers of cytoplasmic motion and should not be incorporated into endocytotic vesicles. I followed the pattern of bead movement prior to and after symmetry breaking. I used Matlab to find the bead position according the areas of high pixel intensity above threshold. Next, I used a function which fits a Gaussian to find the center of the fluorescent blob. The positions were extracted for each timepoint. To connect positions of beads at each timeframe into a trajectory I used a tracking algorithm obtained from <http://physics.georgetown.edu/matlab/>. This algorithm creates a complex matrix to calculate all possible displacements between consecutive timepoints. Particles are assembled into a trajectory according to the minimal squared displacements over time. Automated analysis of the bead movement showed no bulk movement of the beads towards the cortex prior to symmetry breaking. The distance

travelled by the beads implied small movements of the beads (fig. 12), resembling particles moving by Brownian motion. After symmetry breaking, movement of beads close to the male pronucleus was directed towards the cortex, similar to PIV analysis of endogenous granules. Projection of injected bead movies encompassing 150 sec after symmetry breaking clearly illustrates directed motion of the beads towards the cortex (fig. 11).

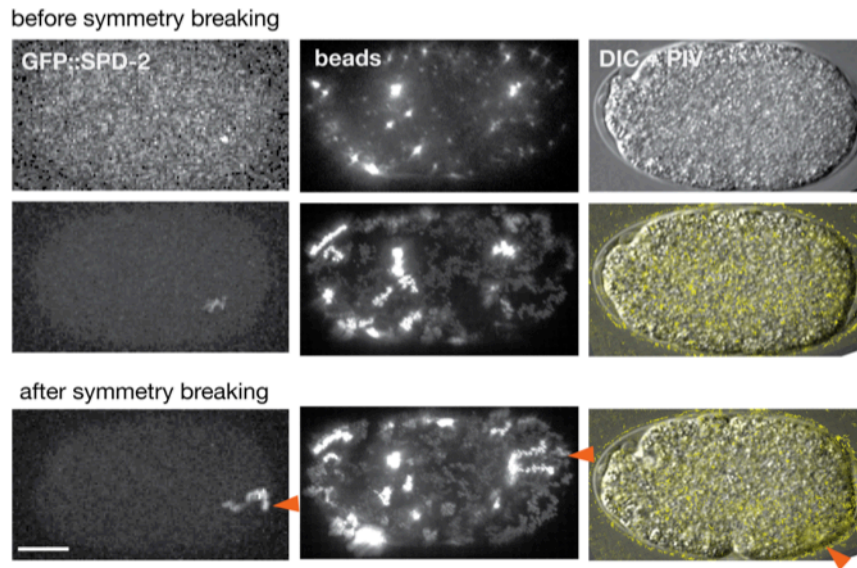


Figure 11. Polarity establishment moves centrosomes, beads and granules to the cortex. **(top)** Single z-images and projections **(middle, bottom)** of centrosomes (GFP::SPD-2) and injected fluorescent beads from time-lapse images before and after symmetry breaking. Projections encompass approximately 150 seconds. Particle image velocimetry (PIV) analysis of endogenous yolk granules and lipid droplets from time-lapse images before (top) and after (bottom) symmetry breaking. In the PIV images, yellow arrows indicate processive motion; high arrow density suggests a coordinated flow field. Symmetry breaking sites are indicated by orange arrowheads.

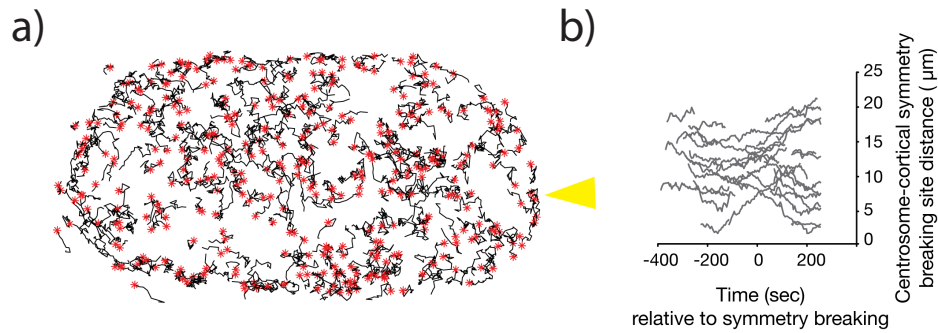


Figure 12. Tracking beads. **(a)** Bead trajectories before symmetry breaking. Black lines: trajectories; red dots: bead position at end of track; yellow arrowhead: symmetry breaking site. **(b)** Bead-cortex distances during symmetry breaking. Distance was determined relative to the site of symmetry breaking on the cortex. Time is indicated relative to symmetry breaking.

3.10 The role of actin in centrosome movement

Based on centrosome trajectories in wild type embryos, I described the motion of centrosomes prior to symmetry breaking as having characteristics of cortically biased random walk. To uncover what part of the cytoskeleton was responsible for centrosome movement, I first investigated the role of actin. I determined the pattern of centrosome movement when the actin cytoskeleton was perturbed. To do so, I used a pharmacological agent - latrunculin -which inhibits actin polymerization. The application of drugs to the embryo by their inclusion in the culture medium is possible due to the permeability of the meiotic eggshell. Successful disruption of actin filament polymerization and dynamics abolishes polarity initiation. Furthermore, cytoplasmic and cortical flows are expected to be absent due to lack of polarity when actin is disrupted. I therefore judged the efficiency of drug penetrance from those features and analyzed only the embryos that showed these phenotypes. Analysis of centrosome motion revealed that centrosomes still moved in a random walk in embryos with a perturbed actin cytoskeleton (fig. 13)

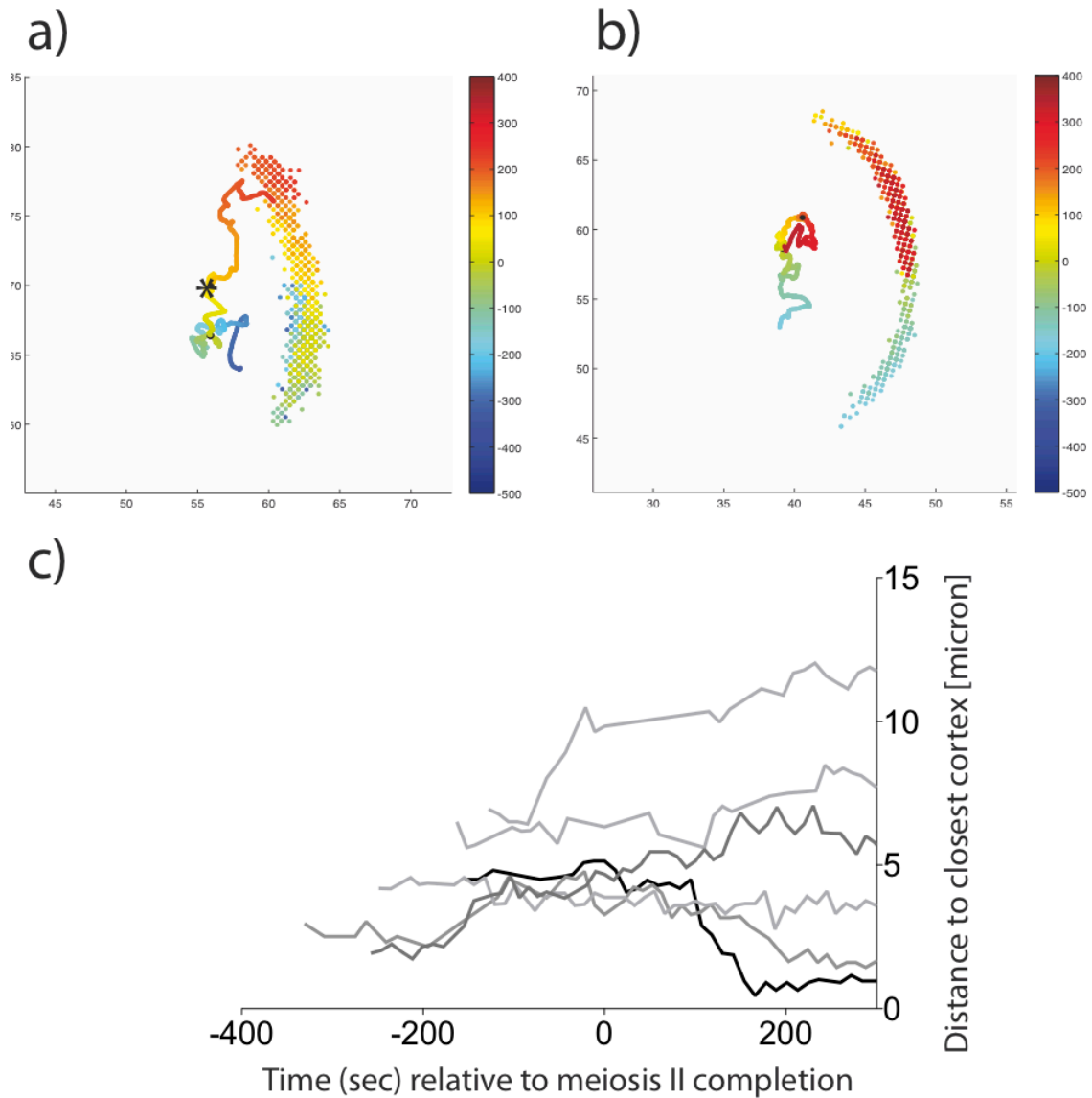


Figure 13. Centrosome motion in a latrunculin-treated embryo. **(a,b)** Centrosome position (linear track) and nearest cortical point (dots) extracted from time-lapse images of GFP::SPD-2 wild type **(a)** and latrunculin A-treated embryos **(b)**. Colors indicate time scale (blue: -500, red: 400). YX axes indicate absolute position. Centrosome position at time “0” is indicated by an arrowhead. In wild type, centrosome position at symmetry breaking is indicated by a star. Polarity establishment does not occur in latrunculin A-treated embryos. **(b)** Centrosome-to-cortex distance. The distance from the centrosome to the closest point on the cortex over time. Each line represents one centrosome. Symmetry breaking does not occur in latrunculin treated embryos.

In some cases, centrosomes approached the cortex. However, centrosomes that were further than approximately 5 μm s away did not reach the cortex (fig 13 bc). Instead they

remained close to the position at which they were at the time “0”. Subsequently, those centrosomes moved towards the middle of the egg, where they appeared to set up the mitotic spindle not approaching cortex at any time.

The failure of centrosomes further than 5 μm from the cortex to ever reach the cortex suggests that the close approximation of centrosomes to the cortex requires actin. As the directional movement of centrosomes towards the cortex occurs once symmetry is broken, it is very likely that actin mediated cytoplasmic flow pushes centrosomes, resembling the movement of beads and granules towards the cortex.

To further investigate contribution of actin to the movement of centrosome I was interested in localizing cytoplasmic actin in the embryo. To do so, I used a strain expressing LifeAct::GFP and SPD-2::GFP. Using this probe I observed LifeAct signal at the cortex. Sporadically there were dots of approximately 1-2 μm size travelling through cytoplasm resembling actin comets. I did not see actin around the centrosome supporting the idea that centrosomes move passively through an actin-dependent process.

3.11 The role of microtubules in centrosome movement

Because the actin cytoskeleton did not seem to be required for centrosome movement before symmetry breaking, I next asked whether microtubules - another component of the cytoskeleton - contributed to centrosome motility. In order to assess the role of microtubules, I used pharmacological agents including nocadazole and taxol, which affect microtubule dynamics. Treatment with nocadazole significantly diminished the distance travelled by centrosomes. If the centrosome was close to the cortex, it most likely stayed close to the cortex and did not move much overall (fig. 14 and fig. 16).

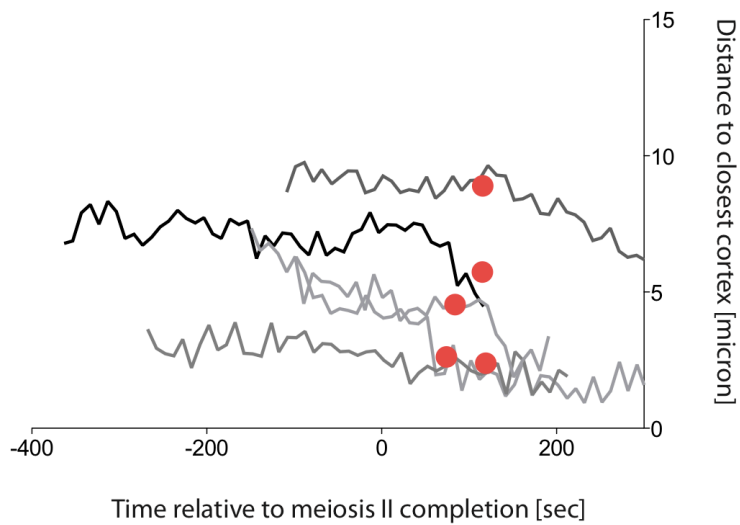


Figure 14. Centrosome-cortex distance in nocadazole treated embryos. The distance from centrosomes to the closest site on the cortex over time. Each line represents one centrosome. Centrosome-cortex distance at time of symmetry breaking is indicated with a red dot.

Measuring centrosomes distance to the closest cortex indicated the reduced mobility of centrosomes: in individual embryos, the distance appears flat over time, signifying decreased motility. To further quantify mobility of the centrosome, I calculated the radius of gyration, which indicates the size of the ensemble of centrosome positions from a given timelapse series. If a particle travels along large area, it has a high radius of gyration (1.0), whereas an object staying largely in place has a low radius of gyration (0.0). Radius of gyration was reduced when microtubules dynamics were inhibited with nocadazole (0.11 for $n=5$) in comparison to wild type embryos (0.31 $n=9$). (fig. 15).

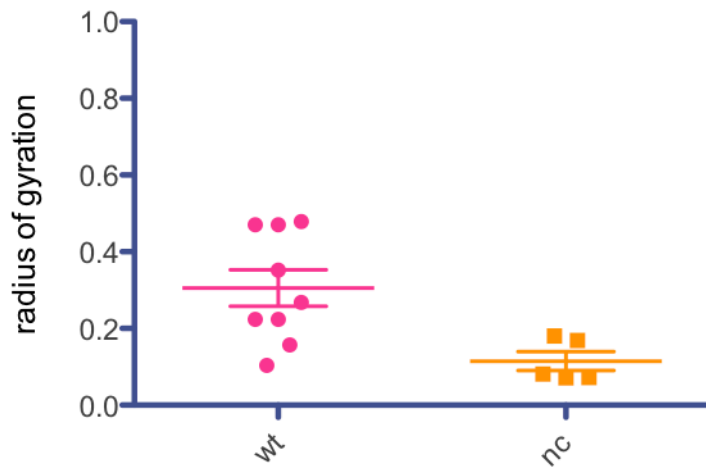


Figure 15. Radius of gyration in wildtype and nocadozole-treated embryos. WT corresponds to wildtype embryos, NC corresponds to nocadozole treated embryos. The radius of gyration is measured for movement of centrosome prior to symmetry breaking.

Furthermore, genetic disruption of tubulin [*tbb-1*(RNAi)] results in centrosomes stuck at the cortex, most likely because those embryos lack a microtubule dependent mechanism to move in away from the cortex before symmetry breaking.

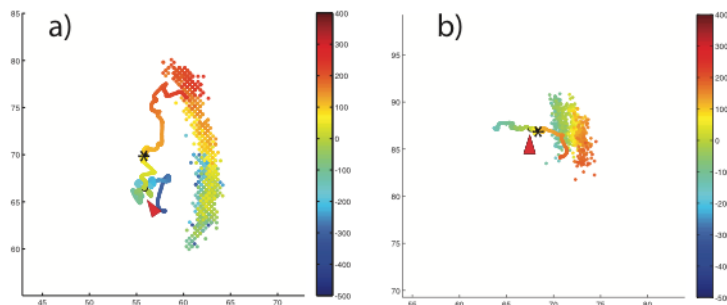


Figure 16. Trajectory travelled by centrosome in (a) wildtype and in (b) nocadozole treated embryo. Centrosome position (linear track) and nearest cortical point (dots) extracted from time-lapse images of GFP::SPD-2 in wildtype (a) and nocadozole treated (b) embryos. Colors indicate time scale (blue: -500, red: 400). YX axes indicate absolute position. Centrosome position at time “0” is indicated by an arrowhead. Centrosome position at symmetry breaking is indicated by a star.

Previous research has shown that centrosomes initiate microtubule nucleation once meiosis II is completed. Thus, explaining the effect on centrosome movement following microtubule perturbation by a depolymerization of centrosomal microtubules is unlikely,

since centrosomal microtubules are not present during the majority of the time the centrosome is moving prior to symmetry breaking. To better understand which microtubules affect centrosomal motility prior to symmetry breaking, I visualized microtubules by immunofluorescence microscopy. Embryos in meiosis showed densely distributed networks of cytoplasmic microtubules throughout the embryo (fig. 17). In particular, cortical sections showed high enrichment of cytoplasmic microtubules. Centrosomes, visualized with centriolar marker SAS-4, did not appear to nucleate microtubules during meiosis, as previously reported (Cowan and Hyman, 2006). To extend this analysis, I tried visualizing tubulin in living one-cell embryos using α tubulin::YFP.

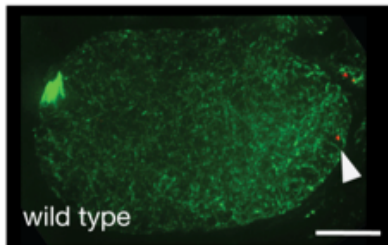


Figure 17. Immunofluorescence of a meiotic embryo showing cytoplasmic microtubules network. Arrowhead points to a red spot which corresponds to the centriole labeled with SAS-4 antibody. Scale bar, 10 μ m

Due to non-optimal imaging conditions, I was not able to obtain satisfactory images. Short movies of α tubulin::YFP indicated the presence of a microtubule network in the cytoplasm. To try to test whether these cytoplasmic microtubules were dynamic and from where they are nucleated, I looked at the microtubule plus-end tracking protein EB-1::GFP. EB-1::GFP was weakly expressed and prone to bleaching. However, I could see that EB-1 signal -in the form of dots - throughout the embryo and EB-1 dots appeared to be highly dynamic.

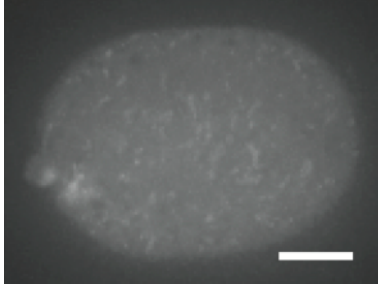


Figure 18. Dynamic noncentrosomal microtubules. Projection of 10 consecutive frames from a timelapse to depict dynamic character of noncentrosomal microtubules visualized with plus-end-binding-protein (EB-1::GFP) prior to symmetry breaking. Scale bar, 10 μm

Projections of 10 consecutive frames ($dt = 0.6$ sec) showed stretches of straight paths of about 2-3 μm travelled within a 6 second interval (fig. 18). A rough approximation from these values suggest growth (growth/sliding) rate of 0.4 μm per second. Microtubule growth rates reported in *C. elegans* embryos during later stages were 0.51 $\mu\text{m}/\text{sec}$ (Kozlowski et al., 2007) or 0-2.0 $\mu\text{m}/\text{sec}$ (Srayko et al., 2005). The maximum instantaneous velocity of centrosome movement was 0.4 $\mu\text{m}/\text{sec}$, in surprisingly good agreement with the apparent rate of microtubule plus-end movement in early embryos. It is therefore likely that centrosome movement is dependent on noncentrosomal microtubules.

3.12 The role of centrosomal microtubules in centrosome movement

Is there any contribution of centrosome-nucleated microtubules to the movement of the centrosomes before symmetry breaking? To test this idea I depleted SPD-5 by RNAi. SPD-5 is a coil-coil protein required for centrosome maturation and assembly of the pericentriolar material (PCM). When SPD-5 function is perturbed, formation of centrosomal microtubule asters is inhibited. Thus, I analyzed centrosome motility in SPD-5 depleted embryos. However, depletion of this protein also abolishes symmetry breaking, as the cue – the centrosome - is no longer functional. Visualization of embryos treated with dsRNA against *spd-5* showed that early centrosome motility retained features of wildtype motion, looking like a random walk (fig. 19). The distribution of centrosome step sizes for wildtype and SPD-5 depleted embryos prior to symmetry breaking overlapped significantly. However, after time “0”, centrosomes in SPD-5

depleted embryos did not approach the cortex (fig. 19), but rather floated around, not showing movement toward the cortex. This result indicates that either the polarization mechanism itself or polymerization of microtubules by centrosomes contributes to the motion of centrosomes towards the cortex after time “0”. Furthermore, a functional centrosome was not essential for early (pre-symmetry breaking) centrosome motility nor for cortical constraint.

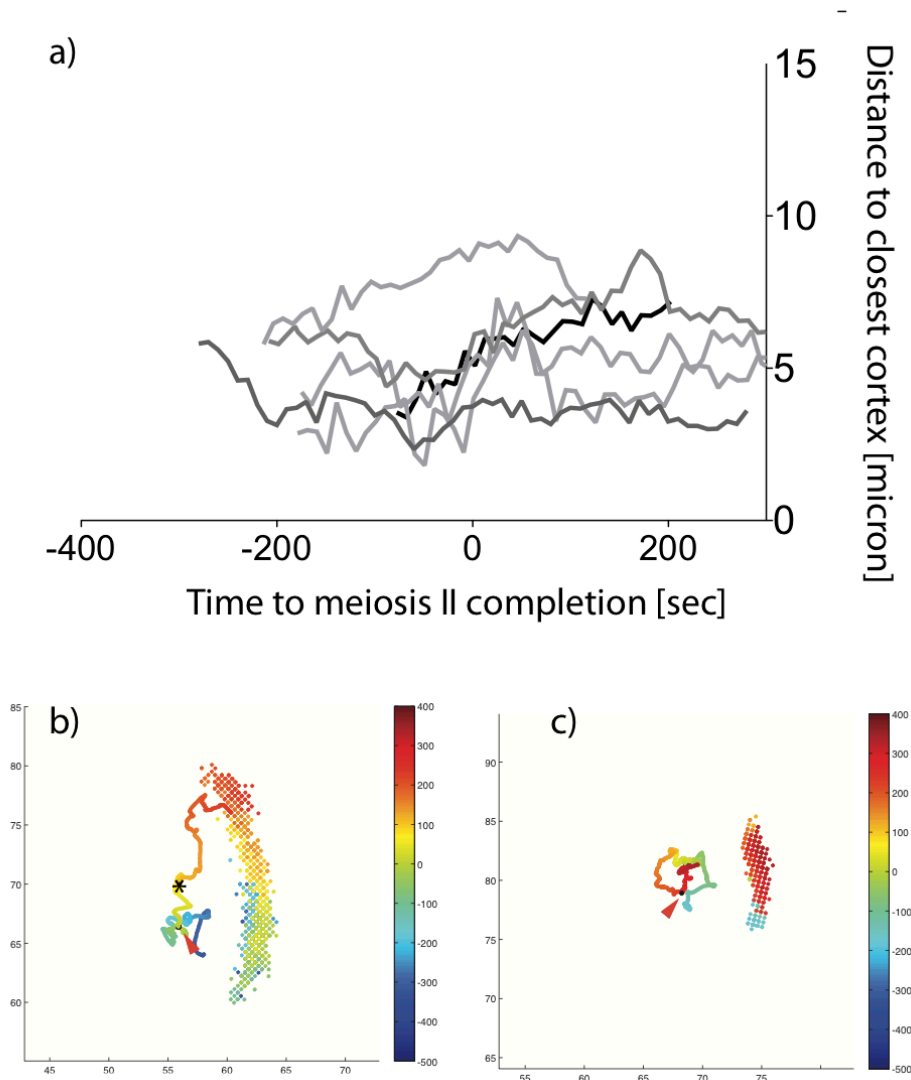


Figure 19. Centrosome movement in *spd-5(RNAi)* (a) Centrosome-cortex distance in *spd-5(RNAi)* embryos. The distance from centrosomes to the closest site on the cortex over time. Each line represents one centrosome. Symmetry breaking does not occur in *spd-5(RNAi)* (b-c) Centrosome position (linear track) and nearest cortical point (dots) extracted from time-lapse images of GFP::SPD-2 in wildtype (b) and *spd-5(RNAi)*-treated (c) embryos. Colors indicate time scale (blue: -500, red: 400). YX axes indicate absolute position. Centrosome position at time “0” is indicated by an arrowhead. In wild type, centrosome position at symmetry breaking is indicated by a star.

3.13 The role of gamma-tubulin in centrosome movement

Since *spd-5*(RNAi) did not allow me to distinguish whether the failure of centrosomes to reach the cortex came from the lack of centrosomal microtubule nucleation or from the lack of symmetry breaking related processes such as flows, I wanted to test how depletion of centrosomal microtubules affected motility of the centrosome and its ability to reach the cortex. γ -tubulin– TBG-1- is an essential component required for microtubule nucleation. Depletion of TBG-1 does not affect polarity, mostly likely because centrosome maturation is not affected. Surprisingly, centrosomes in *tbg-1*(RNAi) embryos showed a novel behavior. Namely, centrosomes appeared more motile than in wildtype embryos prior to symmetry breaking. The overall size of centrosome trajectories was larger than wildtype, and the path taken by centrosomes showed a higher amount of straight motion (fig 20a). The analysis of distance to the closest cortex showed that the average distance to the closest cortex was increased in *tbg-1*(RNAi) embryos, indicating centrosomes were much deeper within the embryo volume (fig 20bc). The average distance to the cortex at symmetry breaking was 5.6 μm (n=17) (wild type =2.8 μm (n=26)). Once symmetry was broken, centrosomes in *tbg-1*(RNAi) embryos moved to the cortex, most likely as a result of cytoplasmic flow. However, in a few cases centrosomes did not reach the cortex. This failure was observed when female and male pronuclei were close to each other and pronuclear meeting occurred during symmetry breaking. Thus, the female pronucleus could immobilize the centrosome away from the cortex, despite cytoplasmic flow. This observation further supports my finding that direct contact with the cortex is not required for symmetry breaking.

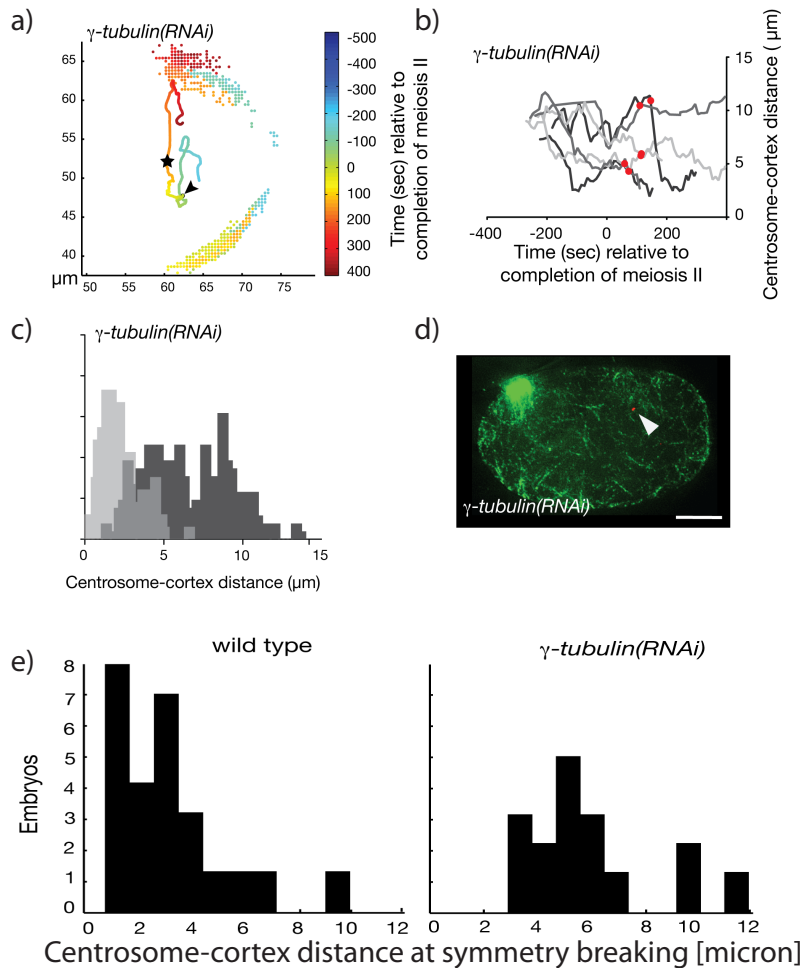


Figure 20. Consequences of TBG-1 depletion on movement of centrosome and microtubules cytoskeleton. **(a)** Centrosome position (linear track) and nearest cortical point (dots) extracted from time-lapse images of GFP::SPD in γ -tubulin-depleted embryos. Colors indicate time scale (blue: -500, red: 400). YX axes indicate absolute position. Centrosome position at time “0” is indicated by an arrowhead. Centrosome position at symmetry breaking is indicated by a star. **(b)** Centrosome-cortex distance in γ -tubulin-depleted embryos. The distance from centrosomes to the closest site on the cortex over time. Each line represents one centrosome. Centrosome-cortex distance at time of symmetry breaking is indicated with a red dot. **(c)** Frequency histogram of centrosome-cortex distances before symmetry breaking in γ -tubulin(RNAi) (n=10) embryos (dark gray bars), the wild type distribution is shown for comparison (light gray bars). **(d)** Microtubules in γ -tubulin-depleted embryo before polarity establishment. Immunofluorescent images show tubulin (green) and the centriolar protein SAS-4 (red, indicated by white arrowheads). **(e)** Distance to cortex at symmetry breaking, comparison between wildtype and *tbg-1*(RNAi) Scale bar, 10 μ m.

To understand the reason for the observed increase of centrosome motility and decrease in cortical constraint in *tbg-1*(RNAi) embryos, I analyzed microtubules when TBG-1 was depleted. Immunostaining of microtubules showed long cytoplasmic microtubules, reaching far into the embryo (fig 20d). The overall density of microtubules was lower

compared to wildtype, also there was an increase of tubulin in the meiotic spindle (fig. 20d). Microtubules could be seen radiating from the meiotic spindle into the cytoplasm. Altogether, depletion of TBG-1 leads to an increase in centrosome motility and an increase in the average distance to the closest cortex, likely due to altered organization of non-centrosomal microtubules.

3.14 Contribution of microtubules regulators

My results showed that the microtubule cytoskeleton makes a large contribution to centrosome motility and cortical constraint prior to symmetry breaking. Trying to understand more about how microtubules exerted this control, I tested whether depletion of well known microtubule motors could phenocopy the aberrant centrosome movement observed in *tbg-1(RNAi)* or nocadazole-treated embryos. I examined centrosome movement in embryos depleted of kinesin-13 (KLP-7), dynein (DHC-1, minus-end microtubule motor) and conventional kinesin-1 (KLC-1, UNC-116)(Yang, 2005). I also tested the small GTPase Ran-1, which is required for non-centrosomal microtubule organization in several systems. Out of the molecules tested, only Ran-1 showed a consistent defect in centrosome motion.

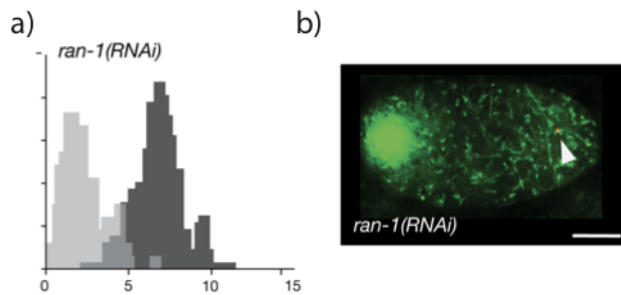


Figure 21. Depletion of RAN-1. (a) Frequency histogram of centrosome-cortex distances before symmetry breaking in *ran-1(RNAi)* (n=8) embryos (dark gray bar), the wild type distribution is shown for comparison (light gray bars). (b) Microtubules in Ran-depleted embryo before polarity establishment. Immunofluorescent images show tubulin (green) and the centriolar protein SAS-4 (red, indicated by white arrowheads). Scale bar, 10 μ m.

Since Ran-1 contributes to nuclear envelope formation, I used a worm strain that expresses SPD-2::GFP together with H2B::mCherry and NMY-2::GFP to assign time “0” according to male pronucleus size measured in the red channel. The centrosome step

sizes in *ran-1(RNAi)* embryos prior to symmetry breaking resembled a Gaussian distribution but with the mean shifted by 4.4 μm compared to wildtype (fig. 21a). As before, I analyzed microtubule distribution in embryos depleted of RAN-1 by immunofluorescence. In meiotic *ran-1(RNAi)* embryos, the network of cytoplasmic microtubules was less dense than in wildtype embryos, and large amounts of tubulin could be found in the meiotic spindle (fig. 21b). Centrosomes were frequently very close to meiotic spindles, perhaps being pulled by the microtubules radiating out of the spindle. The decreased number of cortical microtubules may be the reason for the release of centrosomes from cortical constraint in Ran depleted embryos and allow centrosomes to take larger step sizes.

3.15 The effect of centrosome-cortex distance on polarity: NMY-2 and PAR-2

Depletion of γ -tubulin resulted in an increased distance between centrosomes and the cortex, up to even 14-15 μm . Centrosome could literally be observed in the middle of the embryo, reaching the maximal centrosome-cortex distance achievable according to the geometry of the *C. elegans* egg. Despite the large distances to the cortex, all *tbg-1 (RNAi)* embryos established polarity. I was therefore curious if there were any defects or changes in polarity establishment originating from the increased centrosome distance to the cortex. I concentrated on measuring the delay in symmetry breaking in cases where the centrosome was far from the cortex. I correlated the distance of the centrosome to the cortex with the time required for non-muscle myosin clearance or PAR-2 appearance on the cortex, well-established polarity markers. There was a direct correlation between how far centrosomes were from the cortex and the time required for myosin clearing, meaning the further away the centrosome was, the longer it took. The values of centrosome-cortex distance above 8 μm may not be reliable, because the cortex in the z-dimension may represent the closest cortex. Nevertheless, the further the centrosome was from the cortex, the longer it took from time “0” for myosin to start retracting from the site of symmetry breaking (fig 22).

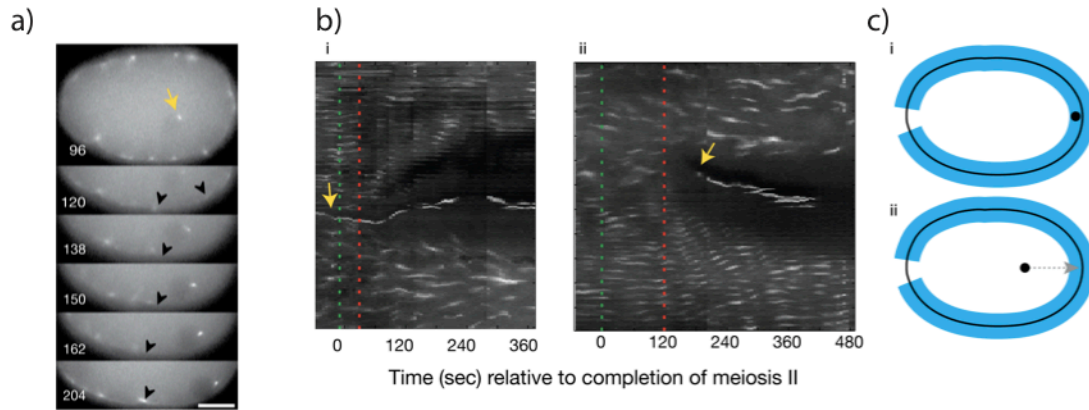


Figure 22. Symmetry breaking at a distance. **(a)** Time-lapse images of centrosomes (GFP::SPD-2) and cortical myosin (NMY-2::GFP) in a γ -tubulin-depleted embryo during symmetry breaking. Time elapsed is indicated relative to completion of meiosis II (time “0”). Yellow arrow: centrosome; black arrowheads: boundary of cortical myosin indicating symmetry breaking and posterior domain establishment. Scale bars, 10 μ m. **(b)** Kymograph of the cortex in GFP::SPD-2; NMY-2::GFP embryos depleted of γ -tubulin. **(c) i)** Centrosomes were 2.1 μ m from the cortex at time of symmetry breaking. **ii)** Centrosomes were 10.1 μ m from the cortex at time of symmetry breaking. The loss of myosin foci from the cortex indicates symmetry breaking and posterior domain establishment. Vertical green lines: time “0”; vertical red lines: symmetry breaking, yellow arrows: centrosomes. Diagrams show kymograph method: black dots, centrosomes; black outline, embryo cortex; blue line, kymograph region. Centrosomes are only detectable in the kymograph when they are directly at the cortex. Scale bar, 10 μ m.

As there is a correlation between centrosome-cortex distance and symmetry breaking, I was interested in examining whether the increased centrosome-cortex distance causes any additional delay in PAR-2 establishment, a posterior polarity marker that localizes to the cortex after symmetry breaking. Such delay would be measured for a period between symmetry breaking and PAR-2 appearance. The analysis of GFP::PAR-2 fluorescence was difficult due to variable levels of intensity. To assign the time of PAR-2's appearance on the cortex in a consistent, unbiased way, I measured a small region on the cortex closest to centrosomes for the entire timelapse series. For each embryo, I standardized the intensity curve to the minimum. The resulting intensity measurement resembled a curve with rising slope, which reaches a plateau when the domain is mature (data not shown).

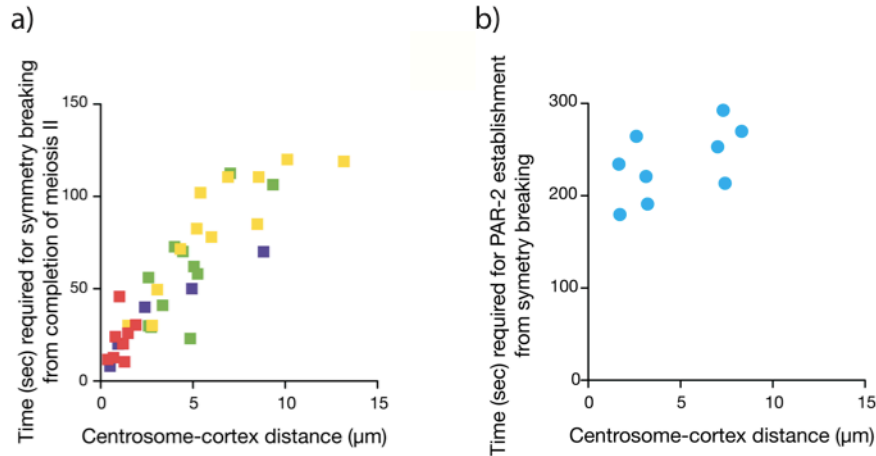


Figure 23. Distance to cortex vs polarity establishment efficiency. **(a)** Centrosome-cortex distance and the time required for symmetry breaking. Centrosome distance to the closest point on the cortex was measured in GFP::SPD-2; NMY-2::GFP embryos at time of symmetry breaking. Time required for symmetry breaking is the interval between time “0” and timeSB. Red: wild type, no compression; purple: wild type, compressed; green: γ -tubulin(RNAi), no compression; yellow: γ -tubulin(RNAi), compressed. **(b)** Centrosome-cortex distance and the time required for PAR-2 establishment. Centrosome distance to the closest point on the cortex was measured in GFP::SPD-2; mCH::PAR-2 embryos at time of symmetry breaking. Time required for PAR-2 establishment is the interval between symmetry breaking and when standardized cortical PAR-2 intensity reaches 0.5.

The timepoint at which the intensity reached 0.5 (ie. 0.5 over background) was considered the 'PAR-2 appearance time'. Next, I measured the delay from symmetry breaking until 'PAR-2 appearance time' and correlated it with centrosome distance to the cortex (fig. 23b). Like I saw for symmetry breaking, there was a delay in PAR-2 appearance that increased with increasing centrosome-cortex distance, even in addition to the initial delay in symmetry breaking itself. This suggests that once symmetry is broken the centrosome-cortex distance may also delay loading of PAR-2 onto the cortex. In conclusion, symmetry can be broken from any position within the embryo, however the distance correlates with a delay in cortical symmetry breaking.

In my study of centrosome movement prior to symmetry breaking I was interested in understanding how position of the centrosome in the embryo affects symmetry breaking. My analysis shows that centrosome can break symmetry from any spot in the zygote. However, the centrosome-cortex proximity enhances the speed of symmetry breaking. If the distance is increased there is a corresponding delay in cortical symmetry breaking.

Furthermore, my data suggests that centrosome movement prior to symmetry breaking has characteristics of a random walk with a cortical constraint. The cortical bias and the motion appear to be dependent on the cytoplasmic microtubules. Cytoplasmic flow moves centrosome towards the cortex once symmetry is broken.

3.16 Visualizing sperm mitochondria in the zygote

Taking advantage of the fact that there are *C.elegans* mutants that are not able to produce sperm, so-called phenotypic females, efficient male-to-female crossing can be performed. I developed an assay in which I specifically stained males with dyes designed for cellular tracking of mitochondria. Next, I crossed the stained males to phenotypic females (*fog-2*) and after approx. 15 hours of mating, I looked for stained mitochondria in newly fertilized embryos. In my experiments, I determined that mitochondrial staining is preserved beyond fertilization and could be used to mark mitochondria delivered by sperm to the oocyte. Thus, I could monitor the location of sperm-supplied mitochondria in living zygotes by time-lapse microscopy.

The use of phenotypic females was not absolutely necessary for persistence of paternal mitochondria in the zygote. Since the male sperm efficiently outcompete hermaphrodite sperm to fertilize the oocyte (LaMunyon and Ward, 2002), the labeled mitochondria from males could be visualized in either phenotypic females or in wild type hermaphrodites.

3.17 Sperm mitochondria in the zygote

Observation of paternally contributed mitochondria was possible with some but not all mitochondrial dyes. I was able to visualize sperm mitochondria in living embryos with Mitotracker CMXRos Red and Rhodamine R6. Mitotracker Green FM did not work, even though FM dyes accumulate in mitochondria regardless of membrane potential.

Two potentiometric mitochondrial dyes, TMRE and JC-1, labeled paternal mitochondria in sperm but were not preserved by paternal mitochondria in the embryo by my labeling procedure.

The previously mentioned dyes, Rhodamine R6, Mitotracker CMXRos and TMRE could label the maternal mitochondria in the embryo when fed to the worm; Mitotracker Green

FM and JC-1 does not label maternal mitochondria in my labeling method (Fig. 24).

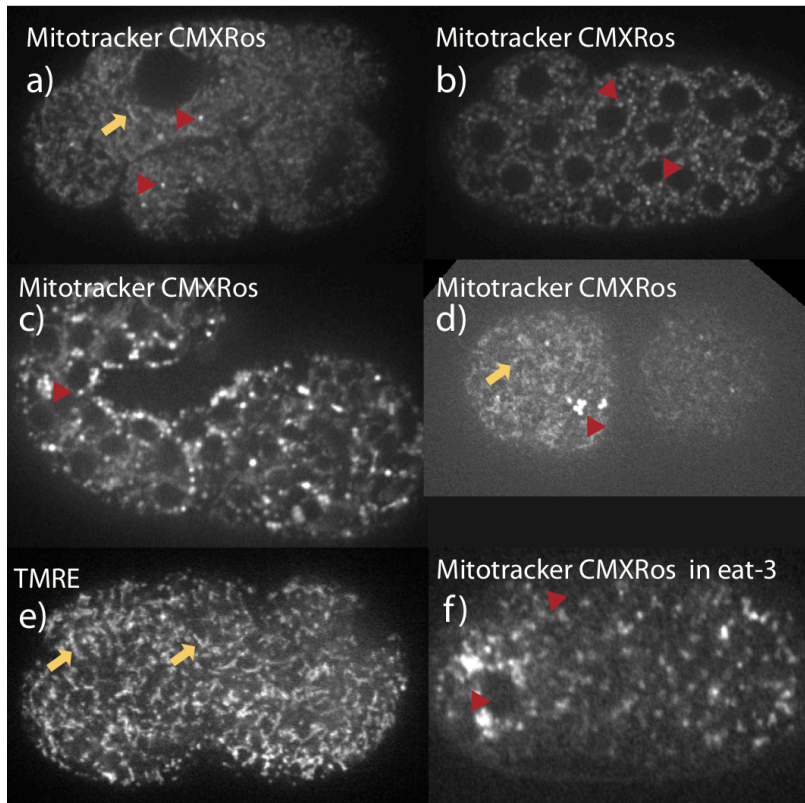


Figure 24. Mitochondria in *C. elegans* embryo. Whole embryo stain. (a) Mitotracker CMXRos staining in 4-cell embryo shows fused (stringy) mitochondria (yellow arrows) and bright circular unfused mitochondria (red arrowhead). (b) Mitotracker CMXRos staining in ~ 20-cell embryo. Arrows point to circular mitochondria. (c) Mitotracker CMXRos staining in coma stage embryo. There is several circular mitochondria visible at this stage. (d) Mitotracker CMXRos staining in 2-cell embryo. Bright circular unfused mitochondria (red arrowhead) are most likely paternal mitochondria. (e) TMRE staining in one-cell embryo shows mainly stringy fused (yellow arrows) mitochondrial network. (f) Mitotracker CMXRos staining in *eat-3* one-cell embryo. Mitochondria have circular unfused appearance (red arrowhead).

One unique aspect of paternal mitochondria compared to maternal mitochondria was their unfused appearance. Sperm mitochondria were circular, about 1 μm in diameter, and showed relatively high intensity of fluorescence when compared with maternal mitochondria. The sperm mitochondria did not appear to fuse either with each other or with the stringy network of maternal mitochondria. The mitochondria dye remained associated with paternal mitochondria and did not spread into the maternal mitochondria, which further suggests that paternal and maternal mitochondria do not undergo fusion. Generally, mitochondria can fuse with each other to form a continuous network that may

allow for exchange of matrix or other components, which appeared to be true of maternal mitochondria in the zygote but not for paternal mitochondria. Mitochondrial fusion is mediated by dynamin superfamily GTPases OPA-1 (*C. elegans* EAT-3) and mitofusins (Wrighton, 2011). Therefore I confirmed that maternal mitochondria are fused by examining embryo mitochondria in *eat-3* mutant. Mitochondria in *eat-3* mutants were circular and looked similar to paternal mitochondria (fig. 24, 25a). Thus paternal mitochondria in the zygote may be prevented from undergoing fusion and thereby retain distinct identity.

3.18 Mitochondria cluster around the male pronucleus and leave the cluster at symmetry breaking

As recent studies show that paternal mitochondria are eliminated from the *C. elegans* embryo, a question is why they are delivered to the zygote in the first place. One possibility is that paternal mitochondria may play a regulatory role in embryonic development. They could function as a signal during symmetry breaking, providing a burst in calcium or other signal. My time-lapse analysis of paternal mitochondria in early zygotes showed that paternal mitochondria cluster around the male pronucleus like beads on a necklace. Paternal mitochondria formed a tight complex and did not move independently (fig. 24a). Identification of individual mitochondria was difficult. Sporadically it was possible to observe a mitochondrion that escaped the cluster and moved away.

Observing localization of sperm mitochondria together with the endoplasmic reticulum (ER) showed that there was ER around the “sperm complex”, giving the impression of a “sperm compartment “ (fig. 26). The ER domain around the sperm mitochondria persisted until symmetry breaking.

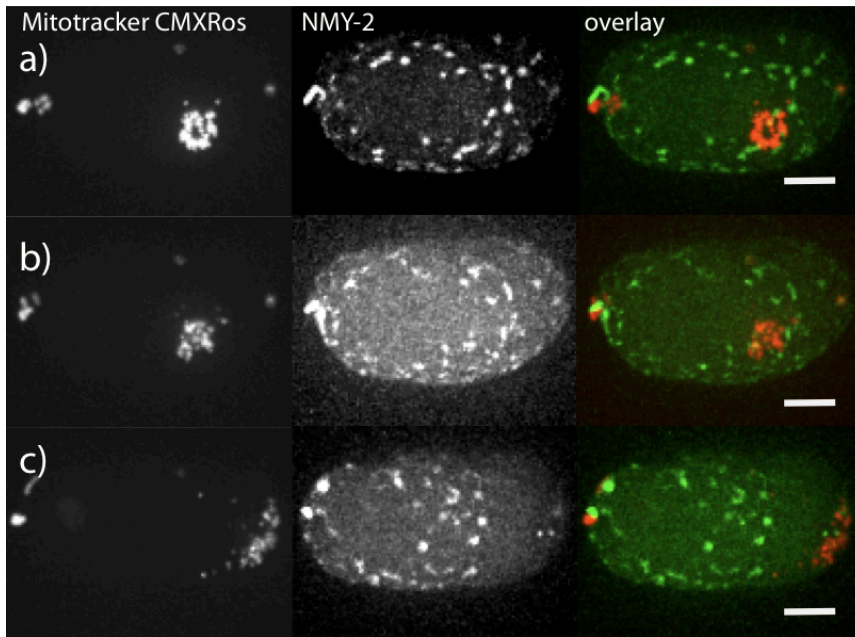


Figure 25. Behavior of sperm mitochondria before and after symmetry breaking. Pictures show projections of about 10 microns to encompass the sperm mitochondria cluster. **(a)** frames before symmetry breaking. Sperm mitochondria are closely associated with each other, two loose mitochondria can be observed close to the cluster. **(b)** 3 frames after symmetry breaking. Sperm cluster is relaxed. Individual mitochondria can be observed. **(c)** Embryo polarity is established. Sperm mitochondria relocate due to cytoplasmic flow. Scale bar, 10 μm .

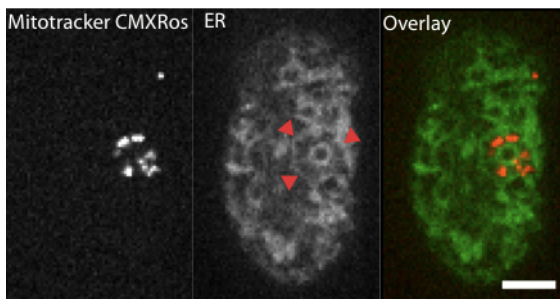


Figure 26. Sperm mitochondria before symmetry breaking are surrounded by endoplasmic reticulum compartment. All pictures are single frames from a timelapse. **(a)** Paternal mitochondria stained with Mitotracker CMXRos clustering around the male pronucleus. The mitochondria form a dense cloud, it is difficult to observe individual mitochondria. Sperm mitochondria signal does not interact with maternal mitochondria. **(b)** ER morphology before symmetry breaking. Red arrowheads indicate ER compartment which encompasses the sperm mitochondria. Male pronucleus surrounded by the ER can be seen inside of the “sperm compartment”. **(c)** Overlay of the two images: red- mitochondria, green – ER.). Scale bar, 10 μm .

During symmetry breaking the association between mitochondria is loosened. Upon the relaxation of the paternal mitochondria cluster, individual mitochondria could be identified and the dye intensity of individual mitochondria appeared to decrease (fig. 24b). Once symmetry is broken, paternal mitochondria move towards the cortex and flow along it towards middle of the egg, probably as a result of cortical flow (fig. 24c). Subsequent movement of mitochondria in the embryo appears to be random. Some mitochondria were displaced over large distances ($\frac{1}{4}$ of the embryo length during 15 sec) with very high straightness, perhaps indicating they move using microtubule tracks. At the time of the first cell division, which generates a P1 and AB cell, paternal mitochondria were distributed randomly. Examination of the number of sperm mitochondria in 5 embryos showed that the AB cell inherited correspondingly: 40, 58, 34, 52 and 37% (average: 44%) of total sperm mitochondria.

3.19 Paternal mitochondrial in the zygote during development

How many mitochondria are there and what happens to them over time? Do they persist during development or are they degraded? Are they able to divide? One study has shown that the number of sperm mitochondria decreases as development proceeds. Already after 4 divisions (16-cell stage) very few sperm mitochondria could be found in the embryo (Sato and Sato, 2011). According to that study, the steep decrease in number occurred between the third and fourth divisions. In my examination I was able to visualize several sperm mitochondria during later development as well, for instance even in a coma-stage embryos. Some cells retained a higher number of paternal mitochondria than others, although this was variable. For example, in one embryo around the 40-cell stage, two cells had more than 30 paternal mitochondria, many other cells had five or less mitochondria, and there were a few cells without any paternal mitochondria.

To investigate fate of sperm mitochondria I performed timelapse imaging of a single embryo from one-cell until 300-cell stage (approx. 4 hours). Despite photobleaching, I was able to visualize paternal mitochondria through the entire period of imaging (fig. 27). It is difficult to say whether there is an overall reduction of sperm mitochondria due to fast photobleaching in mitochondria (fig. 28). Older embryo appears to have high number

of sperm mitochondria compared to one-cell embryo. It remains to be investigated whether division of sperm mitochondria could occur during later embryo development.

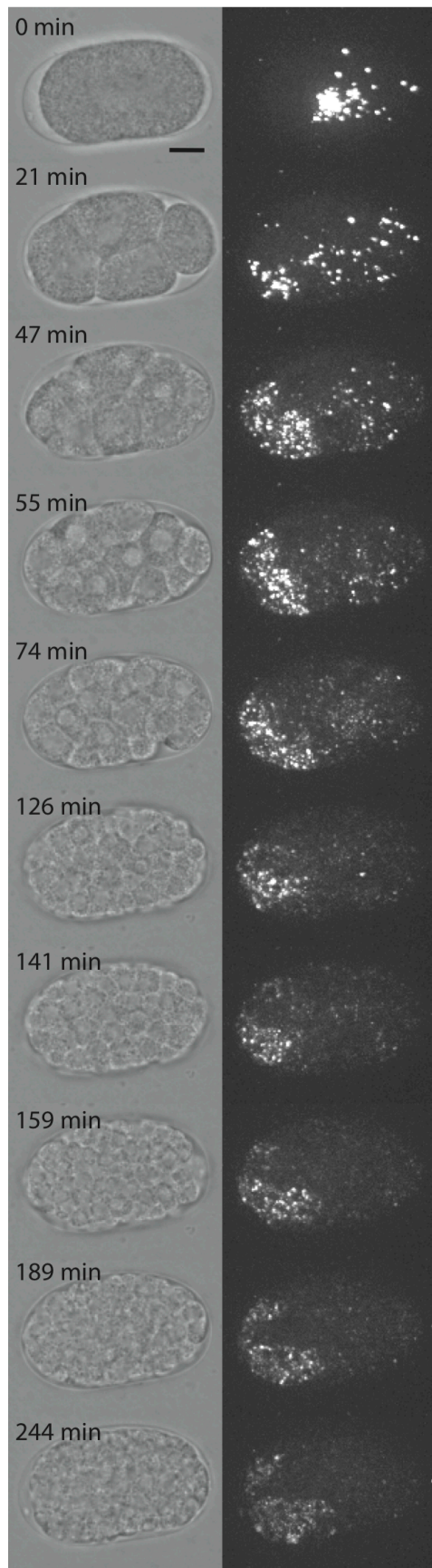


Figure 27. Sperm mitochondria persist during development. Single frames (left, brightfield) and projections (right, Mitotracker CMXRos) from a 4-hour timelapse. Fluorescent images were taken every 5 minutes to minimize photobleaching. Selected stages are shown. Sperm mitochondria can be observed during 4 hour embryo development. The dye intensity goes down with time.

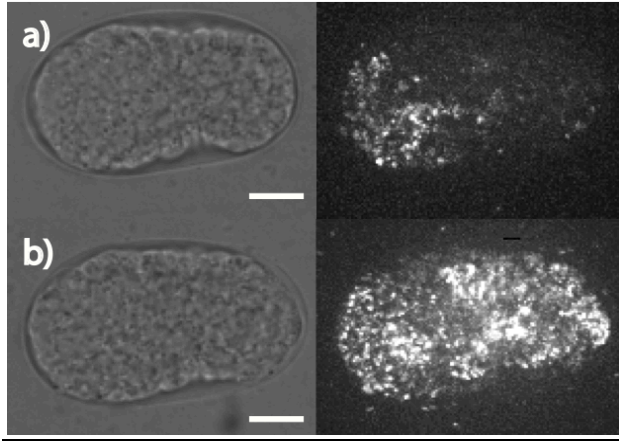


Figure 28. Photobleaching of mitochondrial stain complicates quantification. Comparison of embryo after 4 hour of imaging (from fig. 4) and embryo from the same worm which was not imaged before. There is a reduction in signal in (a) compared to (b). Scale bar, 10 μ m.

3.20 Exclusion of sperm mitochondria from a germline progenitor

Trying to fit my observation that paternally contributed mitochondria persisted in *C. elegans* embryos into the dogma of uniparental mitochondrial transmission, I wondered whether uniparental mitochondria inheritance might be restricted to the germline rather than the whole animal. The first asymmetric division of *C. elegans* zygotes creates a P1 cell that divides asymmetrically three more times to generate the P4 cell at the 16-cell stage. This germline progenitor will divide one more time to give rise to two primordial cells, Z2 and Z3, at the 100-cell embryo stage (Seydoux and Strome, 1999). PIE-1 encodes a cytoplasmic cell fate determinant that localizes to the previously mentioned germline progenitors throughout development (Mello et al., 1996). Thus following cells expressing GFP-tagged PIE-1 allows for unambiguous identification of the germline in the zygote. Therefore I investigated the question of whether the germline progenitor cell inherits sperm mitochondria by examining the presence of sperm mitochondria in PIE-1-positive cells. There was indeed a reduction in the number of paternal mitochondria over time in PIE-1 cells (fig. 29). The reduction could be a result of selective degradation of sperm mitochondria in the germline or by dilution. To estimate the effect of dilution, I

assumed that 50 % of the paternal mitochondria could be lost at each cell division and that the initial number of paternal mitochondria does not exceed 60, as indicated by my counts. With these assumptions a P4 cell experiencing a dilution would have about 6-7 mitochondria at the 16-cell stage. However, I saw almost complete elimination of paternal mitochondria from the germline lineage after only 3 cell divisions, suggesting additional mechanisms of removing paternal mitochondria may exist.

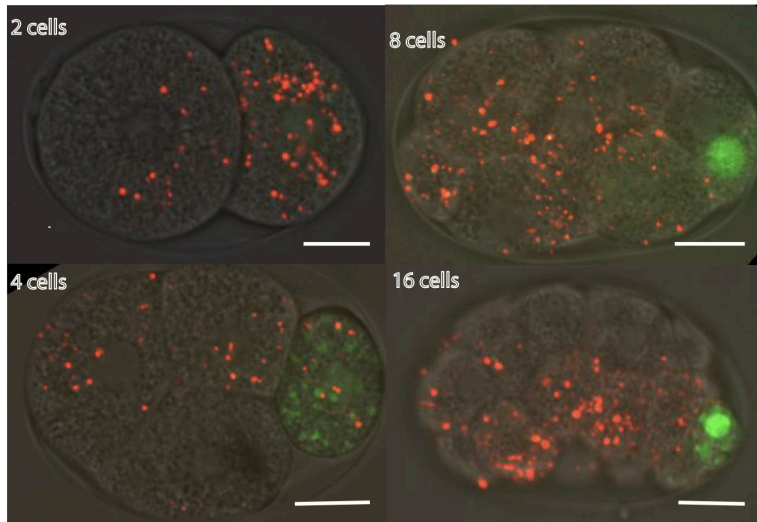


Figure 29. Exclusion of sperm mitochondria from germline. Brightfield images overlaid with z-stack projection of images showing embryos expressing PIE-1::GFP (green) and sperm contributed mitochondria (red) at various stages of development. Scale bar, 10 μ m.

3.21 LGG-1 dependent autophagy

To see whether paternal mitochondria were being degraded, I wanted to see whether labeled paternal mitochondria co-localized with the lysosome. Lysosomes could be observed by LysoTracker Green-labeling in one-cell embryos as well as in older embryos. Are sperm mitochondria inside of those lysosomes? In one-cell embryos, I did not detect lysosomes near the sperm mitochondria. Similarly in older stages (up to 50 cells) lysosomes and sperm mitochondria appeared separate. Thus the paternal mitochondria I can visualize do not appear to be in the process of being degraded.

Next, I looked to see if autophagosome components, labelled by Atg8/LGG-1, co-localized with paternal mitochondria. LGG-1::GFP was expressed under LGG-1 promoter, which does not express in early embryos, thus the GFP signal could only be

observed only during later embryo development (Meléndez et al., 2003). Embryos older than 8-cells, when I could detect both LGG-1::GFP and labeled paternal mitochondria, there was not a strong correlation between LGG-1 signal and Mitotracker CMXRos (fig. 30). This observation complicates the recent suggestion that the autophagy pathway in *C. elegans* embryos degrades paternal mitochondria.

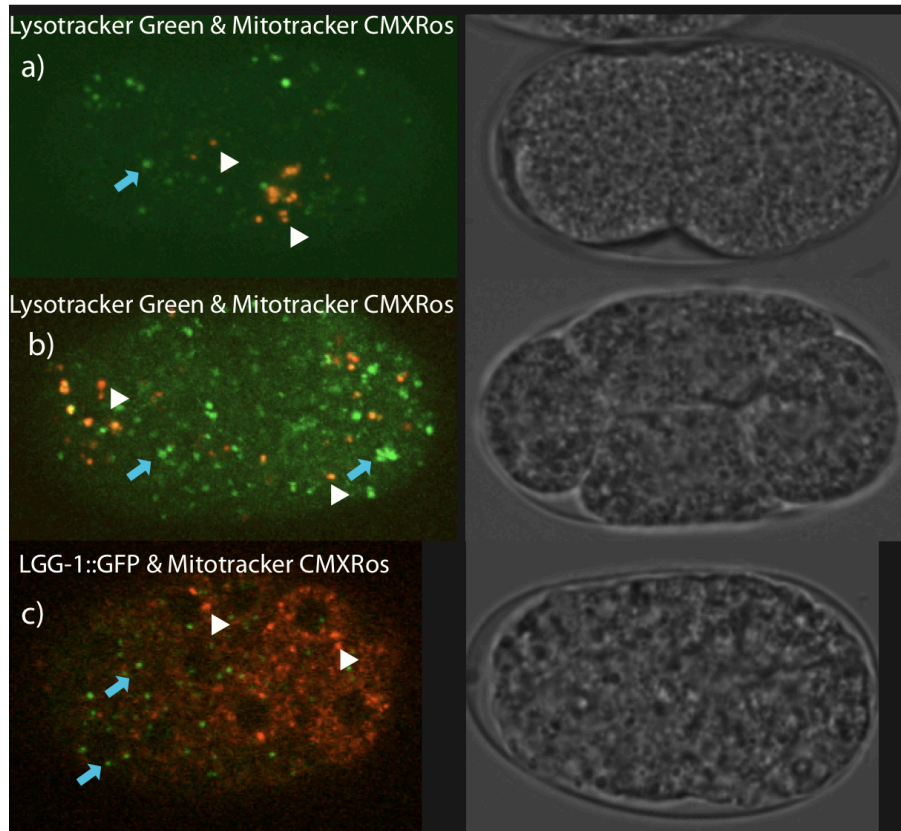


Figure 30. Localization of paternal mitochondria and autophagy components. (a) Two-cell embryo and (b) four-cell embryo with labeled lysosomes (green) and sperm mitochondria (red). The images are projection of z-stacks. (c) Old embryo (~300 cells) expressing LGG-1::GFP (green) with sperm mitochondria labeled (red).

Previous studies have shown contribution of paternally contributed centrosomes to the development of polarity. I was interested in examining whether there are other paternally provided organelles and what is their fate in the embryo. I established an assay for visualizing sperm mitochondria, which allowed me to observe presence in the zygote. Sperm mitochondria are closely associated with each other prior to symmetry breaking and disperse throughout the zygote once symmetry is broken. Those paternal

mitochondria can be observed in later embryo stages with exception of germline progenitor cells. Paternal mitochondria do not appear to colocalize with autophagy or lysosome markers suggesting that *C. elegans* embryo may tolerate presence of paternal mitochondria rather than degrade them after fertilization.

4. Discussion

4.1 High temporal resolution imaging of centrosome movement

The juxtaposition of the centrosome to the cortex during symmetry breaking has been taken for granted as a necessary part of polarity establishment. However, no detailed analysis of centrosome positioning prior to centrosome-cortex association has been performed. Moreover, previous research on polarity establishment has used a relatively wide window of time to demarcate symmetry breaking. During my PhD work, I attempted to understand by what mechanism centrosomes approach the cortex and how the distance to the cortex affects polarization of the zygote. To perform my study I developed conditions to maintain viability of meiotic embryos that would allow for timelapse imaging of centrosomes at high spatial and temporal resolution. In my work, I found that hanging drop embryo mounting and EGM preserved embryo health and the normal timing of development, even in early meiosis I embryos. The major difference between agar pad and hanging drop mounting is that the latter method does not exert mechanical pressure on the specimen, allowing for visualization of sensitive zygotes. In my analysis I tried to be very consistent with time assignment. I first standardized all the embryos according to the cell cycle stage – end of meiosis (male pronucleus size), providing a temporal frame to analyze even those embryos with perturbed polarity. I used the term of symmetry breaking to demarcate a switch between symmetry and asymmetry of the cortex. Using higher temporal and spatial resolution together with precise timing of symmetry breaking revealed the difference in position of centrosome before and after symmetry breaking. The centrosome is not contacting the cortex at the moment of

symmetry breaking but repositions after symmetry breaking. The post-symmetry breaking movement of centrosome towards the cortex takes about 30-60 sec. Thus experiments performed at lower time resolution, for example with acquisition every 60 sec, may have given a false indication of centrosome being at the cortex when symmetry is broken.

In order to perform an unbiased analysis of centrosome position, I developed custom-made image analysis procedures in Matlab to track centrosomes and detect the cortex. These tools have helped analyze how wildtype centrosome moves prior and after symmetry breaking in an unbiased manner, and further, to understand how different pharmacological and genetic perturbations affect centrosome movement.

4.2 Random walk of centrosomes

A cumulative analysis of several aspects of centrosome motion has shown that the early movement of centrosomes is highly heterogeneous and has characteristics of a random walk. There is no detectable directionality in centrosome motion. Considering the invariance of *C. elegans* development, the stochasticity of centrosome movement is somewhat surprising. However, similar random movement of centrosomes that, like centrosomes in early *C. elegans* embryos, do not nucleate microtubules has also been reported in *Drosophila* and HeLa cells (Piel et al., 2000; Rebollo et al., 2007). Those instances illustrate a centrosome whose movement may be not intentional, but rather a consequence of cytoskeleton dynamics. Microtubule network involved in transporting vesicles within the cell exerts pushing which unintentionally moves other organelles passively or actively through attachment of motor protein to those organelles. This contrasts with typically observed pattern of centrosome motion, which depends on microtubules nucleated by centrosome itself.

The speed of the random walk of centrosomes was reduced by inhibition of the microtubule cytoskeleton, resulting in centrosomes that exhibit much less migration. Quantitatively this means a reduction in the distance travelled. Microtubule inhibition

most likely affects noncentrosomal microtubules because centrosomal microtubules are not seen during meiosis in *C. elegans* embryos; microtubule nucleation at the centrosome is initiated only once meiosis II is completed. Furthermore, depletion of SPD-5 does not appear to affect centrosome movement: nonfunctional centrosomes in *spd-5*(RNAi) embryos move similar to wildtype before the end of meiosis II. Both immunofluorescence and live imaging showed a dense and dynamic network of cortical and cytoplasmic microtubules, which I collectively refer to as cytoplasmic microtubules, that are most likely responsible for centrosome movement. Consistent with this idea, depletion of γ -tubulin, required for nucleation of microtubules but which does not affect polarity, showed that centrosome motility was not decreased but rather increased. The phenotype could be attributed to the role of TBG-1 on cytoplasmic microtubules as discussed below.

4.3 Cortical constraint of centrosome movement

Centrosomes could be seen relatively close to the cortex throughout the time prior to symmetry breaking, on average within 5 μm to the cortex. This suggests that there is a mechanism maintaining centrosome-cortex proximity. A cytoplasmic network of microtubules likely prevents exploration of the center of the embryo, constraining centrosome motion. Previous measurements of cytoplasmic microtubules point to cortical enrichment in the network, explaining why centrosomes would stay close to cortex. The authors of those measurements speculate that meiotic embryos exhibit centrally microtubule-directed transport of vesicles (Yang, 2005; McNally et al., 2006). However, the centrosome together with other sperm associated organelles, such as mitochondria and the paternal pronucleus, do not enter the middle but rather stay closer to the cortex, suggesting there may be an active mechanism for keeping such a cortical position.

Alteration of the organization of the cytoplasmic microtubule cytoskeleton by TBG-1 or RAN-1 depletion results in a reduction of cortical constraint. Centrosomes gain the ability to explore the middle of the egg (distances over 10 μm). This phenotype may be explained by a shift in microtubule morphology, density, and cortical bias.

The mechanism of noncentrosomal microtubule nucleation in meiotic worm embryos is not known. However, TBG-1 is likely to be involved in this process. Gamma tubulin is well known for its function in formation of gamma tubulin ring complexes (gamma-TURCs) - core structures involved in nucleation of microtubules. Gamma-TURCs could be distributed outside of centrosome, as satellites, and organize microtubules. Such centriolar satellites could be localized throughout the embryo cytoplasm and cortex, as the staining of a major centriole component SAS-4 resembles a dense pattern of dots. Those SAS-4 punctae could be a source of microtubule nucleation activity. In this case cortical bias could arise from spatial organization in the nucleation activity close to the cortex. Spots of nucleation activity could be anchored directly to the cortex, leading to higher density in microtubules close to cortex and thus contributing the constrained centrosome movement

Depletion of TBG-1 results in a microtubule network of lower density, with individual microtubules appearing longer. As discussed above, a reduction in the number of nucleation sites in *tbg-1*(RNAi) embryos might lead to an excess of free tubulin in the cytoplasm. Such a shift in free tubulin concentration may shift microtubule dynamics toward polymerization and growth, resulting in, long and stable microtubules. Usually the free tubulin concentration is limiting, preventing stabilization of microtubules (Luders and Stearns, 2007). The number of microtubules in *tbg-1*(RNAi) embryos was reduced overall but the microtubules that were present appeared longer than in wild type embryos. Perhaps due to increased microtubule stability in *tbg-1*(RNAi) embryos, the fixation of cytoplasmic microtubules appeared to be improved. Previous research on one-cell *C. elegans* embryo has concluded that microtubules dynamics are largely controlled by tubulin subunits availability and less directly regulated by few proteins (Srayko et al., 2005). The phenotype observed upon depletion of RAN-1, namely reduction in the density and length of noncentrosomal microtubules, may be explained along the same lines. Ran is usually involved in directing zones of microtubule nucleation around the meiotic spindle (Zhang et al., 2008). The distribution and role of the RanGTP gradient is not known for meiotic *C. elegans* embryos. However, perturbation of RAN-1 results in a striking phenotype at the meiotic spindle: the area occupied by meiotic spindle

microtubules was increased and there appeared to be more tubulin in the meiotic spindle than in wildtype. Since tubulin was enriched at the meiotic spindle in *ran-1*(RNAi) embryos, cytoplasmic free tubulin might be lowered, leading to shorter and a more sparse microtubule network.

The random walk of centrosome may be passive and resulting from growth of surrounding microtubules in all possible direction. Measurement of the microtubule growth shows similar magnitude to the maximal instantaneous velocity achieved by centrosomes. The noncentrosomal microtubule network would be therefore responsible for the stochastic character of centrosome motion. Parts of centrosome trajectory when the motion is of high straightness correspond to microtubule pushing centrosome or directly attaching to centrosome and moving it. Dwelling in one spot could occur when the centrosome falls off or when it encounters dense microtubules impeding its movement in a given direction.

Affecting cytoplasmic microtubules has an impact on the motion exerted by centrosomes. I found that centrosomes in *tbg-1*(RNAi) exhibit higher mobility, traveling larger distances with higher straightness. Such a behavior can be explained by lower microtubule density, which allows for more processive movement. Possibly, an individual microtubule can provide a straight track for a longer time than in wildtype. Also, the reduced density allows for movement deeper in the embryo.

In wild type embryos, centrosomes do not enter the egg center. The bias in the motion could result from spatial organization in the microtubule network. The nucleation activity may be enriched at the cortex resulting in higher density of microtubules close to the cortex. Subsequently apart from moving the centrosome, microtubules could also lower its mobility. The centrosome and the associated sperm organelles could be impeded to move when blocked by the dense array of microtubules. When the microtubule density is altered, as with depletion of *tbg-1*(RNAi), and there are long microtubules passing through center of the embryo also the pattern of centrosome motion is different and centrosomes can be observed in egg center.

My data could not discriminate if microtubule motors are involved in the random walk of

centrosomes. I evaluated the role of dynein (DHC-1), kinesin-13 (KLP-7) and kinesin-1 (KLC-1) in the movement. I did not observe significant defects in the motion. However, I would not exclude those motors from playing any role in the motion. The stochastic character of the process and high variability observed in wildtype embryos make the contribution difficult to judge. Furthermore, full depletion of the mentioned motors results in rapid sterility due to their involvement during meiosis.

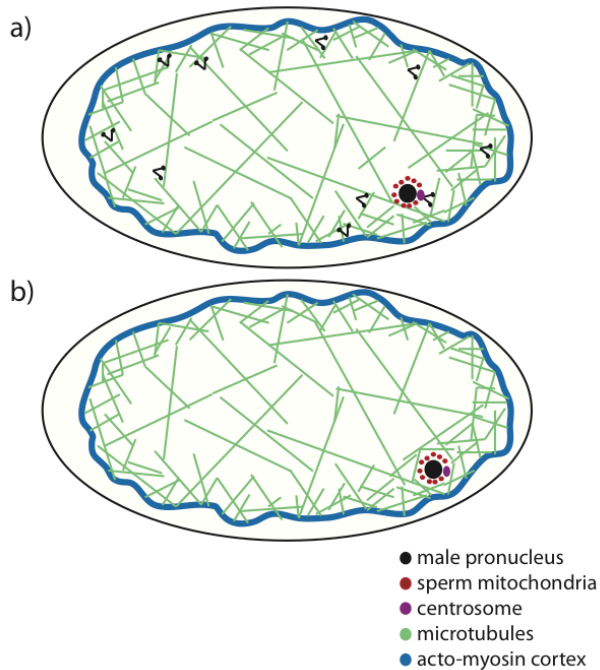


Figure 31. Model for centrosome constraint. **(a)** Centrosome is moved by microtubule motors. Cytoplasmic microtubules are denser close to the cortex. **(b)** Centrosome is immobilized among cytoplasmic microtubules, which are denser close to the cortex. The movement is passive and results from microtubule growth and shrinkage.

Conversely, centrosome and sperm associated organelles may form a complex which is too big and inaccessible for microtubule motors. The movement of such complex would then be passive resulting mainly from growth and shrinkage of the neighboring microtubules. The enrichment of microtubules close to cortex would impede movement of the complex deeper into cytoplasm. This model is not consistent with one of my results, namely that inhibition of microtubule dynamics with nocadazole, lowers mobility of the centrosome. If the movement was passive, then perturbation of microtubules should increase the overall mobility of centrosomes and facilitate movement deeper into cytoplasm which is not the case.

4.4 Movement of centrosomes to the cortex after symmetry breaking

Centrosomes were not directly at the cortex when symmetry was broken, however, they usually achieved close cortex juxtaposition shortly afterwards. The direct repositioning of centrosomes toward the cortex was dependent on polarity establishment, most likely through the action of cytoplasmic flow. Symmetry breaking initiates cytoplasmic flow directed towards the cortex, which could transport organelles such as mitochondria, the male pronucleus and centrosomes, towards the symmetry breaking site. My analysis of cytoplasmic granules, fluorescent beads, and sperm mitochondria revealed that actin-driven flow may transport those objects towards the cortex. In embryos in which the actin cytoskeleton was compromised and the flow was absent, such repositioning did not take place. Inhibition of actin polymerization with latrunculin resulted in some embryos where centrosomes never approached the cortex. In other cases, the centrosome managed to contact the cortex, but this may be because centrosomal microtubules, after time “0”, may generate pulling forces to bring centrosomes towards the cortex. Alternatively, given that pre-symmetry breaking centrosome movement was not affected by actin depolymerization, it may be that the centrosomes reach the cortex “accidentally” during the random walk. Experimental evidence shows that a centrally positioned centrosome aster nucleating microtubules in AB cell can be off-centered when microtubule growth is perturbed by the use of nocadazole (Hird and White, 1993). Additionally the inhibition of microtubules dynamics also triggers a cytoplasmic flow directed towards the proximal cortex, which moves centrosome and nucleus towards the cortex. The requirement for flow in AB cell appears to be perturbation of the microtubule aster. This case illustrates how centrosome can be repositioned towards the cortex as a result of cytoplasmic flow and independent of centrosomal microtubules. This parallels movement of centrosome observed right after symmetry breaking.

After symmetry breaking in wildtype embryos, centrosomes reach the cortex and remain in close proximity to the cortex for about 3 minutes. During this time the male pronucleus and the two centrosomes are close to the cortex and the posterior polarity domain matures. Actin flow may be pushing centrosomes and the pronucleus into direct contact

with the cortex. Centrosomal asters are growing and the number of nucleated microtubules increases. Coincident with termination of the cytoplasmic flow, male pronucleus initiates movement towards the middle of the embryo. The absence of the flow –pushing into cortex force - may allow for movement of the male pronucleus. The reason for maintaining contact between centrosome and male pronucleus is not known. One possibility is that cytoplasmic flow enforces the contact as a byproduct. The flow is essential during polarity development for distribution of cytoplasmic fate determinants.

4.5 Posteriorization

My results emphasize that the position of centrosome at the time of symmetry breaking does not matter for subsequent polarity establishment. There is post-symmetry breaking mechanism that places the centrosome at the pole of embryo along the AP axis called posteriorization. The reorientation is achieved by the whole embryo rotation within the eggshell, aligning geometry axis with polarity axis, which becomes important during division. The mechanism underlying posteriorization is not understood. The possible candidates are microtubules and cytoplasmic flow, but the process merits further investigation. Posteriorization enforces positioning of the sperm complex at the opposite pole (with the caveat of sporadic reverse polarity case) from the female pronucleus. This process may also be important for proper positioning of the posterior domain and consequent distribution of cytoplasmic cell fate determinants such as PIE-1. Defects in the posteriorization may lead to shifts in the posterior domain, which perturb polarity development (Rappleye et al., 2002). Posteriorization extends the flexibility for centrosome position, because centrosome will reach one of the egg poles regardless of its starting position.

4.6 How centrosome-cortex distance affects polarity

Why is centrosome position cortically constrained? Why is the centrosome not free to explore the whole egg volume? I was interested in understanding the reason for keeping centrosomes cortically enriched in relation to polarization efficiency. Centrosomes may

need to stay close to the cortex to facilitate signaling to the cortex during symmetry breaking. To test this idea, I correlated the distance of the centrosome to the cortex with how long it took to see the first signs of myosin II asymmetry. The result was a direct correlation between distance and delay in polarity initiation, indicating that centrosomes close to the cortex were more efficient at breaking symmetry. Centrosomes may generate a signal to break symmetry starting at the end of meiosis II, which then, depending on the position of the centrosome, reaches the cortex with some delay. My data suggests that the time for signaling from 8 μm away from cortex may last about 100 seconds. How is the signal from centrosome transported? Considering the observed delay, the signal could be transduced at the rate of 0.08 $\mu\text{m}/\text{sec}$. 2D diffusion in cytoplasm of dextran molecules was estimated to be 10-30 $\mu\text{m}^2/\text{sec}$ (Gregor et al., 2005), growth rate of microtubules during later stages in *C.elegans* embryo is equivalent to approximately 0.51 $\mu\text{m}/\text{sec}$, transport rate achieved by dynein motor (DHC-1) is 0.75-1.35 $\mu\text{m}/\text{sec}$ (Kozlowski et al., 2007), growth of actin is approximately 0.084 $\mu\text{m}/\text{sec}$ (Zhu and Carlsson, 2006). Considering the mentioned rates actin could be involved in transport of the cue. Thus symmetry breaking cue could be transduced along the cytoplasmic actin filaments. Actin cytoskeleton is required for the symmetry breaking process and it could also be involved mediating the signal.

In my analysis the timing assignment was done according to cortical symmetry breaking. It is possible that centrosomes at a distance from the cortex trigger first a physical change in the cytoplasm – cytoplasmic symmetry breaking – that then is transduced to the cortex and is not visible with the currently known markers of polarity. The current markers do not allow for assessing changes in the cytoplasm, which might indicate that symmetry is broken in cytoplasm. Observation of sperm mitochondria indicates relaxation in the “sperm compartment” correlated with the symmetry breaking event. Preliminary data suggests that the ER surrounds the sperm organelles possibly enforcing their clustered appearance. Cytoplasmic symmetry breaking could then be marked as a relaxation in the “sperm compartment”. Future studies could further investigate the use of “cluster relaxation” as a possible symmetry breaking marker.

In order to study the influence of the centrosome to the cortex I took advantage of genetic

and drug perturbations that maintain centrosome at higher distances from the cortex compared to wildtype. I also attempted to mechanically displace the centrosome. So far, I succeeded at manipulating centrosome position through centrifugation. Symmetry breaking occurred regardless of how far the centrosome was from the cortex. Next, I wanted to use a more controlled method to manipulate centrosome location, namely optical trap. I was not able to displace centrosome or any other organelle. I assumed that centrosome trapping would likewise not be possible without generating too much heat for the embryo. Furthermore centrosome displacement may be further complicated due to the fluid state of centrosomes (David Zwicker and Wallace Mashall pers comm).

Recent literature suggests that PAR-2 is enriched on the microtubules. According to PAR-2 immunofluorescence, PAR-2 signal is enriched at the cytoplasmic microtubules and at the microtubules radiating out of centrosome (Motegi et al., 2011). PAR-2 binding to microtubules protects it from inhibitory phosphorylation by PKC-3. Microtubules, rather than centrosomes, may be a source of active, uninhibited -PAR-2. According to this model, centrosomes would be required to approach the cortex to facilitate cortical localization of this polarity protein.

Thus I wanted to test whether the cortical localization of polarity marker - PAR-2 - can occur when the centrosome does not contact cortex. My data shows that direct contact between centrosome and cortex is not necessary for loading of PAR-2 onto the cortex, however there is a weak correlation between distance to the cortex and the time of PAR-2 appearance on the cortex (fig. 23b), implying that increased distance may delay establishment of cortical PAR-2. This delay is not entirely a consequence of the delay in breaking of symmetry as it was still apparent when I measured the time between symmetry breaking and cortical PAR-2 localization. All in all, centrosome-cortex distance affects timing of polarity establishment. Environmental circumstances combined with delay in a polarity initiation could be detrimental to the embryo development. The ability of centrosomes to initiate polarity from any position within embryo symmetry could be limited when other pathways are defective for example energy production.

4.7 Centrosome-cortex communication to break symmetry

Overall the results of my study imply that centrosomes do not communicate with the cortex through a direct contact, as observed in a TCR synapse (Jenkins et al., 2009), but rather they may provide a signal that reaches the cortex through some other mechanism. Several ways of transducing the symmetry breaking cue are possible. First, there may be a population of actin that reaches from the centrosome to the cortex that ruptures the actomyosin network upon centrosome signaling. Due to lack of tools to visualize cytoplasmic actin, we may not be aware of cytoplasmic actin in the egg that could not only transport the cue but could also be responsible for the motion of centrosome to the cortex. Chromosomes in starfish oocyte are transported towards the centrosome by cytoplasmic actin (Lénárt et al., 2005). Similar contribution have actin filaments in the mouse oocyte, where actin is responsible for movement of chromosomes towards the cortex (Field and Lénárt, 2011).

Thus, cytoplasmic actin could do both: contribute to transport of centrosomes and associated organelles to the cortex as well as communicate to the cortex to break symmetry upon the signal. It would be very interesting to look for cytoplasmic actin with the recently available actin probes, for instance: UtrCh (Field and Lénárt, 2011). This probe allows for cytoplasmic actin detection also in thick specimens which could be highly advantageous in at thick *C. elegans* embryo.

Alternatively a signal could be transduced cytoplasmically through vesicles. So far, dynamin dependent vesicle formation has been shown to play a role in symmetry breaking (Sophia Millonnig pers. Comm.) suggesting a possible role of vesicles. Retraction of actomyosin during symmetry breaking likely reflects changes in the plasma membrane. Certain components brought by vesicles may be incorporated at the cortex to alter curvature of the membrane or its binding affinity for Myosin II or PAR-2. The ER could also transport the signal. Prior to symmetry breaking, the ER forms a continuous network that surrounds the male pronucleus and associated sperm organelle. Furthermore, ER membrane is connected with cortex, offering a potentially efficient way of transporting information. Lastly, biochemical-signaling originating from the centrosome in form of phosphorylation may trigger changes at the cortex. The delay in symmetry breaking could be caused by the time the signal requires to reach the cortex.

4.8 Centrosome cortical constraint: a polarity-independent function?

The reason for the cortical enrichment of centrosomes may be independent of polarity. It could be advantageous for the zygote to decrease the ability of centrosome to explore the egg, for instance to prevent encounter between male and female pronucleus during female meiosis. In wildtype embryos, such an encounter occasionally occurs, but usually the pronuclei remain at the opposite poles of the egg because neither undergoes large net displacement. The female pronucleus undergoes a dramatic reduction of DNA content during meiosis, only half DNA remains in the egg after two rounds of polar body extrusion. Possibly, an encounter between the male and female pronuclei could result in mixing of DNA, leading to a loss of essential paternal chromatin. Worm embryos may therefore prevent premature pronuclear encounter by constraining the paternal pronucleus, and with it centrosome movement. A consistent phenotype observed in TBG-1, RAN-1 and in beta-tubulin (TBB-1) depleted embryos was an increase in the frequency of closely positioned male and female pronuclei during meiosis. Such embryos established polarity, but it is not known whether their DNA content is normal. There are two possibilities how two pronuclei could meet prematurely. First the sperm can enter at the side of the female pronucleus, or second, the sperm complex can move toward the female pronucleus after fertilization, for instance if the cortical constraint mechanism is defective. The meiotic spindle in *tbg-1*(RNAi) and *ran-1*(RNAi) embryos exhibited microtubules radiating out of the spindle into the cytoplasm. Such microtubules might be responsible for bringing the male pronucleus complex together with the centrosome towards the meiotic spindle, which I observed in TBG-1 depleted embryos. Whether there is an underlying preferential positioning of pronuclei at opposite poles remains to be elucidated.

Alternatively, the mechanism underlying cortical constraint of centrosome could be a side effect. Extrusion of polar bodies during meiosis requires placing the female pronucleus in vicinity of cortex. Cytoplasmic microtubules could trap female pronucleus close to the cortex intentionally, while male pronucleus would be trapped as a byproduct of this mechanism.

4.9 Does the centrosome return to a predetermined spot on the cortex?

An unresolved question in the development of *C. elegans* embryos is whether the sperm entry site is also the site on cortex where symmetry is broken. The difficulty lies in imaging development from fertilization until symmetry breaking. So far visualization of the process of fertilization in an isolated embryo is not feasible. Oocytes are very sensitive to the external environment during fertilization. One option to circumvent this problem may be in utero imaging and tracking of the centrosome. This is challenging due to the weak signal intensity of centrosome markers compared to the worm autofluorescence and centrosome signal coming from the surrounding sperms. Finally, the cortex is very dynamic and may rotate within the eggshell, making it difficult to track the site of sperm entry without a stable marker of its position on the cortex.

Goldstein and Hird attempted to address the relationship between the site of symmetry breaking and sperm entry in their paper from 1996. They defined the site as such: “position of the sperm entry was inferred by noting where the sperm pronucleus formed after the oocyte had undergone meiosis”. The inherent problem in such an assignment is the mobility of centrosome and the adjacent sperm pronucleus, which was not appreciated at the time of their analysis. As shown in my analysis, the sperm centrosome-pronucleus complex moves quite a bit within the egg. Considering that time interval between fertilization and the end of meiosis II is more than 20 minutes, such a definition of the sperm entry position is highly imprecise. Considering the trajectories I obtained from my longest timelapses, one may think that centrosome does not seem to be returning to its initial position. But once again, the cortex is not an immobilized unit and may rotate within the eggshell. Symmetry can be broken at the cortex at any spot relative to the geometry of the egg, which suggests that returning to the sperm entry site – or origin – may not be meaningful.

4.10 The sperm mitochondria contribution to the zygote?

The labeling of sperm mitochondria allowed for selective visualization of paternal mitochondria in the zygote. The dyes that gave the clearest signal, namely Mitotracker CMXRos and Rhodamine R6, are both resistant to aldehyde fixation, suggesting this dye

property may be beneficial in labeling paternal mitochondria. In general, selective labeling of mitochondria is achieved according to the membrane potential produced by respiratory chain. Fixed mitochondria lose membrane potential, after which the dye often diffuses out. Maintaining dye in the mitochondria after destroying the membrane potential relies on dye properties independent of mitochondria activity. Since paternal mitochondria in the zygote could be visualized best with fixable dyes, this may indicate that sperm mitochondria have a compromised membrane potential. The dye could have entered the mitochondria when they exhibited high respiratory function and it retained such high dye intensity regardless of later membrane potential. The problem may also lie in the long staining procedure - around 24 hrs - which exposes dyes to temperature and pH changes. Additionally because of the dye feeding strategy I developed, some dyes may be degraded in the intestine or destroyed or sequestered by the *E. coli*.

I have visualized sperm mitochondria with cellular markers that label mitochondria generally. There are several available dyes, which measure other aspects of mitochondrial physiology such as the commercially available markers to detect singlet oxygen species. Future studies could constitute of further characterization of sperm mitochondrial physiology, maybe even answer the question of their functionality in the zygote.

4.11 Sperm mitochondria are an isolated population in the embryo

Sperm mitochondria persist in the zygote in an unfused state. They do not merge with maternal mitochondria to form a fused network. The function of fusion is not entirely known, but current models indicate it could improve mitochondrial health. Some mitochondria show low occurrence of fusion, which is correlated, with low health of that mitochondrion, namely the level of oxidative damage. In other systems, fusion between mitochondria occurs when a fusion receptor is present on the mitochondrial outer membrane. Additionally, OPA-1 destines mitochondria to fuse and lack of this protein is a sign for autophagy to direct the mitochondrion for degradation (Twig et al., 2008). Sperm mitochondria may not fuse due to high oxidative damage accumulated during fertilization (low health). If that, however, was the case, it would be more likely that they should immediately be degraded through the mitophagy machinery to ensure high energetic fitness of the organism (Twig et al., 2008). Based on my time-lapse imaging

and other recent reports, this is not the case; sperm mitochondria can be observed during later development even in coma stage (350 cells). The sperm mitochondria may have lost their membrane potential and thus the ability to fuse with each other. Recent reports show that loss of potential results in cleavage of OPA-1, which inhibits fusion in those mitochondria (Arnoult et al., 2005).

Paternally contributed mitochondria cluster around the nucleus prior to symmetry breaking. Such an aggregation of mitochondria around the nucleus was previously observed in areas of high oxidative need as seen in hamster embryo (Barnett et al., 1996). Symmetry breaking is likely a high-energy event, which requires several functional mitochondria. The symmetry breaking could be initiated by break-up in sperm organelles, which subsequently could be observed as a change in cortical morphology of acto-myosin network. Furthermore, sperm mitochondria show a highly coordinated movement prior to symmetry breaking. There may be a physical barrier or linkage around the mitochondria keeping them together and thus ensuring integrity of sperm complex prior to symmetry breaking.

It would be interesting to selectively destroy the paternal mitochondria and examine consequences on polarity establishment. Photo-caged drugs could be used to locally ablate sperm mitochondria and observe the effects on symmetry breaking.

4.12 Do paternal mitochondria disappear completely during development?

Recent data (Rawi et al., 2011; Sato and Sato, 2011) on sperm mitochondria in the *C. elegans* zygote suggests that disappearance of sperm mitochondria occurs within the first few cell divisions of the embryo (3-4, 8-cell stage). The quantification in (Sato and Sato, 2011) was performed in fixed samples, using males with labeled mitochondria mated to hermaphrodites. Both of those experimental conditions – fixation and the possibility of self-fertilization - may hinder an accurate observation of sperm mitochondria. I performed a time-lapse analysis of paternally contributed mitochondria in living embryos to observe the disappearance of mitochondria rather than just quantifying their absence. I

relied on matings between males to phenotypic females. When matings are done using hermaphrodites, frequently there are some hermaphrodites that are not mated and their embryos do not show any labeled paternal mitochondria. As a consequence, those embryos would lower the total numbers of paternal mitochondria in fixed samples. Considering that immunofluorescence procedure involved crushing multiple worms together, it may be difficult to select for mated worms. The authors reported low occurrence of sperm mitochondria in older embryos, after the 64-cell stage.

A possible explanation for such result may be that embryos with labeled mitochondria did not have enough time to develop and the old embryos were fertilized with unlabeled sperm thus lowering the number of sperm mitochondria. The mating in *C. elegans* is not very robust. Despite excess of males compared to the number of hermaphrodites, it is still frequent to see unmated hermaphrodites. A further complication is that fixation may not allow for accurate quantification due to inherent variability in the fixation procedure. Instead, in my study, I performed live imaging of embryos so that I could, first, confirm that all embryos examined contained labeled paternal mitochondria and second, detect all possible paternal mitochondria within the embryo volume. From my work, I found that there was a difference in the ability to visualize mitochondria according to the type of microscopy applied. For example, fewer paternal mitochondria were detectable by wide-field microscopy - even with deconvolution - than by confocal spinning disk microscopy. The advantage of spinning disk microscopy is high sensitivity and low photobleaching. Using spinning-disk microscopy, I was able to detect sperm mitochondria in later stages of development, in contrast to results reported by the recent publications (Rawi et al., 2011; Sato and Sato, 2011).

Lastly, the method used by (Sato and Sato, 2011) that attempted to provide a quantitative analysis of disappearance of sperm mitochondria was not entirely quantitative. The analysis was performed on an unknown number of embryos and constituted measuring mitochondria according to an “area giving MT intensity [arbitrary units]”. Direct evaluation of the actual number of sperm mitochondria may be more informative. Likewise, such a measurements should be performed in living specimens to provide information how number of sperm mitochondria change over time. The (Rawi et al.,

2011) reported that sperm mitochondria are absent from the zygote at the 8-10-cell stage, unfortunately not providing a quantification.

The recent publications describe colocalization of autophagy marker - LGG-1 - with sperm mitochondria. In my experiments I looked at LGG-1 localization in the later embryo development but I did not find sperm mitochondria to colocalize with LGG-1. The fact that I do not see disappearance of mitochondria may explain the lack of colocalization between the sperm mitochondria and autophagy machinery. The difference in results may be a consequence of differences in strains and microscopy techniques used.

My results suggest that sperm mitochondria enter the egg and persist during further development. There is a reduction in the number in paternal mitochondria in the germline progenitor, suggesting that heteroplasmy in somatic cells may be tolerated but only not favored in the germline. To verify that there are no conditions that favor presence of sperm mitochondria in the germline, further experiments will be necessary. The germline may select for more fit and healthy mitochondria, regardless of their parental origin. For instance, if the oocyte experiences high levels of mtDNA damage and the sperm, in contrast, could provide healthy mtDNA, it may be beneficial to tolerate paternal mitochondria in the germline. The inclusion of paternal mitochondria in such a scenario might facilitate survival. The mechanism for clearance of sperm mitochondria from the germline is completely unknown. The germline could conceivably exclude damaged mitochondria (Jansen, 2000) or select for the fittest mitochondria. Distinguishing these possibilities will require further investigation.

5. References

Agmon, N. (2011). Single molecule diffusion and the solution of the spherically symmetric residence time equation. *J Phys Chem A* *115*, 5838–5846.

Arnoult, D., Grodet, A., Lee, Y.-J., Estaquier, J., and Blackstone, C. (2005). Release of OPA1 during apoptosis participates in the rapid and complete release of

cytochrome c and subsequent mitochondrial fragmentation. *J. Biol. Chem.* *280*, 35742–35750.

- Barnett, D. K., Kimura, J., and Bavister, B. D. (1996). Translocation of active mitochondria during hamster preimplantation embryo development studied by confocal laser scanning microscopy. *Dev. Dyn.* *205*, 64–72.
- Bastock, R., and St Johnston, D. (2008). *Drosophila* oogenesis. *Current Biology* *18*, R1082–R1087.
- Bellion, A., Baudoin, J.-P., Alvarez, C., Bornens, M., and Métin, C. (2005). Nucleokinesis in tangentially migrating neurons comprises two alternating phases: forward migration of the Golgi/centrosome associated with centrosome splitting and myosin contraction at the rear. *Journal of Neuroscience* *25*, 5691–5699.
- Caussinus, E., and Gonzalez, C. (2005). Induction of tumor growth by altered stem-cell asymmetric division in *Drosophila melanogaster*. *Nat Genet* *37*, 1125–1129.
- Conduit, P. T., and Raff, J. W. (2010). Cnn Dynamics Drive Centrosome Size Asymmetry to Ensure Daughter Centriole Retention in *Drosophila* Neuroblasts. *Curr. Biol.* *20*, 2187–2192.
- Cosmides, L. M., and Tooby, J. (1981). Cytoplasmic inheritance and intragenomic conflict. *J. Theor. Biol.* *89*, 83–129.
- Cowan, C. R., and Hyman, A. A. (2004a). Asymmetric cell division in *C. elegans*: cortical polarity and spindle positioning. *Annu. Rev. Cell Dev. Biol.* *20*, 427–453.
- Cowan, C. R., and Hyman, A. A. (2004b). Centrosomes direct cell polarity independently of microtubule assembly in *C. elegans* embryos. *Nature* *431*, 92–96.
- Cowan, C. R., and Hyman, A. A. (2006). Cyclin E-Cdk2 temporally regulates centrosome assembly and establishment of polarity in *Caenorhabditis elegans* embryos. *Nat. Cell Biol.* *8*, 1441–1447.
- CUMMINS, J. (2004). The role of mitochondria in the establishment of oocyte functional competence. *European Journal of Obstetrics & Gynecology and Reproductive Biology* *115*, S23–S29.
- de Anda, F. C., Pollarolo, G., Da Silva, J. S., Camoletto, P. G., Feiguin, F., and Dotti, C. G. (2005). Centrosome localization determines neuronal polarity. *Nature* *436*, 704–708.
- Devreotes, P. N., and Zigmond, S. H. (1988). Chemotaxis in eukaryotic cells: a focus on leukocytes and *Dictyostelium*. *Annu. Rev. Cell Biol.* *4*, 649–686.

- Doerflinger, H., Vogt, N., Torres, I. L., Mirouse, V., Koch, I., Nusslein-Volhard, C., and St Johnston, D. (2010). Bazooka is required for polarisation of the *Drosophila* anterior-posterior axis. *Development* *137*, 1765–1773.
- Doerflinger, H., Benton, R., Torres, I. L., Zwart, M. F., and St Johnston, D. (2006). *Drosophila* anterior-posterior polarity requires actin-dependent PAR-1 recruitment to the oocyte posterior. *Curr. Biol.* *16*, 1090–1095.
- Edgar, L. G. (1995). Blastomere culture and analysis. *Methods Cell Biol.* *48*, 303–321.
- Emelyanov, V. V. (2001). Rickettsiaceae, rickettsia-like endosymbionts, and the origin of mitochondria. *Biosci. Rep.* *21*, 1–17.
- Fan, W., Waymire, K. G., Narula, N., Li, P., Rocher, C., Coskun, P. E., Vannan, M. A., Narula, J., Macgregor, G. R., and Wallace, D. C. (2008). A mouse model of mitochondrial disease reveals germline selection against severe mtDNA mutations. *Science* *319*, 958–962.
- Field, C. M., and Lénárt, P. (2011). Bulk cytoplasmic actin and its functions in meiosis and mitosis. *Curr. Biol.* *21*, R825–30.
- Goldstein, B., and Hird, S. N. (1996). Specification of the anteroposterior axis in *Caenorhabditis elegans*. *Development* *122*, 1467–1474.
- GOMES, E., and GUNDERSEN, G. (2006). Real-Time Centrosome Reorientation During Fibroblast Migration. *Methods in Enzymology* *406*, 579–592.
- Gregor, T., Bialek, W., de Ruyter van Steveninck, R. R., Tank, D. W., and Wieschaus, E. F. (2005). Diffusion and scaling during early embryonic pattern formation. *Proc. Natl. Acad. Sci. U.S.A.* *102*, 18403–18407.
- Gupta, R. S. (2003). Evolutionary relationships among photosynthetic bacteria. *Photosyn. Res.* *76*, 173–183.
- Hamill, D. R., Severson, A. F., Carter, J. C., and Bowerman, B. (2002). Centrosome maturation and mitotic spindle assembly in *C. elegans* require SPD-5, a protein with multiple coiled-coil domains. *Developmental Cell* *3*, 673–684.
- Hao, Y., Boyd, L., and Seydoux, G. (2006). Stabilization of cell polarity by the *C. elegans* RING protein PAR-2. *Developmental Cell* *10*, 199–208.
- He, Y., Wu, J., Dressman, D. C., Iacobuzio-Donahue, C., Markowitz, S. D., Velculescu, V. E., Diaz, L. A., Kinzler, K. W., Vogelstein, B., and Papadopoulos, N. (2010). Heteroplasmic mitochondrial DNA mutations in normal and tumour cells. *Nature* *464*, 610–614.
- Hiiragi, T., and Solter, D. (2004). First cleavage plane of the mouse egg is not

predetermined but defined by the topology of the two apposing pronuclei. *Nature* 430, 360–364.

- Hird, S. N., and White, J. G. (1993). Cortical and cytoplasmic flow polarity in early embryonic cells of *Caenorhabditis elegans*. *The Journal of Cell Biology* 121, 1343–1355.
- Hirokawa, N., Tanaka, Y., and Okada, Y. (2009). Left-right determination: involvement of molecular motor KIF3, cilia, and nodal flow. *Cold Spring Harb Perspect Biol* 1, a000802.
- Hoekstra, R. F. (2000). Evolutionary origin and consequences of uniparental mitochondrial inheritance. *Hum. Reprod.* 15 *Suppl* 2, 102–111.
- Howard, J., Grill, S. W., and Bois, J. S. (2011). Turing's next steps: the mechanochemical basis of morphogenesis. *Nat Rev Mol Cell Biol* 12, 400–406.
- Ivanov, P. L., Wadhams, M. J., Roby, R. K., Holland, M. M., Weedn, V. W., and Parsons, T. J. (1996). Mitochondrial DNA sequence heteroplasmy in the Grand Duke of Russia Georgij Romanov establishes the authenticity of the remains of Tsar Nicholas II.
- Jansen, R. P. (2000). Germline passage of mitochondria: quantitative considerations and possible embryological sequelae. *Hum. Reprod.* 15 *Suppl* 2, 112–128.
- Januschke, J., Llamazares, S., Reina, J., and Gonzalez, C. (2011). *Drosophila* neuroblasts retain the daughter centrosome. *Nature Communications* 2, 243–6.
- Jazin, E. E., Cavelier, L., Eriksson, I., Orelund, L., and Gyllensten, U. (1996). Human brain contains high levels of heteroplasmy in the noncoding regions of mitochondrial DNA. *Proc. Natl. Acad. Sci. U.S.A.* 93, 12382–12387.
- Jenkins, M. R., Tsun, A., Stinchcombe, J. C., and Griffiths, G. M. (2009). The strength of T cell receptor signal controls the polarization of cytotoxic machinery to the immunological synapse. *Immunity* 31, 621–631.
- Jenkins, N., Saam, J. R., and Mango, S. E. (2006). CYK-4/GAP provides a localized cue to initiate anteroposterior polarity upon fertilization. *Science* 313, 1298–1301.
- Johnston, W. L., and Dennis, J. W. (2011). The eggshell in the *C. elegans* oocyte-to-embryo transition. *Genesis*, n/a–n/a.
- Kemphues, K. J., Priess, J. R., Morton, D. G., and Cheng, N. S. (1988). Identification of genes required for cytoplasmic localization in early *C. elegans* embryos. *Cell* 52, 311–320.
- Knoblich, J. A. (2008). Mechanisms of asymmetric stem cell division. *Cell* 132, 583–

597.

- Kosinski, M., McDonald, K., Schwartz, J., Yamamoto, I., and Greenstein, D. (2005). *C. elegans* sperm bud vesicles to deliver a meiotic maturation signal to distant oocytes. *Development* *132*, 3357–3369.
- Kozłowski, C., Srayko, M., and Nedelec, F. (2007). Cortical Microtubule Contacts Position the Spindle in *C. elegans* Embryos. *Cell* *129*, 499–510.
- Kraytsberg, Y., Schwartz, M., Brown, T. A., Ebralidse, K., Kunz, W. S., Clayton, D. A., Vissing, J., and Khrapko, K. (2004). Recombination of human mitochondrial DNA. *Science* *304*, 981.
- LaMunyon, C. W., and Ward, S. (2002). Evolution of larger sperm in response to experimentally increased sperm competition in *Caenorhabditis elegans*. *Proceedings of the Royal Society B: Biological Sciences* *269*, 1125–1128.
- Lénárt, P., Bacher, C. P., Daigle, N., Hand, A. R., Eils, R., Terasaki, M., and Ellenberg, J. (2005). A contractile nuclear actin network drives chromosome congression in oocytes. *Nat. Cell Biol.* *436*, 812–818.
- Li, M., Schönberg, A., Schaefer, M., Schroeder, R., Nasidze, I., and Stoneking, M. (2010). Detecting heteroplasmy from high-throughput sequencing of complete human mitochondrial DNA genomes. *Am. J. Hum. Genet.* *87*, 237–249.
- Luders, J., and Stearns, T. (2007). Microtubule-organizing centres: a re-evaluation. *Nat Rev Mol Cell Biol* *8*, 161–167.
- Mayer, M., Depken, M., Bois, J. S., Jülicher, F., and Grill, S. W. (2010). Anisotropies in cortical tension reveal the physical basis of polarizing cortical flows. *Nature* *467*, 617–621.
- McCarter, J., Bartlett, B., Dang, T., and Schedl, T. (1999). On the control of oocyte meiotic maturation and ovulation in *Caenorhabditis elegans*. *Developmental Biology* *205*, 111–128.
- McNally, K., Audhya, A., Oegema, K., and McNally, F. J. (2006). Katanin controls mitotic and meiotic spindle length. *The Journal of Cell Biology* *175*, 881–891.
- Meléndez, A., Tallóczy, Z., Seaman, M., Eskelinen, E.-L., Hall, D. H., and Levine, B. (2003). Autophagy genes are essential for dauer development and life-span extension in *C. elegans*. *Science* *301*, 1387–1391.
- Mello, C. C., Schubert, C., Draper, B., Zhang, W., Lobel, R., and Priess, J. R. (1996). The PIE-1 protein and germline specification in *C. elegans* embryos. *Nature* *382*, 710–712.

- Motegi, F., Zonies, S., Hao, Y., Cuenca, A. A., Griffin, E., and Seydoux, G. (2011). Microtubules induce self-organization of polarized PAR domains in *Caenorhabditis elegans* zygotes. *Nat. Cell Biol.* *13*, 1361–1367.
- Motosugi, N., Dietrich, J.-E., Polanski, Z., Solter, D., and Hiiragi, T. (2006). Space Asymmetry Directs Preferential Sperm Entry in the Absence of Polarity in the Mouse Oocyte. *Plos Biol* *4*, e135.
- Munro, E., Nance, J., and Priess, J. R. (2004). Cortical Flows Powered by Asymmetrical Contraction Transport PAR Proteins to Establish and Maintain Anterior-Posterior Polarity in the Early *C. elegans* Embryo. *Developmental Cell* *7*, 413–424.
- Noireaux, V., Golsteyn, R. M., Friederich, E., Prost, J., Antony, C., Louvard, D., and Sykes, C. (2000). Growing an Actin Gel on Spherical Surfaces. *Biophysical Journal* *78*, 1643–1654.
- Nonaka, S., Yoshida, S., Watanabe, D., Ikeuchi, S., Goto, T., Marshall, W. F., and Hamada, H. (2005). De Novo Formation of Left–Right Asymmetry by Posterior Tilt of Nodal Cilia. *Plos Biol* *3*, e268.
- OCONELL, K., MAXWELL, K., and WHITE, J. (2000). The *spd-2* gene is required for polarization of the anteroposterior axis and formation of the sperm asters in the *Caenorhabditis elegans* zygote. *Developmental Biology* *222*, 55–70.
- Okada, Y., Takeda, S., Tanaka, Y., Belmonte, J.-C. I., and Hirokawa, N. (2005). Mechanism of Nodal Flow: A Conserved Symmetry Breaking Event in Left-Right Axis Determination. *Cell* *121*, 633–644.
- Paluch, E., van der Gucht, J., and Sykes, C. (2006). Cracking up: symmetry breaking in cellular systems. *The Journal of Cell Biology* *175*, 687–692.
- Pelletier, L., Ozlü, N., Hannak, E., Cowan, C., Habermann, B., Ruer, M., Müller-Reichert, T., and Hyman, A. A. (2004). The *Caenorhabditis elegans* centrosomal protein SPD-2 is required for both pericentriolar material recruitment and centriole duplication. *Curr. Biol.* *14*, 863–873.
- Piel, M., Meyer, P., Khodjakov, A., Rieder, C. L., and Bornens, M. (2000). The respective contributions of the mother and daughter centrioles to centrosome activity and behavior in vertebrate cells. *The Journal of Cell Biology* *149*, 317–330.
- Quann, E. J., Merino, E., Furuta, T., and Huse, M. (2009). Localized diacylglycerol drives the polarization of the microtubule-organizing center in T cells. *Nat. Immunol.* *10*, 627–635.
- Rappleye, C. A., Tagawa, A., Le Bot, N., Ahringer, J., and Aroian, R. V. (2003).

Involvement of fatty acid pathways and cortical interaction of the pronuclear complex in *Caenorhabditis elegans* embryonic polarity. *BMC Dev Biol* 3, 8.

- Rappleye, C., Tagawa, A., Lyczak, R., Bowerman, B., and Aroian, R. (2002). The anaphase-promoting complex and separin are required for embryonic anterior-posterior axis formation. *Developmental Cell* 2, 195–206.
- Rawi, Al, S., Louvet-Vallée, S., Djeddi, A., Sachse, M., Culetto, E., Hajjar, C., Boyd, L., Legouis, R., and Galy, V. (2011). Postfertilization autophagy of sperm organelles prevents paternal mitochondrial DNA transmission. *Science* 334, 1144–1147.
- Rebollo, E., Sampaio, P., Januschke, J., Llamazares, S., Varmark, H., and Gonzalez, C. (2007). Functionally Unequal Centrosomes Drive Spindle Orientation in Asymmetrically Dividing *Drosophila* Neural Stem Cells. *Developmental Cell* 12, 467–474.
- Reese, K. J., Dunn, M. A., Waddle, J. A., and Seydoux, G. (2000). Asymmetric segregation of PIE-1 in *C. elegans* is mediated by two complementary mechanisms that act through separate PIE-1 protein domains. *Mol. Cell* 6, 445–455.
- Ren, X. D. (1999). Regulation of the small GTP-binding protein Rho by cell adhesion and the cytoskeleton. *The EMBO Journal* 18, 578–585.
- Roegiers, F., McDougall, A., and Sardet, C. (1995). The sperm entry point defines the orientation of the calcium-induced contraction wave that directs the first phase of cytoplasmic reorganization in the ascidian egg. *Development* 121, 3457–3466.
- Ryser, J. E., and Vassalli, P. (1982). Role of cell motility in the activity of cytolytic T lymphocytes. *Adv. Exp. Med. Biol.* 146, 23–39.
- Sanders, L. C., Matsumura, F., Bokoch, G. M., and de Lanerolle, P. (1999). Inhibition of myosin light chain kinase by p21-activated kinase. *Science* 283, 2083–2085.
- Sardet, C., Speksnijder, J., Inoue, S., and Jaffe, L. (1989). Fertilization and ooplasmic movements in the ascidian egg. *Development* 105, 237–249.
- Sardet, C., Dru, P., and Prodon, F. (2005). Maternal determinants and mRNAs in the cortex of ascidian oocytes, zygotes and embryos. *Biol. Cell* 97, 35–49.
- Sato, M., and Sato, K. (2011). Degradation of paternal mitochondria by fertilization-triggered autophagy in *C. elegans* embryos. *Science* 334, 1141–1144.
- Seydoux, G., and Strome, S. (1999). Launching the germline in *Caenorhabditis elegans*: regulation of gene expression in early germ cells. *Development* 126, 3275–3283.

- Solecki, D. J., Govek, E. E., Tomoda, T., and Hatten, M. E. (2006). Neuronal polarity in CNS development. *Genes & Development* *20*, 2639–2647.
- Speksnijder, J. E., de Jong, K., Linnemans, W. A., and Dohmen, M. R. (1986). The ultrastructural organization of the isolated cortex of a molluscan egg. *Prog. Clin. Biol. Res.* *217B*, 353–356.
- Srayko, M., Kaya, A., Stamford, J., and Hyman, A. A. (2005). Identification and Characterization of Factors Required for Microtubule Growth and Nucleation in the Early *C. elegans* Embryo. *Developmental Cell* *9*, 223–236.
- Stiernagle, T. (2006). Maintenance of *C. elegans*. *WormBook*, 1–11.
- Stinchcombe, J. C., Majorovits, E., Bossi, G., Fuller, S., and Griffiths, G. M. (2006). Centrosome polarization delivers secretory granules to the immunological synapse. *Nature* *443*, 462–465.
- SULSTON, E., and HORVITZ, H. R. (2003). Post-embryonic Cell Lineages of the Nematode, *Caenorhabditiselegans*. 1–47.
- Sulston, J. E., and HORVITZ, H. R. (1977). Post-embryonic cell lineages of the nematode, *Caenorhabditis elegans*. *Developmental Biology* *56*, 110–156.
- Sutovsky, P., Moreno, R. D., Ramalho-Santos, J., Dominko, T., Simerly, C., and Schatten, G. (2000). Ubiquitinated sperm mitochondria, selective proteolysis, and the regulation of mitochondrial inheritance in mammalian embryos. *Biol. Reprod.* *63*, 582–590.
- Tsang, W. Y., and Lemire, B. D. (2002). Mitochondrial genome content is regulated during nematode development. *Biochem. Biophys. Res. Commun.* *291*, 8–16.
- Turing, A. M. (1952). The Chemical Basis of Morphogenesis. *Philosophical Transactions of the Royal Society B: Biological Sciences* *237*, 37–72.
- Twig, G., Hyde, B., and Shirihai, O. S. (2008). Mitochondrial fusion, fission and autophagy as a quality control axis: the bioenergetic view. *Biochim. Biophys. Acta* *1777*, 1092–1097.
- Wallace, D. C. (2010). Colloquium paper: bioenergetics, the origins of complexity, and the ascent of man. *Proc. Natl. Acad. Sci. U.S.A.* *107 Suppl 2*, 8947–8953.
- Wrighton, K. H. (2011). Autophagy: shaping the fate of mitochondria. *Nat Rev Mol Cell Biol* *12*, 344–345.
- Yamashita, Y. M., and Fuller, M. T. (2008). Asymmetric centrosome behavior and the mechanisms of stem cell division. *The Journal of Cell Biology* *180*, 261–266.
- Yang, H. Y. (2005). Kinesin-1 mediates translocation of the meiotic spindle to the

oocyte cortex through KCA-1, a novel cargo adapter. *The Journal of Cell Biology* *169*, 447–457.

Zhang, X., Ems-McClung, S. C., and Walczak, C. E. (2008). Aurora A phosphorylates MCAK to control ran-dependent spindle bipolarity. *Mol. Biol. Cell* *19*, 2752–2765.

Zhu, J., and Carlsson, A. E. (2006). Growth of attached actin filaments. *Eur Phys J E Soft Matter* *21*, 209–222.

6.1 Acknowledgments

I would like to thank M. Mayer and S. Grill (MPI-CBG, Dresden, Germany) for the PIV code, and members of the Grill, Julicher, and Hyman labs for discussions on early stages of the project. Special thanks to Alex Dammermann and his lab members for comments and discussions.

I would like to thank the faculty and participants of the MBL Physiology Course 2010, particularly: R. Wollman, A. Besser, W. Marshall, and C. Huang for introduction to image processing and analysis.

I thank the reviewers of this thesis: Verena Jantsch and Matthieu Piel and my PhD committee: Verena Jantsch and Vic Small

I am indebted to my parents and my brother for continuous support and encouragement.

I want to thank all the present and past members of the Cowan Group. Great thanks go to Sabina Sans Sanegre, Martin Milk, Harue Wada, Sophie Millonnig, Jakob Zmajkovic, Sylvain Bertho and Jeroen Dobbelaere.

I would like to express huge gratitude to my supervisor Carrie Cowan for surviving four years of my PhD presence. I am grateful for her endless patience, support, encouragement, enthusiasm, guidance, and teaching, simply for being an amazing mentor.

6.2 Matlab scripts

```
##### closecrx.m #####

% write a txt file for closest cortex

function closecrx();
%make extract position of cortex
% have pixel ready!!!!

polarity='not'
if polarity == 'yes'
    disp(' Polarity can be established')
else
    disp(' measuring only according to pn size')
end

close all
% load centrosome position and cortex;
aa=pwd;
embryo=aa(34:43);
name=aa(34:41);
treatment=aa(42:43);
centr=[ 'cen_',treatment,name, '.mat'];
cortx=[ 'cor_',treatment,name, '.mat'];
load(centr);
load(cortx);

% load time, polarity and pixel info
[pol,pixel,dt,his]=inform3(embryo);

last=numel(coorx);
coorx=coorx(1:last);
coory=coory(1:last);
hecho=hecho(1:last);
outline=shapyy(:, :, 1:last);
coorxx=coorx(hecho==1);
cooryy=coory(hecho==1);
outline=outline(:, :, hecho==1);

% create a vector with numbers until last frame tracked
ind=1:last;
% make sure centrosome at a given frame corresponds to cortex
% create a vector only with ind_smoothed where centrosome is detected
ind_smoothed=ind(hecho==1);

corxm=pixel*coorxx;
corym=pixel*cooryy;

% smoothing coordinates

w=1;
for r=11:numel(corxm)-10
    corx(w)=mean(corxm(r-10:r+10));
    cory(w)=mean(corym(r-10:r+10));
    w=w+1;
end
w=w-1;
% indices of smoothed coordinates
ind_smoothed=ind_smoothed(11:numel(corxm)-11);

ind_time=(1:last)*dt;
```

```

tvecreal=ind_time(ind_smoothed);

tzero=find(ind_smoothed==his);
if numel(tzero)==0
    tzero=find(ind_smoothed==his-1);
end

if pol==0
    crxbreak=tzero;
elseif find(ind_smoothed==pol)>0
    crxbreak=find(ind_smoothed==pol);
elseif find(ind_smoothed==(pol+1))>0
    crxbreak=find(ind_smoothed==(pol+1));

elseif find(ind_smoothed==(pol+2))>0
    crxbreak=find(ind_smoothed==(pol+2));

elseif find(ind_smoothed==(pol+3))>0
    crxbreak=find(ind_smoothed==(pol+3));

elseif find(ind_smoothed==(pol+4))>0
    crxbreak=find(ind_smoothed==(pol+4));

elseif find(ind_smoothed==(pol+5))>0
    crxbreak=find(ind_smoothed==(pol+5));

elseif find(ind_smoothed==(pol+6))>0
    crxbreak=find(ind_smoothed==(pol+6));

elseif find(ind_smoothed==(pol-1))>0
    crxbreak=find(ind_smoothed==(pol-1));

elseif find(ind_smoothed==(pol-2))>0
    crxbreak=find(ind_smoothed==(pol-2));

elseif find(ind_smoothed==(pol-3))>0
    crxbreak=find(ind_smoothed==(pol-3));

elseif find(ind_smoothed==(pol-4))>0
    crxbreak=find(ind_smoothed==(pol-4));

elseif find(ind_smoothed==(pol-5))>0
    crxbreak=find(ind_smoothed==(pol-5));

elseif find(ind_smoothed==(pol-31))>0
    crxbreak=find(ind_smoothed==(pol-31));
end

crxbreak=crxbreak-11;
tzero=tzero-11;

trev=tvecreal-tvecreal(tzero);

s=1;
for h=1:numel(ind_smoothed)

    [A,B]=ind2sub(size(outline(:, :, s)), find(outline(:, :, s)==1));
    a=1:numel(A);
    A=A.*pixel;
    B=B.*pixel;
    b=1:numel(B);

    % Calculate distance between cortex and centrosome
    distanceCortex=sqrt((A(a)-corx(s)).^2+(B(b)-cory(s)).^2);

    % the smallest distance

```

```

mnd=min(distanceCortex);
% brute force, only chooses one point, the first one
mnd_ind=find(distanceCortex==mnd);
closest_pointA(s)=A(mnd_ind(1));
closest_pointB(s)=B(mnd_ind(1));

% distance between centrosome and closest cortex
distanceCentrosome(s)=sqrt((closest_pointA(s)-corx(s))^2+(closest_pointB(s)-
cory(s))^2);

%% PLOTTING
if s<50
    colormap(gray)
    plot(B,A, '.', 'MarkerSize',10)
    axis equal
    hold on

plot(cory(s),corx(s), 'ro',closest_pointB(s),closest_pointA(s), 'ro', 'MarkerSize',10, 'Marke
rFaceColor', 'm')
    legend(['frame number: ', int2str(ind_smoothed(s))])
    %axis equal
    pause(0.01)
    hold off
    %saveas(h,[name,int2str(s)], 'tif')
end
% remember position on the cortex at symmetry breaking
if s==crxbreak %%real_pol

    magicX=closest_pointA(s);
    magicY=closest_pointB(s);

end
s=s+1;

% remember spot closest spot on cortex for polarity frame

end
s=s-1;
h=1:numel(ind_smoothed);

dist_cortex_pol=sqrt((magicX-corx(h)).^2+(magicY-cory(h)).^2);

% Reversal of timescale
%
h=figure
plot(trev,dist_cortex_pol, '*g')
hold on
plot(trev,distanceCentrosome, '*r')
plot(trev(crxbreak),1:15, '.k')
title(['movie ', treatment, ' ', name])
xlabel('time in seconds :')
ylabel('distance to cortex, [microns]')
axis([-500 500 0 16])
saveas(h,[name, treatment, 'tzero'], 'tif')

% VELOCITY
t1=find(trev<-trev(crxbreak));
if numel(t1)>0
    index_bef=t1(end);

    % save timepoints: tzero and cortex break
    tt=[-trev(index_bef),trev(tzero),trev(crxbreak)];
    save([name,treatment, 'timepoint', '.mat'], 'tt')
    % instantenous velocity
end
index=1;
for g=2:numel(corx)-1
    velin(index)=sqrt((corx(g)-corx(g-1)).^2+(cory(g)-cory(g-1)).^2)/(trev(g)-trev(g-1));
    index=index+1;
end
index=index-1;

```

```

velin=velin(1:index-1);

% running average on velocity
for q=11:numel(velin)-10
    vel_av(q)=mean(velin(q-10:q+10));
end
%readjust time vector
trev2=trev(7:end-6);

if numel(t1)>0 & polarity=='yes'
    velbef=vel_av(index_bef:tzero);
    tbef=trev(index_bef:tzero);
    velaft=vel_av(tzero:crxbreak);
    taft=trev(tzero:crxbreak);

    %write velocity into a textfile

    ybef=[tbef;velbef];

    yaft=[taft;velaft];

    save([name,treatment,'velocbef','.mat'],'ybef')
    save([name,treatment,'velocaft','.mat'],'yaft')
end
if polarity=='not'
    % special case when there is no polarity
    % like spd-5 rnai when there is no cortex
    % breaking.
    % Time for velocity will be 100 sec .
    t1=find(trev<-99);
    if numel(t1)==0
        t1=1;
        disp('short movie')
        disp(int2str(t1))
    end
    t2=find(trev>=100);
    index_bef=t1(end);
    index_aft=t2(1);

    velbef=vel_av(index_bef:tzero);
    tbef=trev(index_bef:tzero);
    velaft=vel_av(tzero:index_aft);
    taft=trev(tzero:index_aft);
    ybef=[tbef;velbef];

    yaft=[taft;velaft];
    save([name,treatment,'velocbef','.mat'],'ybef')
    save([name,treatment,'velocaft','.mat'],'yaft')

end
y=[trev2;vel_av];
save([name,treatment,'speed','.mat'],'y')
filename=[name,treatment,'speed.txt'];
fid=fopen(filename,'a');
fprintf(fid,'%8s\t %8s\r','time','vel_av');
fprintf(fid,'%8.4f\t %8.4f\t \n',y);
fclose(fid);

cd ..

step10=(trev(1)):10:trev(end);

%step10=floor(trev(1)+2):10:trev(end);
for g=1:numel(step10)
    indixis=find(trev>step10(g));
    %timepoint should have indices of points every 10sec interval
    timepoint(g)=indixis(1);
    clear indixis
end

```

```

trev10=trev(timepoint);
distanceCentrosome10=distanceCentrosome(timepoint);

%save txt files in a directory one higher
y=[trev10;distanceCentrosome10];
% closest cortex
filename=[name,treatment,'closestxyz.txt'];
fid=fopen(filename,'a');
fprintf(fid,'%8.4f\t %8.4f\t \n',y);
fclose(fid);

if polarity=='yes'
    dist_cortex_poll10=dist_cortex_pol(timepoint);
    % distance to polarity site
    z=[trev10;dist_cortex_poll10];
    files=[name,treatment,'polsitexyz.txt'];
    fid=fopen(files,'a');
    fprintf(fid,'%8s\t %8s\r','time','dist');
    fprintf(fid,'%8.4f\t %8.4f\t \n',z);
    fclose(fid);
    % cortex breaking
    file=[name,treatment,'crxbreakt.txt'];
    fid=fopen(file,'a');
    fprintf(fid,'%8.4f\t %8.4f\t \n',trev(crxbreak),distanceCentrosome(crxbreak));
    fclose(fid)
end
if numel(t1)>0
    % how much the centrosome moved from tzero to crxbreak
    % sum every 10 sec
    step_bef=trev(index_bef):10:trev(tzero);
    if polarity=='yes'

        step_aft=trev(tzero):10:trev(crxbreak);
    else

        step_aft=trev(tzero):10:trev(index_aft);
    end
    % create a vector with coordinates evry 10 secs

    for g=1:numel(step_bef)
        indixis_bef=find(trev>=step_bef(g));
        idixis_aft=find(trev>=step_aft(g));
        %timepoint should have indices of points every 10sec interval
        timepoint_bef(g)=indixis_bef(1);
        timepoint_aft(g)=idixis_aft(1);
    end
    timepoint_bef(end+1)=tzero;
    if polarity=='yes'
        timepoint_aft(end+1)=crxbreak;
    else
        timepoint_aft(end+1)=index_aft;
    end
    % how much the centrosome moved from -crxbreak to tzero
    corxbef=corx(timepoint_bef);
    corybef=cory(timepoint_bef);
    corxaft=corx(timepoint_aft);
    coryaft=cory(timepoint_aft);
    % calculate displacements
    dispbef=((diff(corxaft)).^2+(diff(corybef)).^2);
    dispaft=((diff(corxbef)).^2+(diff(coryaft)).^2);

    travelbef=sum(dispbef);
    travelaft=sum(dispaft);

    net_disp_bef=distanceCentrosome(index_bef)-distanceCentrosome(tzero);
    if polarity=='yes'
        net_disp_aft=distanceCentrosome(tzero)-distanceCentrosome(crxbreak);
        dist_crxbreak=distanceCentrosome(crxbreak);
    else
        net_disp_aft=distanceCentrosome(tzero)-distanceCentrosome(index_aft);
    end
end

```

```

dist_crxbreak=distanceCentrosome(index_aft);
end
% distance to cortex at tzero
dist_tzero=distanceCentrosome(tzero);
% distance to cortex at crxbreak

% write into a txt file

filena=[treatment,'disp.txt'];
fid=fopen(filena,'a');
%fprintf(fid,'%8s\t %8s\r','displacement','time');
fprintf(fid,'%8.4f\t %8.4f\t %8.4f\t %8.4f\n', net_disp_bef, net_disp_aft, dist_tzero
,dist_crxbreak);
fclose(fid);
end

##### bead1.m #####

% pre-tracking, image-filtering
%% little addition for tracking

for j=1:25
    a=maxImage(:,j);
    b(:,j)=bpass(a,1,5);
end
% nice(:,j)=b;
pk=pkfnd(b,2,10);
pk(:,3)=j;

    if j<2
        pos=pk;
    else
        pos=vertcat(pos,pk);
    end
    clear pk b a
end

%% BEAD 1
% polarity frame 130
% the longest tracked bead which was also detected at 152
% was tracked from frame 49

% cortex from brightfield

% extract outline from brightfield frame

ref=double(imread('160110bead06_R3D_REF'));

max_ref = max(ref(:));
min_ref =min(ref(:));

norm_ref = (ref - min_ref)./(max_ref-min_ref);
level = graythresh(norm_ref);

thim=im2bw(norm_ref,level);
thim=~thim;
thimblur=bwareaopen(thim,80);
thimclose=imclose(thimblur,strel('disk',15));
outline=edge(thimclose,'canny',[0.025 0.1]);
[A,B]=ind2sub(size(outline),find(outline==1));

% extract outline from the bead 5

ref=double(imread('5bead_01_R3D_REF.tif'));

```

```

max_ref = max(ref(:));
min_ref =min(ref(:));

norm_ref = (ref - min_ref)./(max_ref-min_ref);
level = graythresh(norm_ref);

thim=im2bw(norm_ref,0.55);
thimclose=imclose(thim,strel('disk',7));
thimblur=bwareaopen(thimclose,500);
thimfill=imfill(thimblur,'holes');
outline=edge(thimfill,'canny',[0.025 0.1]);
[A,B]=ind2sub(size(outline),find(outline==1));

% extract outline from bead 6
ref=double(imread('6bead_03_R3D_REF.tif'));
max_ref = max(ref(:));
min_ref =min(ref(:));

norm_ref = (ref - min_ref)./(max_ref-min_ref);
level = graythresh(norm_ref);
thim=im2bw(norm_ref,0.31);
thim=~thim;
thimclose=imclose(thim,strel('disk',5));
thimblur=bwareaopen(thimclose,100);
thimfill=imfill(thimblur,'holes');
thimclose=imclose(thimfill,strel('disk',7));
thimfill=imfill(thimclose,'holes');
outline=edge(thimfill,'canny',[0.025 0.1]);
[A,B]=ind2sub(size(outline),find(outline==1));

pol=130;
% find beads which were found at the polarity timee
late=find(tr(:,3)==pol); % 152 is pol
id=tr(late,4);

% pick the beads that were tracked for more than 10 frames
p=1;
for i=1: numel(id)
    tmp=find(tr(:,4)==id(i));
    if numel(tmp)>6
        particle(p).xyz=tr(tmp,1:3);
        p=p+1;
    end
    clear tmp
end

% how many bead where tracked, in a polarity frame
% and in several frames

good_beads=numel(particle);

% BEAD PLOTTING

%%% option 1:
% one color per bead
cm=colormap(jet(good_beads));
for u=1:good_beads

plot(particle(u).xyz(:,1),particle(u).xyz(:,2),'ro','MarkerSize',2,'MarkerFaceColor',cm(u
,:))
hold on

plot(particle(u).xyz(end,1),particle(u).xyz(end,2),'ro','MarkerSize',5,'MarkerFaceColor'
,'m')
end

% option 2:

```

```

% one color per timepoints
cm=colormap(jet(pol));
p=1;
for h=1:pol
    for g=1:good_beads
        % tpt indexes position
        tpt=find(particle(g).xyz(:,3)==h);
        if tpt>0

plot(particle(g).xyz(tpt,1),particle(g).xyz(tpt,2),'ro','MarkerSize',1,'MarkerEdgeColor',
cm(p,:), 'MarkerFaceColor',cm(p,:));
        hold on
        end
        if (particle(g).xyz(tpt,3)==pol)

plot(particle(g).xyz(tpt,1),particle(g).xyz(tpt,2),'ro','MarkerSize',2,'MarkerFaceColor',
'k','MarkerEdgeColor','k')
        end
        clear tpt
        end

        p=p+1;
    end

% the first five tracks in the bead 1 encompass 200 sec
% the track six encompasses 195 sec
% here the coordinates for 200 sec before polarity are extracted
for u=1:6

    %create a time column (time interval is 5 sec).
    particle(u).xyz(:,4)=(particle(u).xyz(:,3)*5);
    pp=find(particle(u).xyz(:,3)==130);
    time_pp=particle(u).xyz(pp,4);

    first=find(particle(u).xyz(:,4)==(time_pp-200));
    if u==6
        first=1;
    end
    pixel=0.32128;
    cx=particle(u).xyz(first:pp,1)*pixel;
    cy=particle(u).xyz(first:pp,2)*pixel;
    time=particle(u).xyz(first:pp,4);

    % every 10 seconds

    ff=size(cx,1);
    timepoint=1:2:(ff-1);

    r=sqrt((diff(cx(timepoint)).^2+(diff(cy(timepoint)).^2);
    % center of mass
    cm=sum(r)/numel(r);
    bead(u).cm=cm;
    % radius if gyration
    bead(u).rg=sqrt((sum((r-cm).^2)/numel(r));

    %calculate every 10seconds!
    for h=1:2:ff-1
        dist_trav(h)=sqrt((cx(h+1)-cx(h))^2+(cy(h+1)-cy(h))^2);
        vel_in(h)=dist_trav(h)/(time(h+1)-time(h));
    end

    % average velocity
    vel_av=mean(vel_in);
    bead(u).vel=vel_av;
    % total dist traveled
    bead(u).dist_tot=sum(dist_trav);

    % distance from first to last point travelled
    bead(u).dist_ori=sqrt((cx(ff)-cx(1))^2+(cy(ff)-cy(1))^2);
    sqrt((cx(ff)-cx(1))^2+(cy(ff)-cy(1))^2)

```



```

    %figure
    % plot(cy,cx, '.')
    %clear vel_in dist_trav cx cy r cm
end

filename=['bead', '.txt']
fid=fopen(filename, 'a');
%
% % writes into file the total distance travelled, dist from first frame
% % tracked until where pol is assigned. Then time from start elapsed
% % lastly, the fourth column contain the name of the embryo
%
for u=1:6
fprintf(fid, ' %8.4f\t %8.4f\t %8.4f\t %8.4f\t %8.4f\t %8.4f\t
%8.1f\r', bead(u).dist_ori, bead(u).dist_tot, 200, bead(u).vel, bead(u).cm, bead(u).rg,
u)
end
fclose(fid);
%

##### main.m #####

%% used for recess poster, updated 30/09/2010
function main();

close all

aa=pwd;
prefix=aa(33:41);
polarity=['pol', prefix];
treatment=aa(25:31);
name=prefix;
name_cortex=[prefix, 'cortex.mat'];
name_centrosome=[prefix, 'centrosome.mat'];
load(name_cortex)
load(name_centrosome)

% use min_distance=10 when tracking things until polarity
min_distance=10;

%%
%% The thing with pixel size is that it's always 0.32128, cannot be 0.20080
%% There is aux magnification that changes that in software, but on microscope it
%% was always set for 1.0, even if software says 1.6
%%

first_frame=1;
##### polarity assignment
switch polarity
case 'pol130309_05'
    pol=27;
    pixel=0.32128; %0.2008;
    hours=load('130309_05.txt');
case 'pol150909_17'
    pol=32;
    pixel=0.32128; % 0.2008;
    hours=load('150909_17.txt');

```

```

case 'pol150909_01'
    pol=55;
    pixel=0.32128; % 0.2008;
    hours=load('150909_01.txt');
case 'pol240309_01'
    pol=20;
    pixel=0.32128; %0.2008;
    hours=load('240309_01.txt');
case 'pol240309_05'
    pol=30;
    pixel=0.32128; % 0.2008;
    hours=load('240309_05.txt');
case 'pol151009_01'
    pol=63;
    pixel=0.32128; % 0.2008;
    hours=load('151009_01.txt');
case 'pol240309_07'
    pol=45;
    pixel=0.32128; % 0.2008;
    hours=load('240309_07.txt');
case 'pol240309_08'
    pol=40;
    pixel=0.32128; % 0.2008;
    hours=load('240309_08.txt');
case 'pol260309_04'
    pol=61;
    pixel=0.32128; %0.2008;
    hours=load('260309_04.txt');
case 'pol310708_14'
    pol=22;
    pixel=0.32128;
    hours=load('310708_14.txt');
case 'pol240708_01'
    pol=24;
    pixel=0.16064;
    hours=load('240708_01.txt');
    min_distance=20;
    % case 'pol300708_37'
    %     pol=16;
    %     pixel=0.32128;
    %     time=load('300708spd2_37.txt');
case 'pol271108_23'
    pol=35;
    pixel=0.32128; %0.2008;
    hours=load('271108_23.txt');
case 'pol280708_03'
    first_frame=2;
    pol=23;
    pixel=0.16064;
    min_distance=30;
    hours=load('280708_03.txt');
case 'pol140808_00'
    pol=36;
    pixel=0.32128;
    hours=load('140808_00.txt');
case 'pol130309_01'
    pol=33;
    pixel=0.32128; %0.2008;
    hours=load('130309_01.txt');
case 'pol140808_12'
    pol=40; %35;
    pixel=0.32128;
    hours=load('140808_12.txt');
case 'pol220808_09'
    pol=60;
    pixel=.32128;
    hours=load('220808_09.txt');
case 'pol260309_07'
    pol=57; % maybe 60.
    pixel=0.32128; % 0.2008;
    hours=load('260309_07.txt');
case 'pol271108_06'
    pol=63;

```

```

    pixel=0.32128; % 0.2008;
    hours=load('271108_06.txt');

case 'pol160909_02'
    pol=47;
    pixel=0.32128;
    hours=load('160909_02.txt');
    first_frame=33;

    %% latrunculin
case 'pol050809_03'
    pol=26;
    pixel=0.32128; % 0.2008;
    hours=load('050809_03.txt');
    % case 'pol050809_17'
    % hours=load('050809_17.txt');
    % pixel=0.32128; % 0.2008;
case 'pol120809_01'
    pixel=0.32128; % 0.2008;
    pol=30;
    first_frame=4;
    hours=load('120809_01.txt');
case 'pol120809_08'
    hours=load('120809_08.txt');
    pixel=0.32128; % 0.2008;
    pol=35;
case 'pol120809_18'
    hours=load('120809_18.txt');
    pixel=0.32128; % 0.2008;
    pol=49;
    first_frame=1;
case 'pol120809_28'
    hours=load('120809_28.txt');
    pixel=0.32128; % 0.2008;
    pol=29;
    first_frame=17;
    % case 'pol130809_01' high contractility
    % hours=load('130809_01.txt');
    % first_frame=3;
    % pol=33;
    % min_distance=20;
    % pixel=0.32128; % 0.2008;
case 'pol130809_04'
    hours=load('130809_04.txt');
    pixel=0.32128; % 0.2008;
    pol=47;
    first_frame=23;
case 'pol130809_07'
    hours=load('130809_07.txt');
    pol=64;
    pixel=0.32128; % 0.2008;
    first_frame=14;
case 'pol260809_01'
    hours=load('260809_01.txt');
    pol=44;
    pixel=0.32128; % 0.2008;

case 'pol260809_13'
    pol=64;
    pixel=0.32128; % 0.2008;
    hours=load('260809_13.txt');
    min_distance=15;
case 'pol260809_17'
    hours=load('260809_17.txt');
    pixel=0.32128; % 0.2008;
    pol=20;
    first_frame=3;

case 'pol260809_20'
    hours=load('260809_20.txt');
    pol=58;
    pixel=0.32128; % 0.2008;
case 'pol260809_24'

```

```

hours=load('260809_24.txt');
pol=42;
pixel=0.32128; % 0.2008;
case 'pol270809_01'
hours=load('270809_01.txt');
pol=15;
pixel=0.32128; % 0.2008;
case 'pol270809_04'
hours=load('270809_04.txt');
pixel=0.32128; % 0.2008;
first_frame=20;
pol=29;
%moves on slide
case 'pol270809_13'
hours=load('270809_13.txt');
pol=23;
first_frame=14;
pixel=0.32128; % 0.2008;
case 'pol270809_15'
hours=load('270809_15.txt');
pixel=0.32128; % 0.2008;
pol=38;
first_frame=15;
case 'pol310809_01'
hours=load('310809_01.txt');
pixel=0.32128; % 0.2008;
pol=38;
first_frame=26;
case 'pol310809_02'
hours=load('310809_02.txt');
pixel=0.32128; % 0.2008;
pol=37;

%%% spd-5 rnai %%%%
case 'pol300709_11'
hours=load('300709_11.txt');
pixel=0.32128;
pol=38;

case 'pol300709_13'
hours=load('300709_13.txt');
pixel=0.32128;
pol=4;

case 'pol300709_14'
hours=load('300709_14.txt');
pixel=0.32128;
pol=6;

case 'pol300709_21'
hours=load('300709_21.txt');
pixel=0.32128;
pol=34;

case 'pol300709_24'
hours=load('300709_24.txt');
pixel=0.32128;
pol=34;

case 'pol300709_34'
hours=load('300709_34.txt');
pixel=0.32128;
pol=7;

case 'pol310709_01'
hours=load('310709_01.txt');
pixel=0.32128;
pol=16;

case 'pol310709_07'
hours=load('310709_07.txt');
pixel=0.32128;

```

```

pol=22;
case 'pol310709_08'
hours=load('310709_08.txt');
pixel=0.32128;
pol=30;
min_distance=10;

case 'pol310709_12'
hours=load('310709_12.txt');
pixel=0.32128;
pol=35;
min_distance=8;

case 'pol310709_15'
hours=load('310709_15.txt');
pixel=0.32128;
pol=36;
first_frame=7;

##### Nocadozole #####
case 'pol150410_03'
hours=load('150410_03.txt');
pixel=0.32128;
pol=26;

case 'pol150410_04'
hours=load('150410_04.txt');
pixel=0.32128;
pol=62;

case 'pol150410_08'
hours=load('150410_08.txt');
pixel=0.32128;
pol=74;

#####

#### nmy-2 rnai #####

case 'pol080510_08'
hours=load('080510_08.txt');
pixel=0.32128; % 0.2008;
pol=17;
first_frame=2;

case 'pol080510_10'

hours=load('080510_10.txt');
pixel=0.32128; % 0.2008;
pol=47;
first_frame=25;

case 'pol080510_22'

hours=load('080510_22.txt');
pixel=0.32128; % 0.2008;
pol=11;

case 'pol130510_05'

hours=load('130510_05.txt');
pixel=0.32128; % 0.2008;
pol=14;

case 'pol180510_02'

hours=load('180510_02.txt');
pixel=0.32128; % 0.2008;
pol=18;

```

```

case 'pol180510_04'
    first_frame=2;
    hours=load('180510_04.txt');
    pixel=0.32128; % 0.2008;
    pol=16;

case 'pol310809_16'
    first_frame=17;
    hours=load('310809_16.txt');
    pixel=0.32128; % 0.2008;
    pol=40;
    min_distance=10;

%% nocadozole

case 'pol101109_04'
    pol=57;
    pixel=0.32128;
    hours=load('101109_04.txt');

case 'pol101109_06'
    pol=43; pixel=0.32128;
    hours=load('101109_06.txt');

case 'pol101109_09'
    pol=32; pixel=0.32128;
    hours=load('101109_09.txt');
    first_frame=2;

case 'pol130809_05'
    pol=70; pixel=0.32128;
    first_frame=4;
    hours=load('130809_05.txt');

case 'pol130809_09'
    pol=21; pixel=0.32128;
    hours=load('130809_09.txt');
    first_frame=4;

case 'pol200310_03'
    pol=30; pixel=0.32128;
    hours=load('200310_03.txt');

case 'pol210709_16'
    pol=27; pixel=0.32128;
    hours=load('210709_16.txt');

case 'pol230709_03'
    pol=38; pixel=0.32128;
    hours=load('230709_03.txt');
    first_frame=14;

case 'pol230709_11'
    pol=35; pixel=0.32128;
    hours=load('230709_11.txt');
    first_frame=11;

case 'pol230709_16'
    pol=61; pixel=0.32128;
    hours=load('230709_16.txt');

    first_frame=37;
    %%% cyk-1 rnai noc %%%
case 'pol030609_01'
    pol=24; pixel=0.32128;
    hours=load('030609_01.txt');
    first_frame=2;

case 'pol030609_05'

```

```

    pol=33; pixel=0.32128;
    hours=load('030609_05.txt');
    first_frame=12;

case 'pol1030609_08'
    pol=34; pixel=0.32128;
    hours=load('030609_08.txt');

case 'pol1060809_01'
    pol=60; pixel=0.32128;
    hours=load('060809_01.txt');

case 'pol1220609_01'
    pol=28; pixel=0.32128;
    hours=load('220609_01.txt');
    first_frame=2;

case 'pol1220609_08'
    pol=49; pixel=0.32128;
    hours=load('220609_08.txt');

case 'pol1220609_10'
    pol=73; pixel=0.32128;
    hours=load('220609_10.txt');

case 'pol1220609_13'
    pol=63; pixel=0.32128;
    hours=load('220609_13.txt');

    %%%%% ran-1 rnai %%%%%%%%%%%%%%%

case 'pol140310_07'
    pol=62; pixel=0.32128;
    hours=load('140310_07.txt');
    first_frame=40;

case 'pol150310_01'
    pol=25; pixel=0.32128;
    hours=load('150310_01.txt');

case 'pol170210_01'
    pol=26; pixel=0.32128;
    hours=load('170210_01.txt');

case 'pol170210_04'
    pol=15; pixel=0.32128;
    hours=load('170210_04.txt');

case 'pol170210_08'
    pol=15; pixel=0.32128;
    hours=load('170210_08.txt');

case 'pol170210_12'
    pol=22; pixel=0.32128;
    hours=load('170210_12.txt');
    first_frame=2; % or 2

case 'pol190210_02'
    pol=35; pixel=0.32128;
    hours=load('190210_02.txt');

case 'pol190210_13'
    pol=40; pixel=0.32128;
    hours=load('190210_13.txt');
    first_frame=2; % or 7

case 'pol190210_18'
    pol=40; pixel=0.32128;
    hours=load('190210_18.txt');

    %%%%%% dhc-1 rnai

```

```

case 'pol080510_01'
  pol=31; pixel=0.32128;
  hours=load('080510_01.txt');
  first_frame=11;

case 'pol080510_10'
  pol=32; pixel=0.32128;
  hours=load('080510_01.txt');
  first_frame=9;

case 'pol080510_16'
  pol=7; pixel=0.32128;
  hours=load('080510_16.txt');
  min_distance=20;

case 'pol080510_19'
  pol=41; pixel=0.32128;
  hours=load('080510_19.txt');
  first_frame=4;

case 'pol080510_23'
  pol=19; pixel=0.32128;
  hours=load('080510_23.txt');
  first_frame=4;
  min_distance=10;

case 'pol130510_08'
  pol=34; pixel=0.32128;
  hours=load('130510_08.txt');
  first_frame=7;

case 'pol130510_11'
  pol=38; pixel=0.32128;
  hours=load('130510_11.txt');
  min_distance=10;

case 'pol130510_14'
  pol=43; pixel=0.32128;
  hours=load('130510_14.txt');
  first_frame=21;

case 'pol180510_01'
  pol=10; pixel=0.32128;
  hours=load('180510_01.txt');

case 'pol180510_10'
  pol=49; pixel=0.32128;
  hours=load('180510_10.txt');
  first_frame=5;

case 'pol220410_07'
  pol=48; pixel=0.32128;
  hours=load('220410_07.txt');
  first_frame=39;

  %%%%%%%%% klp-7 rnai %%%%%%%%%

case 'pol210410_03'
  pol=49; pixel=0.32128;
  hours=load('210410_03.txt');
  first_frame=13;

case 'pol210410_13'
  pol=29; pixel=0.32128;
  hours=load('210410_13.txt');

case 'pol220410_05'
  pol=30; pixel=0.32128;
  hours=load('220410_05.txt');
  first_frame=3;

```



```

case 'pol220410_12'
  pol=30; pixel=0.32128;
  hours=load('220410_12.txt');
  first_frame=4;

case 'pol230410_10'
  pol=54; pixel=0.32128;
  hours=load('230410_10.txt');

case 'pol230410_12'
  pol=52; pixel=0.32128;
  hours=load('230410_12.txt');
  first_frame=23;

case 'pol230410_22'
  pol=50; pixel=0.32128;
  hours=load('230410_22.txt');
  first_frame=7;

case 'pol230410_28'
  pol=45; pixel=0.32128;
  hours=load('230410_28.txt');

  first_frame=8;
case 'pol240410_22'
  pol=53; pixel=0.32128;
  hours=load('240410_22.txt');
  first_frame=2;

case 'pol260410_03'
  pol=33; pixel=0.32128;
  hours=load('260410_03.txt');
  % the dis is so large because the embryo
  % moves a lot on the slide
  min_distance=80;

  %%% noc plus %%%

case 'pol011109_11'
  %polarity from top
  pol=58; pixel=0.32128;
  hours=load('011109_11.txt');

case 'pol021109_05'
  pol=17; pixel=0.32128;
  hours=load('021109_05.txt');

case 'pol021109_09'
  pol=56; pixel=0.32128;
  hours=load('021109_09.txt');

case 'pol021109_18'
  pol=47; pixel=0.32128;
  hours=load('021109_18.txt');

case 'pol031109_01'
  pol=63; pixel=0.32128;
  hours=load('031109_01.txt');

case 'pol031109_06'
  pol=59; pixel=0.32128;
  hours=load('031109_06.txt');

case 'pol031109_10'
  pol=64; pixel=0.32128;
  hours=load('031109_10.txt');

```

```

case 'pol061109_05'
  pol=39; pixel=0.32128;
  hours=load('061109_05.txt');

case 'pol091109_01'
  pol=49; pixel=0.32128;
  hours=load('091109_01.txt');

case 'pol091109_04'
  pol=53; pixel=0.32128;
  hours=load('091109_04.txt');

case 'pol091109_05'
  pol=53; pixel=0.32128;
  hours=load('091109_05.txt');
  first_frame=17;

case 'pol091109_06'
  pol=59; pixel=0.32128;
  hours=load('091109_06.txt');
  min_distance=80;

case 'pol271009_03'
  pol=52; pixel=0.32128;
  hours=load('271009_03.txt');
  first_frame=4;
  min_distance=10;

case 'pol291009_01'
  pol=65; pixel=0.32128;
  hours=load('291009_01.txt');

  %%%%%%%%% centrifuged %%%%%%%%%
case 'pol090909_10'
  pol=43; pixel=0.32128;
  hours=load('090909_10.txt');
  first_frame=20;

case 'pol090909_17'
  pol=34; pixel=0.32128;
  hours=load('090909_17.txt');

case 'pol090909_24'
  pol=17; pixel=0.32128;
  hours=load('090909_24.txt');

case 'pol100909_40'
  pol=14; pixel=0.32128;
  hours=load('100909_40.txt');

case 'pol110909_01'
  pol=29; pixel=0.32128;
  hours=load('110909_01.txt');

case 'pol110909_06'
  pol=45; pixel=0.32128;
  hours=load('110909_06.txt');

case 'pol110909_12'
  pol=32; pixel=0.32128;
  hours=load('110909_12.txt');
  min_distance=30;

case 'pol141009_11'
  pol=71; pixel=0.32128;
  hours=load('141009_11.txt');
  first_frame=8;

case 'pol151009_01'

```

```

    pol=58; pixel=0.32128;
    hours=load('151009_01.txt');

    %%% taxol things (like dhc-1)
case 'pol190510_03'
    pol=6; pixel=0.32128;
    hours=load('190510_03.txt');

case 'pol190510_05'
    pol=21; pixel=0.32128;
    hours=load('190510_05.txt');

case 'pol190510_09'
    pol=67; pixel=0.32128;
    hours=load('190510_09.txt');
    first_frame=55;

case 'pol190510_12'
    pol=35; pixel=0.32128;
    hours=load('190510_12.txt');
    first_frame=3;

case 'pol280410_01'
    pol=21; pixel=0.32128;
    hours=load('280410_01.txt');
    first_frame=3;
case 'pol280410_03'
    pol=35; pixel=0.32128;
    hours=load('280410_03.txt');
    first_frame=5;

case 'pol280410_09'
    pol=43; pixel=0.32128;
    hours=load('280410_09.txt');
    first_frame=3;

case 'pol290410_02'
    pol=66; pixel=0.32128;
    hours=load('290410_02.txt');

case 'pol290410_11'
    pol=43; pixel=0.32128;
    hours=load('290410_11.txt');
    first_frame=4;
    min_distance=10;

    %%% taxol and dhc-1 rnai
case 'pol010610_15'
    pol=37; pixel=0.32128;
    hours=load('010610_15.txt');

case 'pol010610_20'
    pol=20; pixel=0.32128;
    hours=load('010610_20.txt');

case 'pol010610_21'
    pol=12; pixel=0.32128;
    hours=load('010610_21.txt');

case 'pol030610_01'
    pol=49; pixel=0.32128;
    hours=load('030610_01.txt');

case 'pol030610_04'
    pol=32; pixel=0.32128;
    hours=load('030610_04.txt');

case 'pol030610_05'
    pol=54; pixel=0.32128;
    hours=load('030610_05.txt');

case 'pol030610_06'

```

```

    pol=27; pixel=0.32128;
    hours=load('030610_06.txt');

case 'pol290410_03'
    pol=7; pixel=0.32128;
    hours=load('290410_03.txt');

case 'pol290410_04'
    pol=24; pixel=0.32128;
    hours=load('290410_04.txt');
    first_frame=12;

    %%%% wve-1 rnai %%%%%%%%%%%%%%%

case 'pol140709_05'
    pol=15;
    pixel=0.32128; %0.2008;
    hours=load('140709_05.txt');
case 'pol140709_07'
    pol=22;
    pixel=0.32128; %0.2008;
    hours=load('140709_07.txt');

case 'pol140709_09'
    pol=36;
    pixel=0.32128;
    hours=load('140709_09.txt');

    first_frame=1;
case 'pol150709_09'
    pol=23;
    pixel=0.32128; %0.2008;
    hours=load('150709_09.txt');
    first_frame=3;
case 'pol150709_13'
    pol=27;
    pixel=0.32128; %0.2008;
    hours=load('150709_13.txt');
    first_frame=3;
case 'pol160709_01'
    pol=59;
    pixel=0.32128; %0.2008;
    hours=load('160709_01.txt');
case 'pol160709_06'
    pol=29;
    pixel=0.32128; %0.2008;
    hours=load('160709_06.txt');
case 'pol160709_08'
    pol=28;
    pixel=0.32128; %0.2008;
    hours=load('160709_08.txt');
    first_frame=2;
case 'pol220709_08'
    pol=24;
    pixel=0.32128; %0.2008;
    hours=load('220709_08.txt');
case 'pol220709_10'
    pol=23;
    pixel=0.32128; %0.2008;
    hours=load('220709_10.txt');
end

if exist('hours')==1
    for (c=1:(length(hours)))
        tt(c,1)=hours(c,1)*3600+hours(c,2)*60+hours(c,3);
    end
    for (g=1:(length(tt)))
        time(g)=tt(g)-tt(length(g));
    end
end

```

```

end

%% the idea is to graph things passed polarity, like 10 more timepoints
%last=pol;

last=size(image_thresholded,3)
for ii=1:last
    centro_dots(:, :, ii)=bwmorph(image_thresholded(:, :, ii), 'shrink', Inf);
end

% sometimes need to start everything at second or third frame,
% but the default will be 1.

%pol130309_05=24; %pol150909_17=32; %pol240309_01=20; %pol151009_01=24 %% check?
%pol240309_08=35; %pol260309_04=61; %pol310708_14=22; %pol300708_37=15;
%pol271108_23=32; %pol140808_00=36; %240309_05=30;

tracker

corx=coorx(hecho==1);
cory=coory(hecho==1);
% special case for one movie
if prefix=='130809_07'
    disp('i do it')
    corx=corx+70;
    cory=cory+70;
end

if prefix=='280708_03'
    disp('i do it')
    cory=cory+125;
end

end

if prefix=='190510_05'
    disp('i do it')
    cory=cory+100;
end

if prefix=='270809_04'
    disp('i do it')
    corx=corx+50;
    cory=cory+50;
end

if prefix=='140709_09'
    corx=corx+50;
    cory=cory+150;
end

cortex=edgeImage(:, :, first_frame:last);
outline=cortex(:, :, (hecho==1));
tpt=1:numel(corx);
time=time(first_frame:last);
indices=tpt(hecho==1);
time=time(hecho==1);

s=1;

h=figure
for h=1:numel(indices)

    [A,B]=ind2sub(size(outline(:, :, s)), find(outline(:, :, s)==1));
    a=1:numel(A);
    A=A; %.*pixel;
    B=B; %.*pixel;
    b=1:numel(B);
    % put a sqrt
    distanceCortex=sqrt((A(a)-corx(s)).^2+(B(b)-cory(s)).^2);

```

```

% the smallest distance
mnd=min(distanceCortex);
% brute force, only chooses one point, the first one
mnd_ind=find(distanceCortex==mnd);
closest_pointA(s)=A(mnd_ind(1));
closest_pointB(s)=B(mnd_ind(1));

% distance between centrosome and closest cortex
distanceCentrosome(s)=sqrt((closest_pointA(s)-corx(s))^2+(closest_pointB(s)-
cory(s))^2);

colormap(gray)
imagesc(outline(:,s))
hold on

plot(cory(s),corx(s),'ro',closest_pointB(s),closest_pointA(s),'ro','MarkerSize',10,'Marke
rFaceColor','m')
legend(['frame number: ', int2str(indices(s))])
%axis equal
%pause(0.1)

hold off
%saveas(h,[prefix,int2str(s)],'tif')
s=s+1;
%close all
end
s=s-1;
close all

corx=coorx(hecho==1).*pixel;
cory=coory(hecho==1).*pixel;

if prefix=='130809_07'
    disp('i do it')
    corx=corx+70*pixel;
    cory=cory+70*pixel;
end

if prefix=='190510_05'
    disp('i do it')
    cory=cory+100*pixel;
end

if prefix=='280708_03'
    disp('i do it')
    cory=cory+125*pixel;
end

if prefix=='270809_04'
    disp('i do it')
    corx=corx+50*pixel;
    cory=cory+50*pixel;
end

if prefix=='140709_09'
    corx=corx+50*pixel;
    cory=cory+150*pixel;
end
% subtract from polarity the number of frames taken out by first_frame-1
polarity=pol-first_frame-1;

% real_pol takes into account that centrosome was missed/not tracked
% in some frames and thus corx(polarity) is not really position at the
% polarity

real_pol=sum(hecho(1:polarity));
% calculation of the closest distance to cortex, things in microns

s=1;

```

```

for h=1:numel(indices)

    [A,B]=ind2sub(size(outline(:,:,s)),find(outline(:,:,s)==1));
    a=1:numel(A);
    A=A.*pixel;
    B=B.*pixel;
    b=1:numel(B);
    % put a sqrt
    distanceCortex=sqrt((A(a)-corx(s)).^2+(B(b)-cory(s)).^2);

    % the smallest distance
    mnd=min(distanceCortex);
    % brute force, only chooses one point, the first one
    mnd_ind=find(distanceCortex==mnd);
    closest_pointA(s)=A(mnd_ind(1));
    closest_pointB(s)=B(mnd_ind(1));

    % distance between centrosome and closest cortex
    distanceCentrosome(s)=sqrt((closest_pointA(s)-corx(s))^2+(closest_pointB(s)-
cory(s))^2);
    colormap(gray)
    plot(B,A, '.')
    axis equal
    hold on

plot(cory(s),corx(s), 'ro',closest_pointB(s),closest_pointA(s), 'ro', 'MarkerSize',10, 'Marke
rFaceColor', 'm')
    legend(['frame number: ', int2str(indices(s))])
    %axis equal

    pause(0.01)
    hold off

    if s<=real_pol
        y(s,:)= [cory(s),corx(s),closest_pointB(s),closest_pointA(s)]
    end
    %saveas(h,[prefix,int2str(s)], 'tif')
    if s==real_pol

        magicX=closest_pointA(s);
        magicY=closest_pointB(s);

    end
    s=s+1;

    % remember spot closest spot on cortex for polarity frame
end
s=s-1;

h=1:numel(indices);
dist_cortex_pol=sqrt((magicX-corx(h)).^2+(magicY-cory(h)).^2);

% time=time-time(end);
% h=figure
% plot(time,distanceCentrosome, '*')
% title(['movie ', treatment, ' ', prefix])
% xlabel('time in seconds :')
% ylabel('distance to cortex, [microns]')
% axis([-1000 0 0 16])
% saveas(h,[prefix, treatment, '_dist_cortex'], 'tif')
%figure
%
%
% for t=1:numel(indices)
%     cm=colormap(jet(numel(corx)));
%     plot(cory(t),corx(t), 'ro', 'MarkerFaceColor', cm(t,:))
%     hold on
%     plot(closest_pointB(t),closest_pointA(t), 'ro', 'MarkerFaceColor', cm(t,:))
%     title('color-coded centrosome and closest crtx')
% end

```

```

%save([prefix, 'distcor'],'time' , 'distanceCentrosome');

%% graph to show dist to cortex overall, goes passed timepoint '0'
zero_time=real_pol;
time2=time-time(real_pol);
trev=time2;
ind200=find(time2<1 & time2>=-220);
corx200=corx(ind200);
cory200=cory(ind200);
time200=time2(ind200);
indear=find(time2>=time2(1) & time2<=-220);
last_one=numel(ind200);

t_pol=size(y,1);
ty=trev(1:t_pol);
y(:,5)=ty';
save([name,treatment,'cencrx','.mat'],'y')

r=figure
plot(time2,distanceCentrosome, '*')
title(['movie ', treatment, ' ', prefix])
xlabel('time in seconds :')
ylabel('distance to cortex at each timepoint, [microns]')
axis([-1000 400 0 16])
saveas(r,[prefix, treatment, '_dist_cortex_overall'],'tif')

%% graph distance of centrosome to cortex at the time of polarity

c=figure
plot(time2,dist_cortex_pol, '*')
title(['movie ', treatment, ' ', prefix])
xlabel('time in seconds :')
ylabel('distance to cortex at polarity, [microns]')
axis([-1000 400 0 16])

saveas(c,[prefix, treatment, '_dist_cortex_atpolarity'],'tif')

% track in the embryo
g=figure
[A,B]=ind2sub(size(outline(:, :, real_pol)), find(outline(:, :, real_pol)==1));
A=A*pixel;
B=B*pixel;
plot(B,A, '.')
hold on
plot(cory(1:real_pol), corx(1:real_pol))
mcx=mean(corx(1:real_pol));
mcy=mean(cory(1:real_pol));
plot(cory(real_pol), corx(real_pol), '.', 'MarkerSize', 5)
axis([mcy-10 mcy+10 mcx-10 mcx+10])
legend([treatment, ' ', prefix])
saveas(g,[prefix, treatment, 'track'],'tif')
% calculate distance travelled until frame
% with polarity establishment
saveas(g,[prefix, treatment, 'track'],'psc2');
% for l=1:real_pol-1
%   dist_travelled(l)=sqrt((corx(l+1)-corx(l))^2+(cory(l+1)-cory(l))^2);
% end
%
% % distance between ori and polarity position
% dist_ori=sqrt((corx(real_pol)-corx(1))^2+(cory(real_pol)-cory(1))^2);
% % total dist
% dist_tot=sum(dist_travelled);

% measuring things in the last 200 sec prior to polarity
% find indices for time interval -220 sec until polarity (t=0)

for h=1:(last_one-1)
    dist_trav200(h)=sqrt((corx200(h+1)-corx200(h))^2+(cory200(h+1)-cory200(h))^2);

```



```

    vel_in(h)=dist_trav200(h)/(time200(h+1)-time200(h));
end
vel_av200=mean(vel_in);
dist_ori200=sqrt((corx200(last_one)-corx200(1))^2+(cory200(last_one)-cory200(1))^2);
dist_tot200=sum(dist_trav200);

% distance to closest cortex from centrosome at the first timepoint
% from range -220sec-175 sec ==> ind200(1)
cen_cortex_closest=distanceCentrosome(ind200(1));

%distance to closest-cortex-at-polarity from centrosome
% from range -220sec-175 sec
cen_cortex_pol=dist_cortex_pol(ind200(1));
% distance to cortex of centrosome at time zero== polarity
cen_cortex_at_pol=dist_cortex_pol(ind200(last_one));
cen_cortex_end=distanceCentrosome(end);
if numel(indear)>1
    cen_crx_early=distanceCentrosome(indear(1))-cen_cortex_closest;
    cen_polsite_early=dist_cortex_pol(indear(1))-cen_cortex_pol;
    cen_crx_0=cen_cortex_closest-cen_cortex_at_pol;
    cen_polsite_0=cen_cortex_pol-cen_cortex_at_pol;
    cen_crx_end=cen_cortex_end-cen_cortex_at_pol;
end

%obtain maximum distance to polarity site: dist_cortex_polarity
dtx=max(dist_cortex_pol(1:zero_time));
% index of the maximum distance to polarity site, useful in time vector
ind_dtx=find(dist_cortex_pol==dtx);
dtx_time=trev(ind_dtx(1));
%distance to cortex at polarity
dt_pol=dist_cortex_pol(ind200(last_one));
x_bar=dtx-dt_pol;

cx=corx(1:real_pol);
cy=cory(1:real_pol);
% r defines displacement
r=sqrt((diff(cx)).^2+(diff(cy)).^2);
cm=sum(r)/numel(r);
rg=sqrt((sum((r-cm).^2)/numel(r));

cd ..

%write the data into a txt file
% Maximum displacemet
filena=['mxdisp',treatment, '.txt'];
fid=fopen(filena,'a+');
fprintf(fid, '%8.4f\t %8.4f\r', x_bar, dtx_time);
fclose(fid);

filus=[treatment, 'distances.txt']
fid=fopen(filus,'a+');
% write distance to cortex at first timepoin, -200, and 0 sec
fprintf(fid, ' %8.4f\t %8.4f\t %8.4f\t %8.4f\t %8.4f\t %8.9s\r',
distanceCentrosome(1),time2(1),cen_cortex_closest,cen_cortex_at_pol,time200(1),prefix);
fclose(fid);

filename=[treatment, 'crx.txt']
fid=fopen(filename,'a');

% writes into file the total distance travelled, dist from first frame
% tracked until where pol is assigned. Then time from start elapsed
% lastly, the fourth column contain the name of the embryo

fprintf(fid, ' %8.4f\t %8.4f\t %8.4f\t %8.4f\t
%8.9s\r',cen_cortex_closest,cen_cortex_pol,cen_cortex_at_pol,time200(1),prefix);
fclose(fid);

if numel(indear)>1

```

```

        filok=['netdisp',prefix,'.txt'];
        fid=fopen(filok,'a+');
        fprintf(fid,'%8.4f\t %8.4f\t %8.4f\t %8.4f\t %8.4f\t %8.9s\r',
cen_crx_early,cen_polsite_early,cen_crx_0,cen_polsite_0,cen_crx_end,prefix);
        fclose(fid)
end
filename=[treatment,'good.txt']
fid=fopen(filename,'a');
% wrtiting distances, rg, prefix etc.
fprintf(fid, '%8.4f\t %8.4f\t %8.4f\t %8.4f\t %8.4f\t %8.4f\t
%8.9s\r',dist_ori200,dist_tot200,time200(1),vel_av200,cm,rg, prefix)
fclose(fid);

% save time200 and distance to cortex in a text file,
% two columns
y=[time2;distanceCentrosome]; % need to put the variables in matrix
filename=[prefix,'closestcrx.txt'];
fid=fopen(filename,'a');
fprintf(fid, '%8s\t %8s\r', 'time', 'distance');
fprintf(fid, '%8.4f\t %8.4f\t \n',y);
fclose(fid);

x=[time2;dist_cortex_pol']; % need to put the variables in matrix
filename=[prefix,'polaritycrx.txt'];
fid=fopen(filename,'a');
fprintf(fid, '%8s\t %8s\r', 'time', 'distance');
fprintf(fid, '%8.4f\t %8.4f\t \n',x);
fclose(fid);

##### tracker.m #####
% vector initialization

p=1; % having internal indexing so reading a move can start anywhere

previous_good=0;
hecho=zeros(last-first_frame,1);
coorx=zeros(last-first_frame,1);
coory=zeros(last-first_frame,1);
coorxi=zeros(last-first_frame,1);
cooryi=zeros(last-first_frame,1);
coorxa=0;
coorya=0;
% min_distance specifies a step that can be taken by a centrosome
% on a average

%% jumps
% it may happen that there is a jump of centrosome
% need to manually specify it
%% for 061009spd2h2b_03
% if k==3
%     min_distance=40;
% end

%min_distance=30;
dist_two_centrosomes=5;

for k=first_frame:last
    %extra condition for movie 061009spd2h2b_03
    %     if k==3
    %         min_distance=40;
    %     end

    disp([' Doing frame : ',int2str(k)])
    %%% Centrosome initialization
    sample=centro_dots(:, :,k);

```

```

% 'nr' is number of row, 'nc' is number of column
[nr,nc]=size(sample);
% find indices above the threshold
ind=find(sample > 0);
howmany=numel(ind);
%convert index from find to row and column
rc=[mod(ind,nr),floor(ind/nr)+1];

% hopefully this is the right dot which represents centrosome...
if previous_good==0 && howmany==1
    coorx(p)=rc(1,1);
    coory(p)=rc(1,2);
    hecho(p)=1;
    previous_good=p;
    disp('i got the first one')
end
% Catching centrosome for the second time, self-check
% if more than one point in the first frame
if previous_good==0 && howmany>1
    coorx(p)=rc(1,1);
    coory(p)=rc(1,2);
    hecho(p)=1;
    previous_good=p;
    %alternative initializing centrosome
    for u=1:howmany
        coorxa(p)=rc(u,1);
        coorya(p)=rc(u,2);
    end
end

%%%%% second centrosome catching
if sum(hecho==1)
    % one spot found and it's close to previously found spot
    if howmany==1 && sqrt((rc(1,1)-coorx(previous_good))^2+(rc(1,2)-
coory(previous_good))^2)<min_distance
        % correction mechanism if previous frame had two spots in close
        % distance and the wrong one was picked
        if coorxa>0 && sqrt((rc(1,1)-coorxa(previous_good))^2+(rc(1,2)-
coorya(previous_good))^2)<sqrt((rc(1,1)-coorx(previous_good))^2+(rc(1,2)-
coory(previous_good))^2)
            coorx(p-1)=coorxa(previous_good);
            coory(p-1)=coorya(previous_good);
            hecho(p)=1;
            previous_good=p;
            disp('alternative cnetrosome initialization')
        end
        coorx(p)=rc(1,1);
        coory(p)=rc(1,2);
        hecho(p)=1;
        previous_good=p;
        disp('one spot found')
    end

    if howmany>1
        % calculate sd to the first point for all of them
        for u=1:howmany
            sd(u)=(sqrt((rc(u,1)-coorx(previous_good))^2+(rc(u,2)-
coory(previous_good))^2));
        end
        % sort the distances
        sorted_dist=sort(sd);
        % indices of the spots in close vicinity
        within_range=find(sorted_dist<min_distance);
        indo=numel(within_range);
        % save the closest point
        % case there is one point in vicinity
        if indo==1
            first=find(sd==sorted_dist(1));
            coorx(p)=rc(first,1);
            coory(p)=rc(first,2);
            hecho(p)=1;
            previous_good=p;
        end
    end
end

```



```

        first=find(sd==sorted_dist(1));
        coorx(p)=rc(first,1);
        coory(p)=rc(first,2);
        hecho(p)=1;
        previous_good=p;
        second=find(sd==sorted_dist(2));
        coorxi(p)=rc(second,1);
        cooryi(p)=rc(second,2);
        hecho(p)=1;
        previous_good=p;
        disp('multiple spots in close vicinity')
        if indo>2
            disp('more than two spots in close vicinity, need to work on it')
        end
    end
end
% in case nothing at all was detected
if howmany==0
    hecho(p)=0;
    disp(['nothing in frame', intstr(k)])
end
end
%% internal indexing
p=p+1;
clear indx howmany rc indo sd sorted_dist within_range ind
end
p=p-1;

% % sorry, you need to click on the first centrosome!
% imagesc(centrosome(:, :, 2));
% [x, y] = ginput(1);
% x=ceil(x);
% y=ceil(y);
% if howmany==1

%     norm_sub=sample;
%     mx=[];
%     if howmany>1
%         k=1:howmany
%     end

%     close_pixels_x=x-6:x+6;
%     close_pixels_y=y-6:y+6;
%
%     h=0;
%     for k=1:howmany
%
%         if find(close_pixels_x==rc(k,1))>0 & find(close_pixels_y==rc(k,2))>0
%             h=h+1;
%             blobx(h)=rc(k,1);
%             bloby(h)=rc(k,2);
%         end
%     end
%
%     x_center=ceil(mean(blobx));
%     y_center=ceil(mean(bloby));

##### major_scripto.m #####

% need to load cortex mask usually from rfp, sometimes from
% gfp channel
clear all
close all
pathnow=pwd;
prefix=pathnow(33:48);

```

```

name_cortex=[prefix, 'cortex.mat'];
name_histone=[prefix, 'rfpimage_thres.mat'];
name_centrosome=[prefix, 'gfpimage_thres.mat'];
cd rfp
% % load the cortex mask
if exist(name_cortex)==2
    load(name_cortex)
    cortex=edgeImage;
end
% load the histone mask
load(name_histone)
histone=image_thresholded;
clear image_thresholded;
cd ..
cd gfp
% load the cortex mask, extracted with cortex.m
if exist(name_cortex)==2
    load(name_cortex)
    cortex=edgeImage;
end
% load centrosome mask
load(name_centrosome)
centrosome=image_thresholded;
% actually it will need an image thinned down to a single dot

last=size(centrosome,3);
%extra for 081009spd2h2b_01
% last=25
%extra for 131009spd2h2b_02
%last=56
for ii=1:last
    centro_dots(:,:,ii)=bwmorph(centrosome(:,:,ii),'shrink',Inf);
end
clear image_thresholded;
cd ..

% run the tracker to obtain the coordinates for centrosome

tracker % tracker.m

% find the middle of the centroid

% since the male nucleus has to be in proximity
% of the centrosome, then create a zoom area with
% centrosome being in the middle

% hicho equals one when histone is detected in a frame
hicho=zeros(last,1);
g=1;
first=1;
for h=1:last
    if hecho(h)==1
        hista=histone(:,:,h);
        % zoom in the vicinity of centrosome
        % to be close to male pronucleus

        % zoomy and zoomx are vectors
        % which encompass +/- 20 neighbourhood
        y=coory(h);
        x=coorx(h);
        zoomy=[ y-15 y-15 y-10 y-10 y-10 y-5 y-5 y-5 y y y y y y y y+5
y+5 y+5 y+10 y+10 y+10 y+15 y+15 y+15];
        zoomx=[ x x-15 x x+10 x-10 x x-5 x+5 x x x+5 x-5 x+10 x-10 x+15 x+15
x+5 x-5 x x+10 x-10 x x+15 x-15];

        L=bwselect(hista,zoomy,zoomx);

```

```

        % save center of mass for male histone
        stats=regionprops(L,'Centroid');
        if numel(stats)==1
            disp(int2str(h))
            histx(h)=stats(1).Centroid(1,1);
            histy(h)=stats(1).Centroid(1,2);
            hicho(g)=1;
            g=g+1;
        end
    else
        disp(int2str(h))
    end
end
g=g-1;
last_tracked=g;

save([prefix, 'H2B_SPD2'], 'coorx', 'coory', 'hecho', 'histx', 'histy', 'hicho')
coorx=coorx(hecho==1);
coory=coory(hecho==1);
histxx=histx(hecho==1);
histyy=histy(hecho==1);

for w=1:last_tracked
    imagesc(cortex(:, :, w))
    title(int2str(w))
    plot(coory(w), coorx(w), 'ro')
    hold on
    if histx(w)>0
        plot(histxx(w), histyy(w), '+')
    end
    pause(0.5)
end
%%%%%%%%%%%%%%%%%%%%%%%%%%%%%%%%%%%%%%%%%%%%%%%%%%%%%%%%%%%%%%%%%%%%%%%%%%
% find closest spot on cortex

tpt=1:numel(coorx);
indices=1:tpt;

indices=tpt(hecho==1);

%% Only work with things where centrosome has been found
% sometimes when histone was detected but centrosome wasn't
% this will be ignored
outline=cortex(:, :, (hecho==1));

s=1;

h=figure
for h=1:numel(indices)

    [A,B]=ind2sub(size(outline(:, :, s)), find(outline(:, :, s)==1));
    a=1:numel(A);
    b=1:numel(B);
    % put a sqrt
    distanceCortex=sqrt((A(a)-coorx(s)).^2+(B(b)-coory(s)).^2);

    % the smallest distance
    mnd=min(distanceCortex);
    % brute force, only chooses one point, the first one
    mnd_ind=find(distanceCortex==mnd);
    closest_pointA(s)=A(mnd_ind(1));
    closest_pointB(s)=B(mnd_ind(1));

    % distance between centrosome and closest cortex
    distanceCentrosome(s)=sqrt((closest_pointA(s)-coorx(s))^2+(closest_pointB(s)-
coory(s))^2);

    % in case there is a centrosome and no histone... ignore histone
    if histx(s)>0
        % distance between histone and closest cortex to centrosome
        distanceHistone(s)=sqrt((closest_pointA(s)-histx(s))^2+(closest_pointB(s)-
histy(s))^2);

```

```

end
%h=figure
colormap(gray)
imagesc(outline(:,:,s))
hold on

plot(cory(s),corx(s), 'ro',closest_pointB(s),closest_pointA(s), 'ro', 'MarkerSize',10, 'Marke
rFaceColor', 'm')
legend(['frame number: ', int2str(s)])
%axis equal
pause(0.5)

hold off
%saveas(h,[prefix,int2str(s)], 'tif')
s=s+1;
%close all
end
s=s-1;

t=figure
plot(indices,distanceCentrosome, 'ro')
hold on
for d=1:numel(indices)
    if distanceHistone(d)>0
        plot(indices(d),distanceHistone(d), '+')
    end
    title([prefix, 'movie'])
    xlabel('indices')
    ylabel('closest distance to cortex for centrosome [units]')
    legend('centrosome', 'male pronucleus')
end

saveas(t,[prefix, 'spd2h2b'], 'tif')

```

```

##### closest_point_cortex.m #####

```

```

% find closest spot on cortex

tpt=1:numel(coorx);
indices=1:tpt;
corx=coorx(hecho==1);
cory=coory(hecho==1);
indices=tpt(hecho==1);

%%
liny=outline(:,:, (hecho==1));

%for s=1:numel(files)
s=1;
%for h=starting_frame:ending_frame
h=figure
    for h=1:numel(indices)

[A,B]=ind2sub(size(liny(:,:,s)),find(liny(:,:,s)==1));

% find a way of finding the very first point

a=1:numel(A);
b=1:numel(B);
% put a sqrt
distanceCortex=sqrt((A(a)-corx(s)).^2+(B(b)-cory(s)).^2);
% the smallest distance
mnd=min(distanceCortex);
% brute force, only chooses one point, the first one
mnd_ind=find(distanceCortex==mnd);

```



```

closest_pointA(s)=A(mnd_ind(1));
closest_pointB(s)=B(mnd_ind(1));

%h=figure
    colormap(gray)
    imagesc(linyy(:, :, s))
    hold on

plot(cory(s), corx(s), 'ro', closest_pointB(s), closest_pointA(s), 'ro', 'MarkerSize', 10, 'MarkerFaceColor', 'm')
    legend(['frame number: ', int2str(s)])
    axis([50 500 100 500])
    %axis equal
    pause(0.001)

    hold off
%saveas(h,[prefix,int2str(s)], 'tif')
    s=s+1;
    %close all
end

% find a way of finding the very first point
% s=s-1;
% for t=1:numel(indices)
%     cm=colormap(jet(numel(indices)));
%     plot(cory(t), corx(t), 'ro', 'MarkerFaceColor', cm(t, :))
%     hold on
%     plot(closest_pointB(t), closest_pointA(t), 'ro', 'MarkerFaceColor', cm(t, :))
%
% end
%
```

```
##### centrosome_extrax #####
```

```

function [coorx, coory, hecho]=centrosome_extrax(tpt, maxImage)

p=1; % having internal indexing so reading a move can start anywhere

previous_good=0;
hecho=zeros((tpt), 1);

for j=1:tpt

    disp(['frame: ', int2str(j)])

    sub=maxImage(:, :, j);
    max_sub = max(sub(:));
    min_sub = min(sub(:));

    norm_sub = (sub - min_sub)./(max_sub-min_sub);

    % find threshold value
    % 'nr' is number of row, 'nc' is number of column
    [nr, nc]=size(norm_sub);
    % zb is number of bins
    zb=10;
    [freq, binVal]=hist(reshape(norm_sub(:), nr*nc, 1), zb);
    % set a threshold intensity
    th=binVal(zb);

    % find indices above the threshold
    ind=find(norm_sub > th);

    mx=[];
    n=numel(ind);

    %convert index from find to row and column

```

```

for i=1:n
    r=rc(i,1);c=rc(i,2);

    if r>1 & r<nr & c>1 & c<nc
        if norm_sub(r,c)>=norm_sub(r-1,c-1) & norm_sub(r,c)>=norm_sub(r,c-1) &
norm_sub(r,c)>=norm_sub(r+1,c-1) & ...
            norm_sub(r,c)>=norm_sub(r-1,c) & norm_sub(r,c)>=norm_sub(r+1,c) &
...
            norm_sub(r,c)>=norm_sub(r-1,c+1) & norm_sub(r,c)>=norm_sub(r,c+1) &
norm_sub(r,c)>=norm_sub(r+1,c+1)
                mx=[mx,[r,c]'];
            end
        end
    end
end

mx=mx';

[npks,crap]=size(mx);
nmx=npks;
%disp(int2str(npks))
%% initialize first centrosome
if previous_good==0 & npks==1
    coorx(p)=mx(1,1);
    coory(p)=mx(1,2);
    hecho(p)=1;
    previous_good=p;
    disp('i got the first one')
end

% in case the first centrosome are two bright spots next to each other
if previous_good==0 && npks==2 && sqrt((mx(1,1)-mx(2,1))^2+(mx(1,2)-mx(2,2))^2)<8
    disp('i got the first centrosome')
    disp([int2str(j)])
    coorx(p)=ceil(mx(1,1)+mx(2,1))/2;
    coory(p)=ceil(mx(1,2)+mx(2,2))/2;
    hecho(p)=1;
    previous_good=p;
end

if previous_good==0 && npks==2
    coorx(p)=mx(1,1);
    coory(p)=mx(1,2);
    hecho(p)=1;
    previous_good=p;
    %alternative initializing centrosome
    coorxa(p)=mx(2,1);
    coorya(p)=mx(2,2);
end

if sum(hecho)==1
    if npks==1 && sqrt((mx(1,1)-coorx(previous_good))^2+(mx(1,2)-
coory(previous_good))^2)<10
        coorx(p)=mx(1,1);
        coory(p)=mx(1,2);
        hecho(p)=1;
        previous_good=p;

        disp('one')
    end
    if npks==1 && sqrt((mx(1,1)-coorxa(previous_good))^2+(mx(1,2)-
coorya(previous_good))^2)<10
        coorx(p)=mx(1,1);
        coory(p)=mx(1,2);
        hecho(p)=1;
        previous_good=p;
        coorx(p-1)=coorxa(1);
        coory(p-1)=coorya(1);
    end
end

```

```

        disp('two')
    end
    if npks==2 && sqrt((mx(1,1)-coorx(previous_good))^2+(mx(1,2)-
coory(previous_good))^2)<8 && sqrt((mx(2,1)-coorx(previous_good))^2+(mx(2,2)-
coory(previous_good))^2)<10
        disp('two centrosomes in the frame')
        disp([int2str(j)])
        coorx(p)=ceil(mx(1,1)+mx(2,1))/2;
        coory(p)=ceil(mx(1,2)+mx(2,2))/2;
        hecho(p)=1;
        previous_good=p;
        disp('three')
    end
    if npks==2 && sqrt((mx(1,1)-coorxa(previous_good))^2+(mx(1,2)-
coorya(previous_good))^2)<8 && sqrt((mx(2,1)-coorxa(previous_good))^2+(mx(2,2)-
coorya(previous_good))^2)<8
        disp('two centrosomes in the frame')
        disp([int2str(j)])
        coorx(p)=ceil(mx(1,1)+mx(2,1))/2;
        coory(p)=ceil(mx(1,2)+mx(2,2))/2;
        hecho(p)=1;
        previous_good=p;
        coorx(p-1)=coorxa(1);
        coory(p-1)=coorya(1);
        disp('four')
    end

end

if sum(hecho)>1
    % Centrosome tracking
    if npks==1 && sqrt((mx(1,1)-coorx(previous_good))^2+(mx(1,2)-
coory(previous_good))^2)<20
        coorx(p)=mx(1,1);
        coory(p)=mx(1,2);
        hecho(p)=1;
        previous_good=p;
    end

    if npks==2 && sqrt((mx(1,1)-coorx(previous_good))^2+(mx(1,2)-
coory(previous_good))^2)<8 && sqrt((mx(2,1)-coorx(previous_good))^2+(mx(2,2)-
coory(previous_good))^2)<10
        disp('two centrosomes in the frame')
        disp([int2str(j)])
        coorx(p)=ceil(mx(1,1)+mx(2,1))/2;
        coory(p)=ceil(mx(1,2)+mx(2,2))/2;
        hecho(p)=1;
        previous_good=p;
    end

    if npks==2 && sqrt((mx(1,1)-coorx(previous_good))^2+(mx(1,2)-
coory(previous_good))^2)>10 && sqrt((mx(2,1)-coorx(previous_good))^2+(mx(2,2)-
coory(previous_good))^2)>10
        r=1:npks;
        sd(r)=sqrt((mx(r,1)-coorx(previous_good)).^2+(mx(r,2)-coory(previous_good)).^2);
        ind_close=find(sd<24);
        closest_point=find(sd==min(sd));
        coorx(p)=(mx(closest_point,1));
        coory(p)=(mx(closest_point,2));
        hecho(p)=1;
        previous_good=p;
    end

end

if npks>2
    r=1:npks;
    sd(r)=sqrt((mx(r,1)-coorx(previous_good)).^2+(mx(r,2)-coory(previous_good)).^2);
    ind_close=find(sd<10);
    closest_point=find(sd==min(sd));
    disp([int2str(ind_close)])

    % it's important to be checking for numel(ind_close) because
    % this is just an index, when it's 2 doesn't mean the were two
    % pairs that were found...

```

```

    if numel(ind_close)==2
        coorx(p)=ceil(mx(ind_close(1),1)+mx(ind_close(2),1))/2;
        coory(p)=ceil(mx(ind_close(1),2)+mx(ind_close(2),2))/2;
        hecho(p)=1;
        previous_good=p;
        disp('case 1')
    end
    if numel(ind_close)==1
        coorx(p)=mx(ind_close,1);
        coory(p)=mx(ind_close,2);
        hecho(p)=1;
        previous_good=p;
        disp('case 2')
    end
    if numel(ind_close)>2 & sd(closest_point)<6
        coorx(p)=mx(closest_point,1);
        coory(p)=mx(closest_point,2);
        hecho(p)=1;
        previous_good=p;
        disp('case 3')
    end
end
end
clear ind_close closest_point sd mx

%end
clear norm_sub
p=p+1;
end
p=p-1;

% Display the centrosome
%
% mnx=min(coorx(hecho==1));
% mxx=max(coorx(hecho==1));
% mny=min(coory(hecho==1));
% mxy=max(coory(hecho==1));
%
% cm=colormap(jet(numel(coorx)));
% for f=1:numel(coorx)
%     plot(coorx(f),coory(f),'ro','MarkerFaceColor',cm(f,:))
%     axis([mnx-5 mxx+5 mny-5 mxy+5])
%     legend(['frame number', int2str(f)])
%     pause(0.1)
%     hold on
% end
%
%
% for h=1:tpt
%     imagesc(linyy(:, :,h))
%     colormap(gray)
%     hold on
%     plot(coory(h),coorx(h),'ro')
%     pause(0.5)
% end

##### cortex_extrax.m #####

function [linyy]=cortex_extrax(tpt,meanImage)

for k=1:tpt
    %normalize the image
    sub=meanImage(:, :,k);
    max_sub = max(sub(:));
    min_sub = min(sub(:));

```

```

norm_sub = (sub - min_sub)./(max_sub-min_sub);

    % mask the image
disks = graythresh(norm_sub);
BW = im2bw(norm_sub,disks);
    % clean the mask to obtain nice edges
aBW=bwareaopen(BW,25);
BW_fill = imfill(aBW, 'holes');
closeIm=imclose(BW_fill,strel('disk',3));
edIm=edge(closeIm,'canny',[0.025 0.1]);
dilIm=imdilate(edIm,strel('disk',5));
erodIm=imerode(dilIm,strel('disk',5));
thinIm=bwmorph(erodIm,'thin',Inf);
liny(:, :,k)=thinIm;

end

%% Graph extracted lines
% for k=1:tpt
% imagesc(liny(:, :,k))
% axis equal
% colormap(gray)
% pause(0.5)
% end

end

##### angle_power2.m #####

% % % % % angle power
coorxx=coorx(hecho==1);
cooryy=coory(hecho==1);
o=1;
% instanteneous angle
for g=2:numel(coorxx)
    beta(o)=atan2((cooryy(g)-cooryy(g-1)),(coorxx(g)-coorxx(g-1)));
    if o>1

        teta(o)=beta(1)+beta(o);
    end
    o=o+1;

    beta_d(g)=beta(o)*(180/3.14);
%     beta_start(g)=atan2((cooryy(g)-cooryy(1)),(coorxx(g)-coorxx(1)));
%     beta_start_d(g)=beta_start(g)*(180/3.14);
%     if beta_start_d(g)>0 && beta_start_d(g)<89.99
%         turni(g)=1;
%     end
%     if beta_start_d(g)>=89.99 && beta_start_d(g)<200
%         turni(g)=2;
%     end
%     if beta_start_d(g)>-200 && beta_start_d(g)<=-90
%         turni(g)=3;
%     end
%     if beta_start_d(g)>-90 && beta_start_d(g)<=0
%         turni(g)=4;
%     end

end

% dot product angle calculation

%%% dot product gives lots of zeros...

% for c=1:(numel(coorxx)-2)
%     len(c,1)=sqrt((coorxx(c+1)-coorxx(c))^2+(cooryy(c+1)-cooryy(c))^2);
%     len(c,2)=sqrt((coorxx(c+2)-coorxx(c+1))^2+(cooryy(c+2)-cooryy(c+1))^2);
%     len(c,3)=sqrt((coorxx(c)-coorxx(c+2))^2+(cooryy(c)-cooryy(c+2))^2);
%     len(c,4)=(len(c,1)^2+(len(c,2))^2-(len(c,3))^2)/(2*(len(c,1))*(len(c,2)));

```

```

%     len(c,5)=acosd(len(c,4))
% end

% h = findobj(gca,'Type','patch');
% set(h,'FaceColor','r','EdgeColor','w')
% hold on
h1=hist(beta_d(1:124),4)
h2=hist(beta_d(125:248),4)
h3=hist(beta_d(275:323),4)
h4=hist(beta_d(324:373),4)

##### stream_cen.m #####

clear all
close all
clc

% centrosome detection in a stream movie

% there is no filtering with large window to avoid losing autofluorescence
files=dir('*.tif');
%for n=1:numel(files)

starting_frame=1;
ending_frame=numel(files); %last;

p=1; % having internal indexing so reading a movie can start anywhere

min_dist=15;
previous_good=0;
hecho=zeros((ending_frame),1);
tracker=1;
for j=starting_frame:ending_frame
    display(['Doing frame: ',int2str(j)])
    raw=double(imread(files(j).name));
    % raw=SampleMovie(:,:,p);

    % using gaussian filtering with 1sigma
    Ss = fspecial('gaussian',7,1);
    Filter_Ss = imfilter(raw,Ss,'symmetric');

    % background dispersion

    Ls = fspecial('gaussian',210,30);
    Filter_Ls = imfilter(raw, Ls, 'symmetric');

    imSmooth = Filter_Ss - Filter_Ls;
    sub=imSmooth;
    % normalize the norm_subage
    max_sub = max(sub(:));
    min_sub = min(sub(:));

    norm_sub = (sub - min_sub)./(max_sub-min_sub);

    % find threshold value
    % 'nr' is number of row, 'nc' is number of column
    [nr,nc]=size(norm_sub);
    % zb is number of bins
    zb=8;
    [freq,binVal]=hist(reshape(norm_sub(:),nr*nc,1),zb);
    % set a threshold intensity
    th=binVal(zb);

    % find indices above the threshold

```

```

ind=find(norm_sub > th);

mx=[];
n=numel(ind);

%convert index from find to row and column
rc=[mod(ind,nr),floor(ind/nr)+1];
for i=1:n
    r=rc(i,1);c=rc(i,2);

    if r>1 & r<nr & c>1 & c<nc
        if norm_sub(r,c)>=norm_sub(r-1,c-1) & norm_sub(r,c)>=norm_sub(r,c-1) &
norm_sub(r,c)>=norm_sub(r+1,c-1) & ...
norm_sub(r,c)>=norm_sub(r-1,c) & norm_sub(r,c)>=norm_sub(r+1,c) &
...
norm_sub(r,c)>=norm_sub(r-1,c+1) & norm_sub(r,c)>=norm_sub(r,c+1) &
norm_sub(r,c)>=norm_sub(r+1,c+1)
            mx=[mx,[r,c]'];
        end
    end
end

mx=mx';

[npks,crap]=size(mx);
nmx=npks;
%disp(int2str(npks))
%% initialize first centrosome
if previous_good==0 & npks==1
    coorx(p)=mx(1,1);
    coory(p)=mx(1,2);
    hecho(p)=1;
    previous_good=p;
    disp('i got the first one')
end

if npks==1 && sqrt((mx(1,1)-coorx(previous_good))^2+(mx(1,2)-
coory(previous_good))^2)<min_dist
    coorx(p)=mx(1,1);
    coory(p)=mx(1,2);
    hecho(p)=1;
    previous_good=p;
end

if npks==2 && sqrt((mx(1,1)-coorx(previous_good))^2+(mx(1,2)-
coory(previous_good))^2)<min_dist && sqrt((mx(2,1)-coorx(previous_good))^2+(mx(2,2)-
coory(previous_good))^2)<min_dist
    disp('two centrosomes in the frame')
    disp([int2str(j)])
    coorx(p)=ceil(mx(1,1)+mx(2,1))/2;
    coory(p)=ceil(mx(1,2)+mx(2,2))/2;
    hecho(p)=1;
    previous_good=p;
end

if npks>2
    r=1:npks;
    sd=sqrt((mx(r,1)-coorx(previous_good)).^2+(mx(r,2)-coory(previous_good)).^2);
    ind_close=find(sd<8);
    closest_point=find(sd==min(sd));
    disp([int2str(ind_close)])

    % it's important to be checking for numel(ind_close) because
    % this is just an index, when it's 2 doesn't mean the were two
    % pairs that were found...
    if numel(ind_close)==2
        coorx(p)=ceil(mx(ind_close(1),1)+mx(ind_close(2),1))/2;
        coory(p)=ceil(mx(ind_close(1),2)+mx(ind_close(2),2))/2;
        hecho(p)=1;
    end
end

```

```

        previous_good=p;
        disp('case 1')
    end
    if numel(ind_close)==1
        coorx(p)=mx(ind_close,1);
        coory(p)=mx(ind_close,2);
        hecho(p)=1;
        previous_good=p;
        disp('case 2')
    end
    if numel(ind_close)>2 & sd(closest_point)<6
        coorx(p)=mx(closest_point,1);
        coory(p)=mx(closest_point,2);
        hecho(p)=1;
        previous_good=p;
        disp('case 3')
    end
end
clear ind_close closest_point sd mx

%% %% %% clearing some variables just in case...
% % intensity calc
% if hecho(p)==1
%     c=ceil(coorx(p));
%     r=ceil(coory(p));
%     matryca=raw(c-5:c+5,r-5:r+5);
%     stored(:,:,sum(hecho(1:p)))=matryca;
% end
% int(p)=sum(sum(matryca));
%
% c_bg=c-20;
% r_bg=r-20;
% matryca_bg=raw(c_bg-5:c_bg+5,r_bg-5:r_bg+5);
% stored_bg(:,:,p)=matryca_bg;
% int_bg(p)=sum(sum(matryca_bg));
%

    p=p+1;
end
p=p-1;

%
% inth=int(hecho==1);
% for e=6:365
%     int_av(e)=mean(inth(e-5:e+5));
%     int_avbg(e)=mean(int_bg(e-5:e+5));
% end
%
%     for e=6:365
%         imagesc(stored(:,:,ind_det(e)))
%         pause(0.5)
%     end
%

mnx=min(coorx(hecho==1));
mxx=max(coorx(hecho==1));
mny=min(coory(hecho==1));
mxy=max(coory(hecho==1));

cm=colormap(jet(numel(coorx)));
for f=1:numel(coorx)
    plot(coorx(f),coory(f),'ro','MarkerFaceColor',cm(f,:))
    axis([mnx-5 mxx+5 mny-5 mxy+5])
    legend(['frame number', int2str(f)])
    pause(0.1)
    hold on
end

% Create time information, time interval is 0.33 sec

```



```

%
% i=1:250;
% tvec(i)=i.*0.33;
% tvec_adjust=tvec(hecho==1);
%
% plot(tvec(1:25),mean_squared_d(1:25),'*')
% hold on
% plot(tvec(1:25),2*tvec(1:25),'ro')
%
% % velocity measurement
%
% % instanteneous velocity
% for z=2:numel(coorxx)
%     vel_in(z)=sqrt((coorxx(z)-coorxx(z-1)).^2+(cooryy(z)-cooryy(z-1)).^2)/(tvec_adjust(z)-tvec_adjust(z-1));
%
% end
% % average velocity / over each ten points that were detected
% % maybe better to account only for like every 10*0.33sec points.. missing
% % and gaps
%
% t=2:10:numel(coorxx);
% for k=2:ceil(numel(coorxx)/10)
%     vel_av(k)=mean(vel_in(t(k-1):t(k)));
% end
% % time adjustment
% tvec_av= tvec(t); % only choose timepoints used in averaging
%
%
% figure
% plot(tvec_adjust,vel_in)
% hold on
% plot(tvec_av,vel_av)
% title('instantenous velocity vs average velocity')
%

```

outlinestream.m

```

clear all
close all

% this code is good for bleached streaming movies from spinning disk
% there is no filtering with large window to avoid losing autofluorescence
files=dir('*.tif');
%for n=1:numel(files)
p=1; % having internal indexing so reading a movie can start anywhere
for n=1:numel(files)
    files(n).name
    SampleMovie(:,:,p)=double(imread(files(n).name));
    p=p+1;
end

disp('Now doing the loop')
%for j=1:numel(files)

%% specify how many files are being used
nn_images=numel(files);

for j=1:nn_images
    raw=SampleMovie(:,:,j);
    %noise and background filtering

    % using gaussian filtering with 1sigma

```

```

Ss = fspecial('gaussian',7,1);
Filter_Ss = imfilter(raw,Ss,'symmetric');

%   % background dispersion
%   Ls = fspecial('gaussian',210,30); % 210 30
%   Filter_Ls = imfilter(raw, Ls, 'symmetric');
%
%   imSmooth = Filter_Ss - Filter_Ls;
%   sub=imSmooth;
sub=Filter_Ss;
% normalize the norm_subage
max_sub = max(sub(:));
min_sub = min(sub(:));

norm_sub = (sub - min_sub)./(max_sub-min_sub);

%create a binary image
level = graythresh(norm_sub);
level=level*1.35;

image1=im2bw(norm_sub,level);
%figure
%imshow(image1,[])

image1(:,1)=zeros(size(image1(:,1)));
image1(:,end)=zeros(size(image1(:,end)));
image1(1,:)=zeros(size(image1(1,:)));
image1(end,:)=zeros(size(image1(end,:)));

newImage=image1;

for c=1:35
display(['Loop: ',int2str(c)])
level=0.99*level;
currentImage=im2bw(norm_sub,level);
currentImage(:,1)=zeros(size(currentImage(:,1)));
currentImage(:,end)=zeros(size(currentImage(:,end)));
currentImage(1,:)=zeros(size(currentImage(1,:)));
currentImage(end,:)=zeros(size(currentImage(end,:)));

tmp=currentImage-newImage;
[nr,nc]=find(tmp);

points_in=[];

% look for bright neighbours => 4x check
for i=1:length(nr)
if (newImage(nr(i)+1,nc(i))==1 || newImage(nr(i)-1,nc(i))==1)...
|| (newImage(nr(i),nc(i)+1)==1 || newImage(nr(i),nc(i)-1)==1) || ...
(newImage(nr(i)+1,nc(i)+1)==1 || newImage(nr(i)-1,nc(i)-1)==1)...
|| (newImage(nr(i)+1,nc(i)-1)==1 || newImage(nr(i)-1,nc(i)+1)==1)
points_in=vertcat(points_in,[nr(i) nc(i)]);

end
end

goesIn=zeros(size(tmp));
for f=1:length(points_in)
goesIn(points_in(f,1),points_in(f,2))=1;
end

newImage=newImage+goesIn;
newImage=bwareaopen(newImage,3);
% figure(115)
% imagesc(newImage)
% pause(0.1)
end
workIm=newImage;
opArIm=bwareaopen(workIm,10);

```

```

closeIm=imclose(opArIm,strel('disk',3));
edIm=edge(closeIm,'canny',[0.025 0.1]);
dilIm=imdilate(edIm,strel('disk',5));
erodIm=imerode(dilIm,strel('disk',5));
thinIm=bwmorph(erodIm,'thin',Inf);

%subplot(2,1,1)cc
%imshow(thinIm,[]);
%subplot(2,1,2)
%imshow(SampleMovie(:,:,j),[]);

%% get coordinates of the line
[A,B]=ind2sub(size(thinIm),find(thinIm==1));

% save the coordinates marking timeframe
outline(j).xc=A;
outline(j).yc=B;

imagesc(thinIm)
shape(:,:,j)=thinIm;
pause(0.1)
end

```

Dominika Bienkowska

CONTACT INFORMATION	IMP Dr. Bohr-Gasse 7 1030, Vienna , AUSTRIA dominika.bienkowska@imp.ac.at	<i>nationality:</i> Polish date of birth: 24. 07.1985
OBJECTIVE	I would like to pursue an innovative career in a challenging cell biology research which combines new approaches such as computation and microscopy	
QUALIFICATION	Research Institute of Molecular Pathology, IMP , Vienna, Austria Ph.D. Student, January 2008 (expected graduation date: March 2012) <ul style="list-style-type: none">• Supervisor: Carrie R. Cowan University of Wisconsin-Madison , Madison , Wisconsin, USA B.S., Molecular Biology, December, 2007	
RESEARCH EXPERIENCE	Research Institute of Molecular Pathology, IMP , Vienna, Austria Ph.D. Student, February 2008 (expected graduation date: March 2012) <ul style="list-style-type: none">• Dissertation Topic: "Analysis of molecular mechanics required for symmetry breaking in <i>C. elegans</i> zygote"• Supervisor: Carrie R. Cowan• Techniques: microscopy and fluorescent imaging (Spinning Disk, Delta Vision, DIC), image processing, worm genetics, protein expression and purification, Western Blot, immunofluorescence, microinjection,• Teaching Experience: supervised Master Student on the project: "Fate of paternal mitochondria in <i>C. elegans</i> zygote" University of Wisconsin-Madison , Madison, Wisconsin, USA Honors Senior Thesis, September, 2006- June, 2007 <ul style="list-style-type: none">• Thesis Topic: "Calcium dynamics during cytokinesis in living embryos"• Supervisor: John White, Mentor: Jayne Squirrell• Techniques: reengineering GFP probes (calcium markers), microscopy (Two-photon imaging), laser ablation Undergraduate Research, September, 2005- September, 2007 <ul style="list-style-type: none">• Topic: "Analyzing the role of two novel genes in ER and mitotic spindle organization in nematode embryos"• Supervisor: John White, Mentor: Jayne Squirrell• Techniques: general molecular biology (cloning), microparticle bombardment Independent Project, Spring 2005 <ul style="list-style-type: none">• Topic: "wormclassroom.org - an educative resource for undergraduates"• Project conducted at the Laboratory for Optical Computation and Instrumentation, LOCI• Techniques: website design	
HONORS AND AWARDS	Hilldale Undergraduate Research Fellowship (5 000 USD) for the project " Calcium dynamics in <i>C. elegans</i> embryo " Madison, USA, May, 2007 Benjamin Kaminer Scholarship (4 300 USD) for MBL Physiology Course 2010, Woods Hole, MA, USA, June, 2010	

PAPERS ACCEPTED Bienkowska, D. and Cowan C.R. 2011. Centrosomes can initiate a single polarity axis from any position within one-cell *C. elegans* embryos. "Current Biology".

ATTENDED "Analysis of molecular mechanics required for symmetry breaking in worm zygote"
 CONFERENCES Poster presentation, Biophysical Mechanisms of Development, EMBO Workshop, Lisboa, May 2011.

"Centrosome migration to the cortex during symmetry breaking in *C. elegans* zygote"
 Poster presentation, ASCB 50th Annual Meeting, Philadelphia, PA, December 2010.

"Exploration of endoplasmic reticulum organization during cell division in *C. elegans* embryos",
 Poster presentation, European Worm Meeting 2008, Carmona, Spain, March 2008.

"Exploration of endoplasmic reticulum organization during cell division in *C. elegans* embryos",
 Poster presentation, ASCB, 47th Annual Meeting, Washington, D.C., December 2007.

COURSES ATTENDED "Modern Cell Biology Using Microscopic, Biochemical and Computational Approaches",
 Physiology Course 2010, Woods Hole, MA, USA, June-July 2010

"Supramolecular Structure and Function" 10th International Summer School on Biophysics,
 Rovinj, Croatia, September, 2010

Presentation Workshop by Leonie Ringrose, Vienna, Austria, July 2008

COMPUTER SKILLS • Programs: Metamorph, ImageJ, Fiji, Illustrator, Soft Worx, Prism GraphPad
 • Languages: Octave, Bash, MatLab, C++, LaTeX
 • Algorithms: Basic experience programming Monte Carlo

OTHER SKILLS **Foreign Languages:** Polish - Native Tongue, English and Spanish - Professional Working Proficiency, German, French and Portuguese - Elementary Proficiency,

REFERENCES • **Dr. Carrie R. Cowan (Thesis Supervisor)**
 Group Leader
 Research Institute of Molecular Pathology, IMP
 Dr. Bohr-Gasse 7
 1030, Vienna, Austria

• **Dr. Barry Dickson**
 Scientific Director
 Research Institute of Molecular Pathology, IMP
 Dr. Bohr-Gasse 7, 1030, Vienna, Austria

• **Dr. Wallace Marshall**
 Assistant Professor
 Department of Biochemistry and Biophysics
 UCSF Mission Bay, 600 16th St.
 San Francisco, CA 94143-2200

• **Dr. Kerwyn Casey Huang**
 Assistant Professor
 Department of Bioengineering
 Stanford University
 Clark Center S325 MC:5444, CA 94305